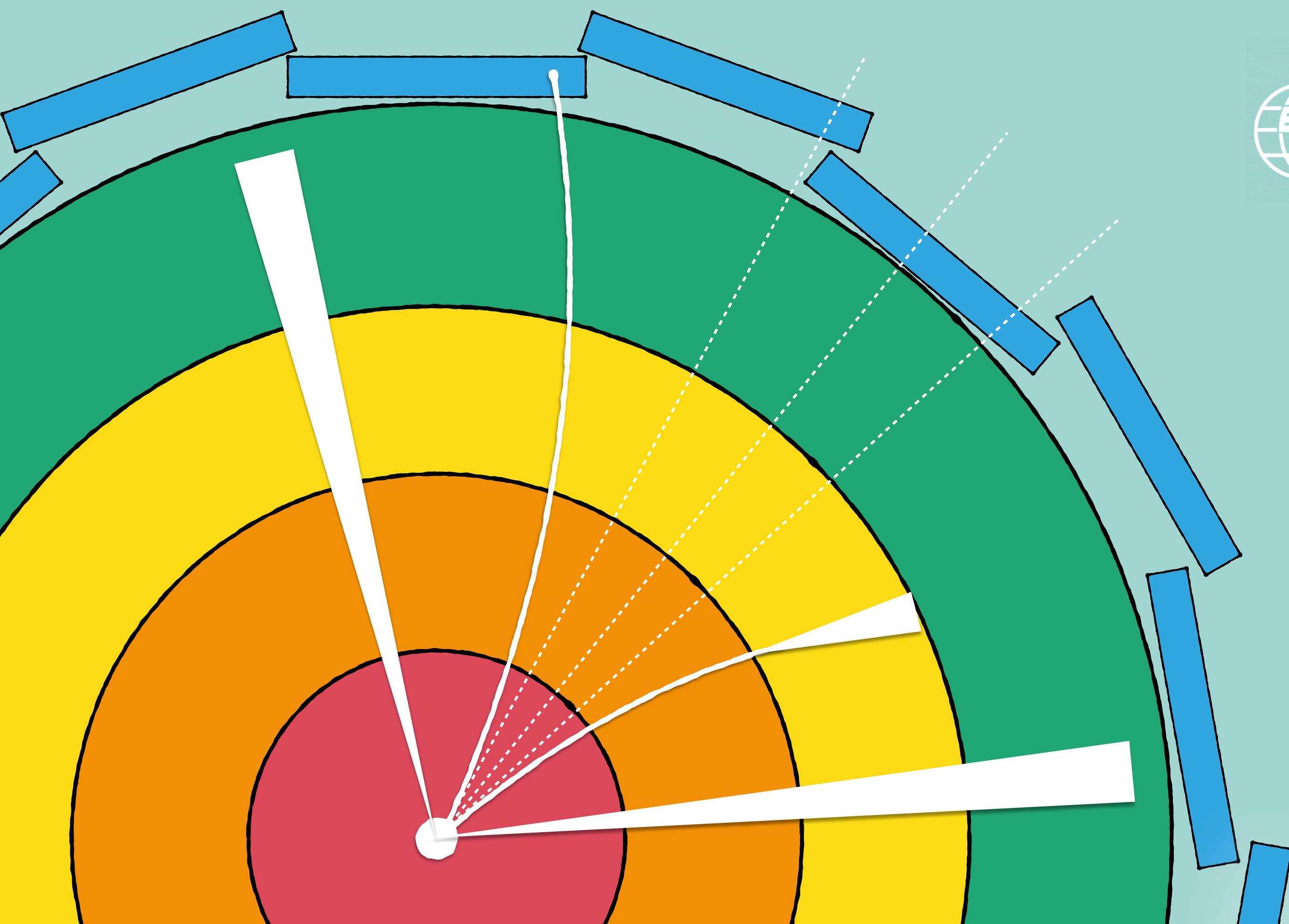


# Searches for Leptoquarks with the ATLAS detector

Christian Appelt, *on behalf of the ATLAS collaboration*

22. Aug 2023



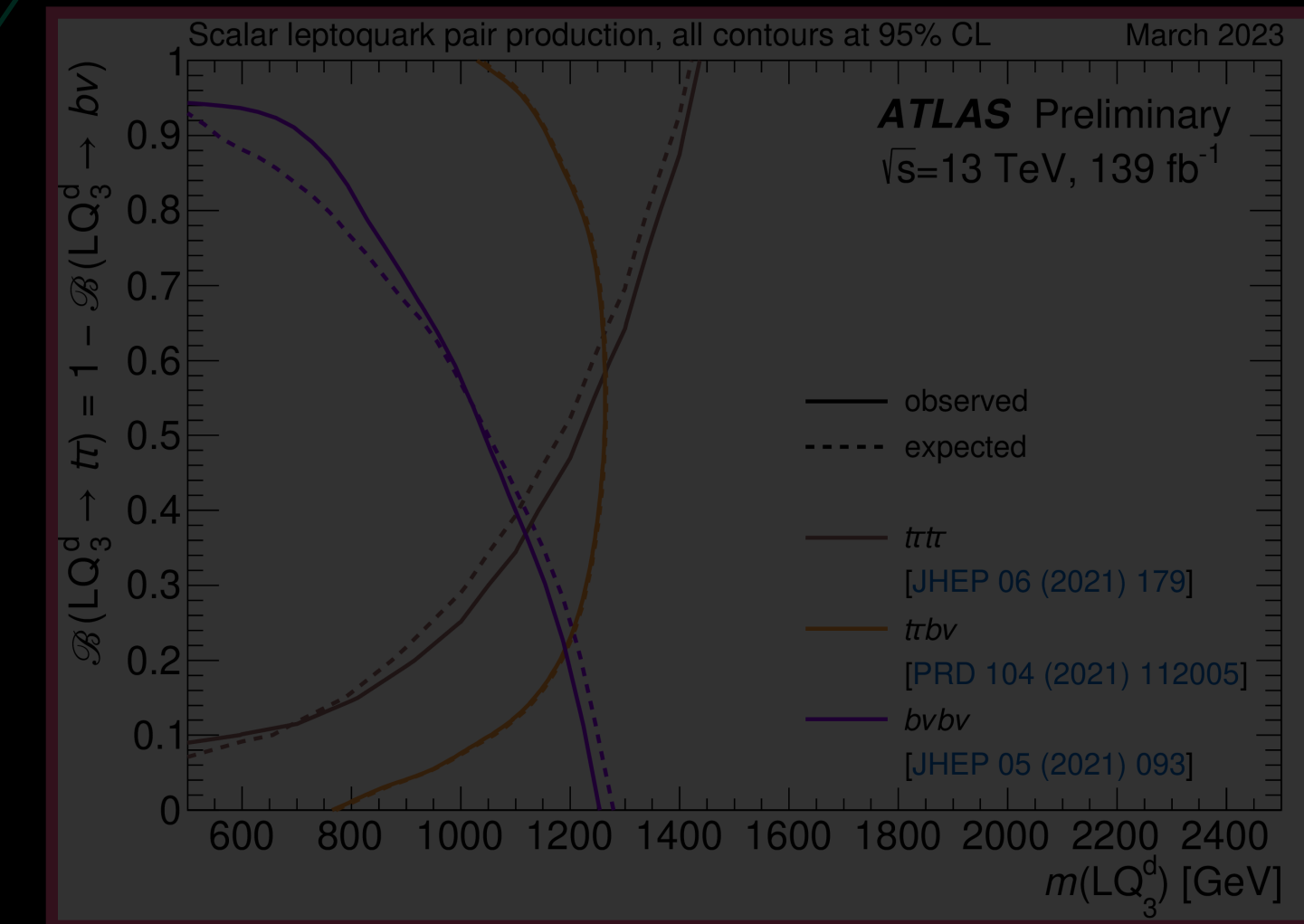
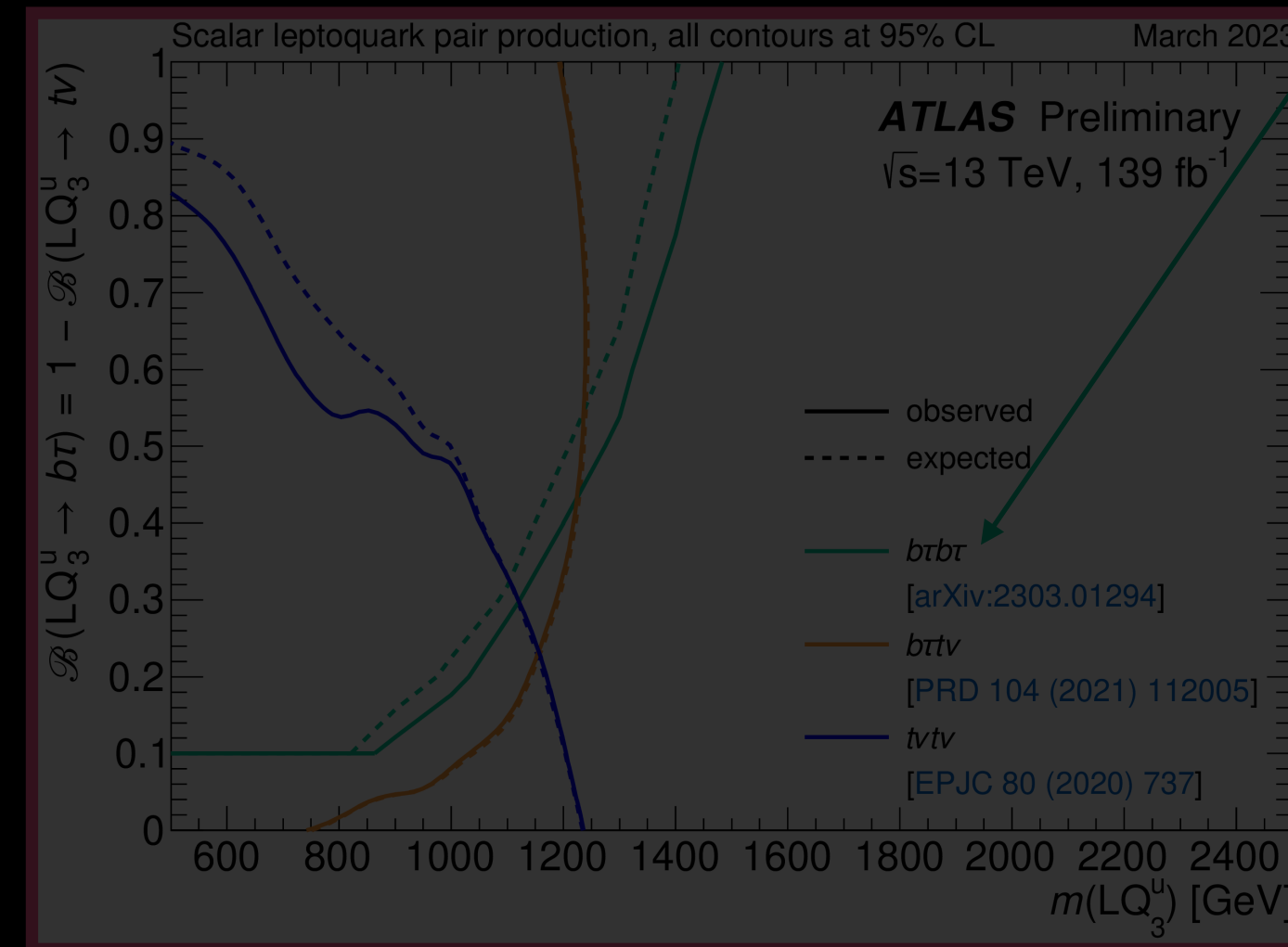
# Why Leptoquarks?

in a nutshell

- Many extensions to the SM predict particles known as **Leptoquarks (LQ)\***.
- **LQs** provide a connection between the lepton and quark sectors.
- **LQs** can be scalar (spin 0) or vector (spin 1) bosons.
- **LQs** carry colour and a fractional electric charge.
- **LQs** potentially explain hints of violations of **lepton universality** in flavour experiments (recent results from [BaBar](#), [Belle](#), and [LHCb](#) in B-meson decays).
- $4.2\sigma$  deviation to the SM in the **anomalous magnetic moment** measurement could be caused by **LQ contributions to the magnetic moment**.

## Scalar $LQ_3$ summary plots

Discussed in this talk + one more analysis!



[ATL-PHYS-PUB-2023-006]

\* [Phys. Rev. D 10 (1 1974) 275, Phys. Rev. Lett. 32 (8 1974) 438, Nuclear Physics B 155 (1979) 237, Nuclear Physics B 168 (1980) 69, Physics Letters B 90 (1980) 125, Nuclear Physics B 292 (1987) 59, Physics Letters B 177 (1986) 377]

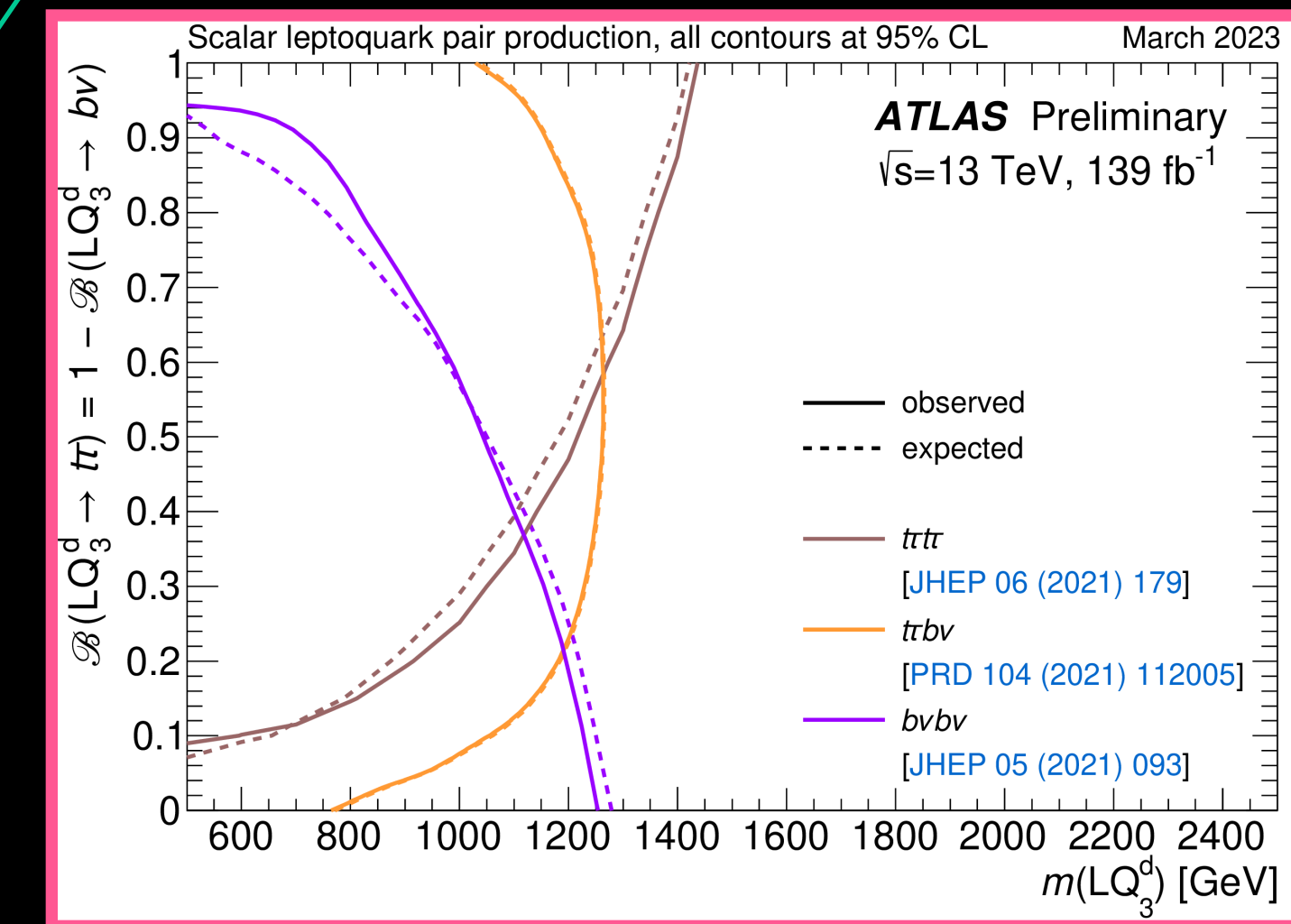
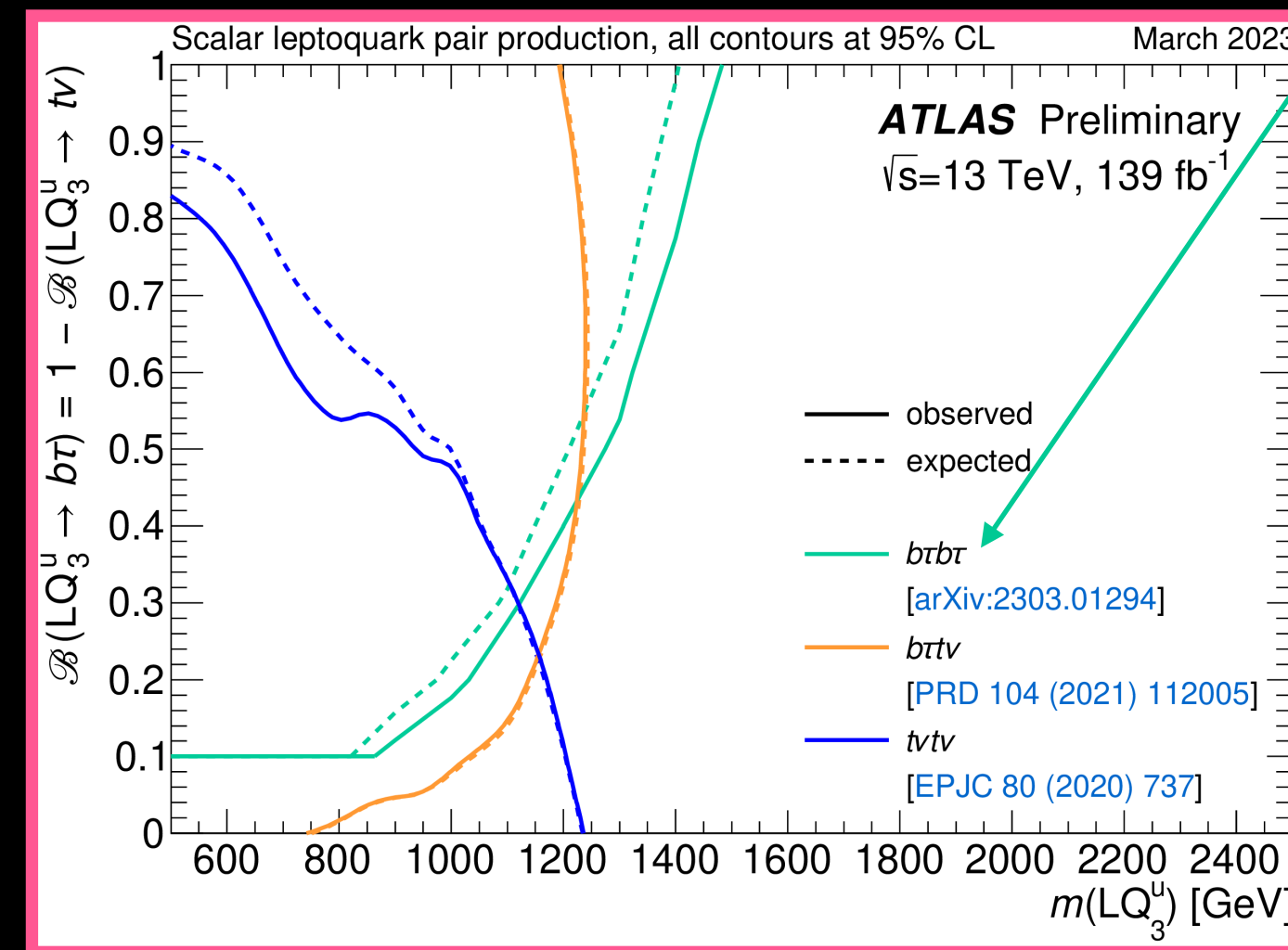
# Why Leptoquarks?

in a nutshell

- Many extensions to the SM predict particles known as **Leptoquarks (LQ)\***.
- LQs** provide a connection between the lepton and quark sectors.
- LQs** can be scalar (spin 0) or vector (spin 1) bosons.
- LQs** carry colour and a fractional electric charge.
- LQs** potentially explain hints of violations of **lepton universality** in flavour experiments (recent results from [BaBar](#), [Belle](#), and [LHCb](#) in B-meson decays).
- 4.2  $\sigma$  deviation to the SM in the **anomalous magnetic moment** measurement could be caused by **LQ contributions to the magnetic moment**.

## Scalar LQ<sub>3</sub> summary plots

Discussed in this talk + one more analysis!

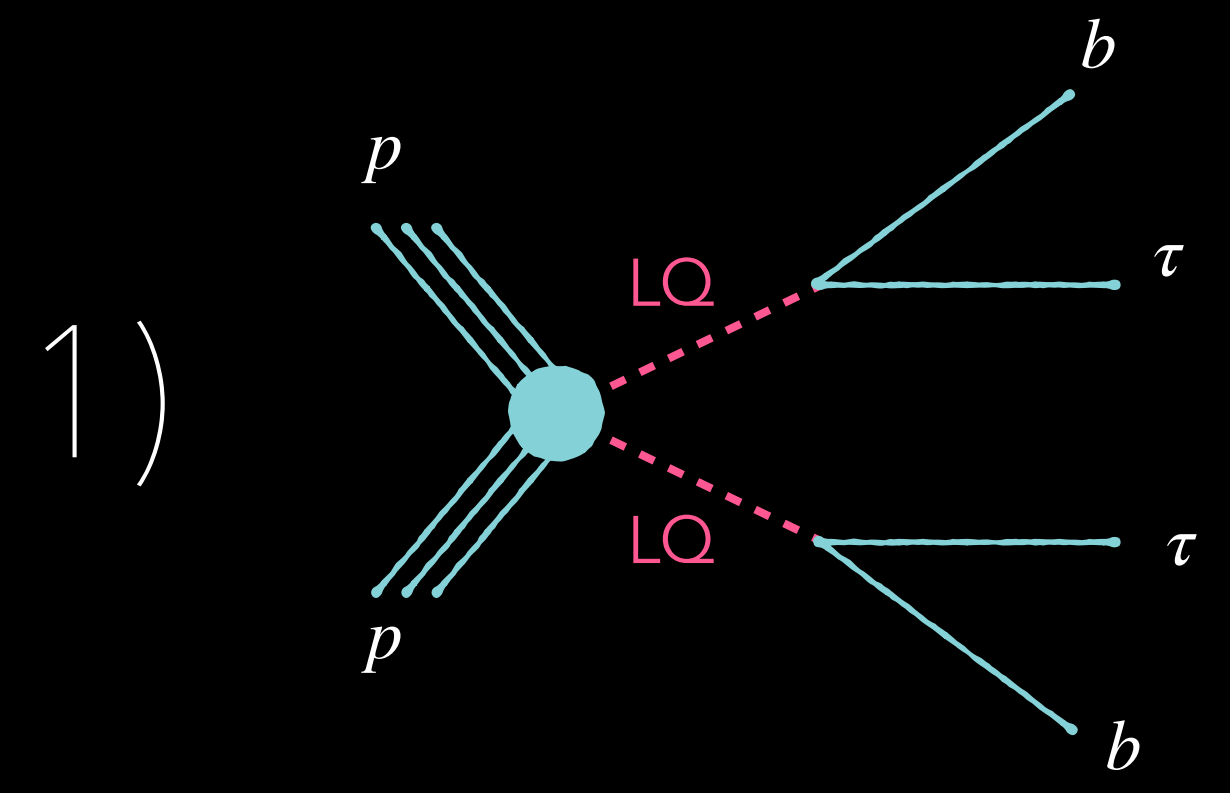


[ATL-PHYS-PUB-2023-006]

\* [Phys. Rev. D 10 (1 1974) 275, Phys. Rev. Lett. 32 (8 1974) 438, Nuclear Physics B 155 (1979) 237, Nuclear Physics B 168 (1980) 69, Physics Letters B 90 (1980) 125, Nuclear Physics B 292 (1987) 59, Physics Letters B 177 (1986) 377]

# Outline

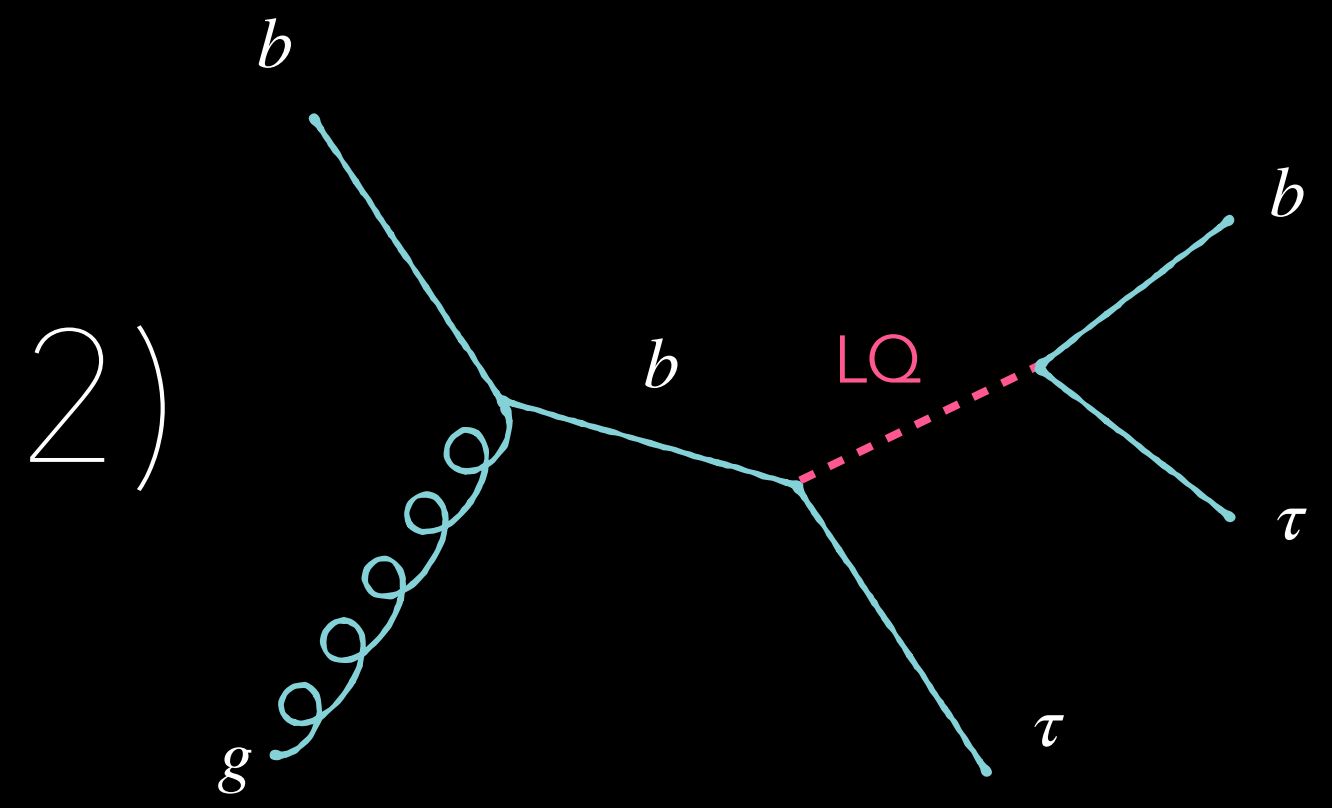
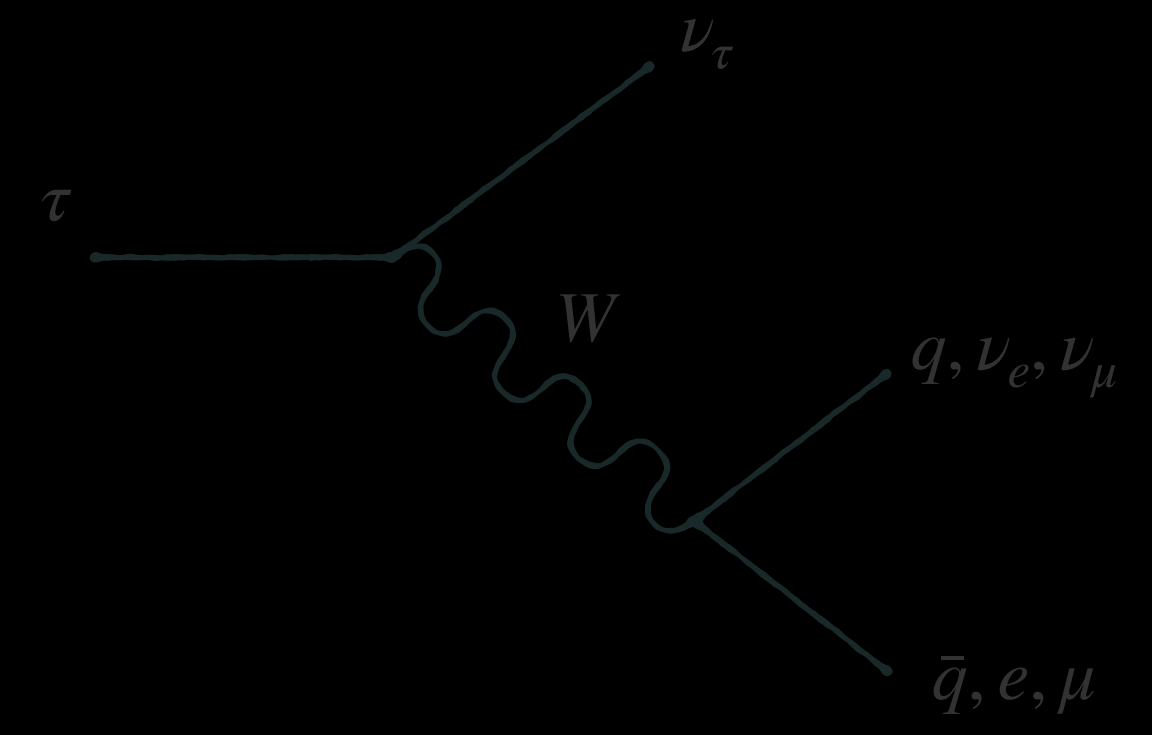
Both in  $\sqrt{s} = 13 \text{ TeV } pp$  collisions with  $L = 139 \text{ fb}^{-1}$



Search for pair production of third-generation leptiquarks decaying into a bottom quark and  $\tau$ -lepton with the ATLAS detector.

[[arXiv:2303.01294](https://arxiv.org/abs/2303.01294)]  
Submitted to: EPJC  
March 2023

$\tau$  decays either hadronically or leptonically:



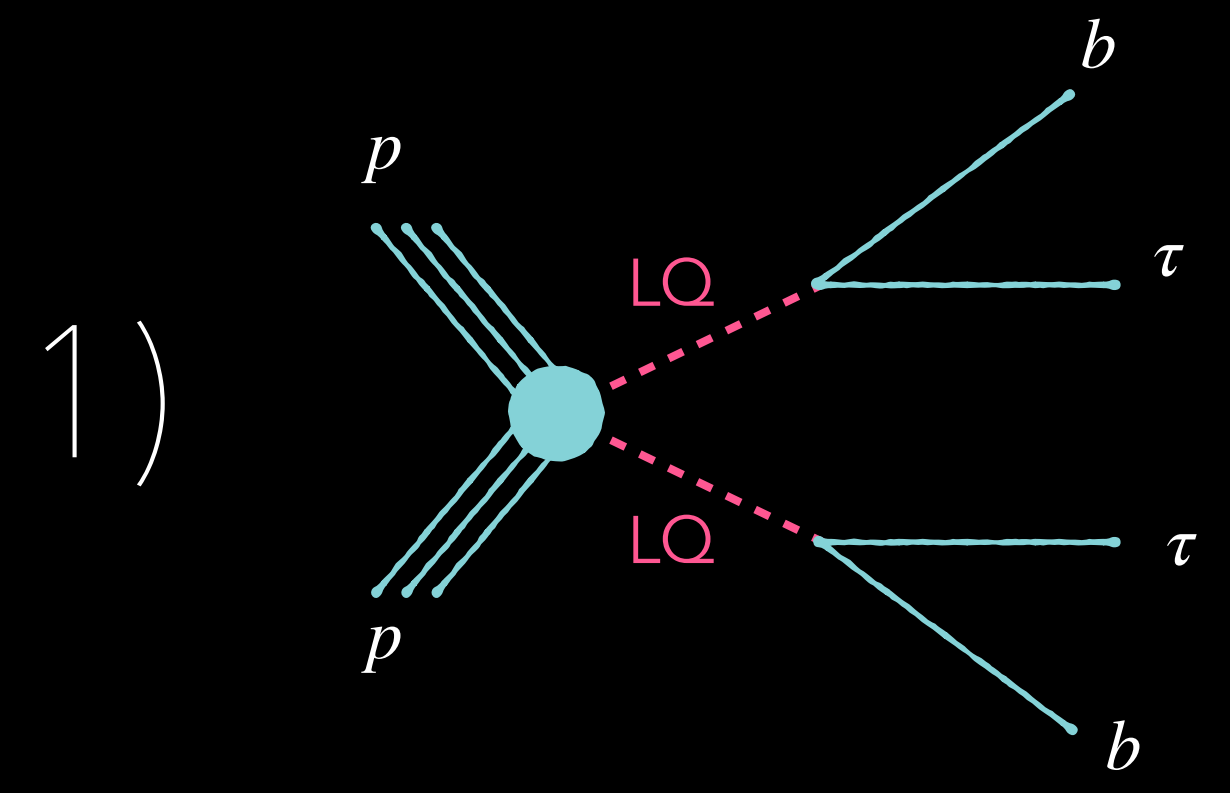
Search for leptiquarks decaying into the  $b\tau$  final state with the ATLAS detector.

[[arXiv:2305.15962](https://arxiv.org/abs/2305.15962)]  
Submitted to: JHEP  
May 2023



# Outline

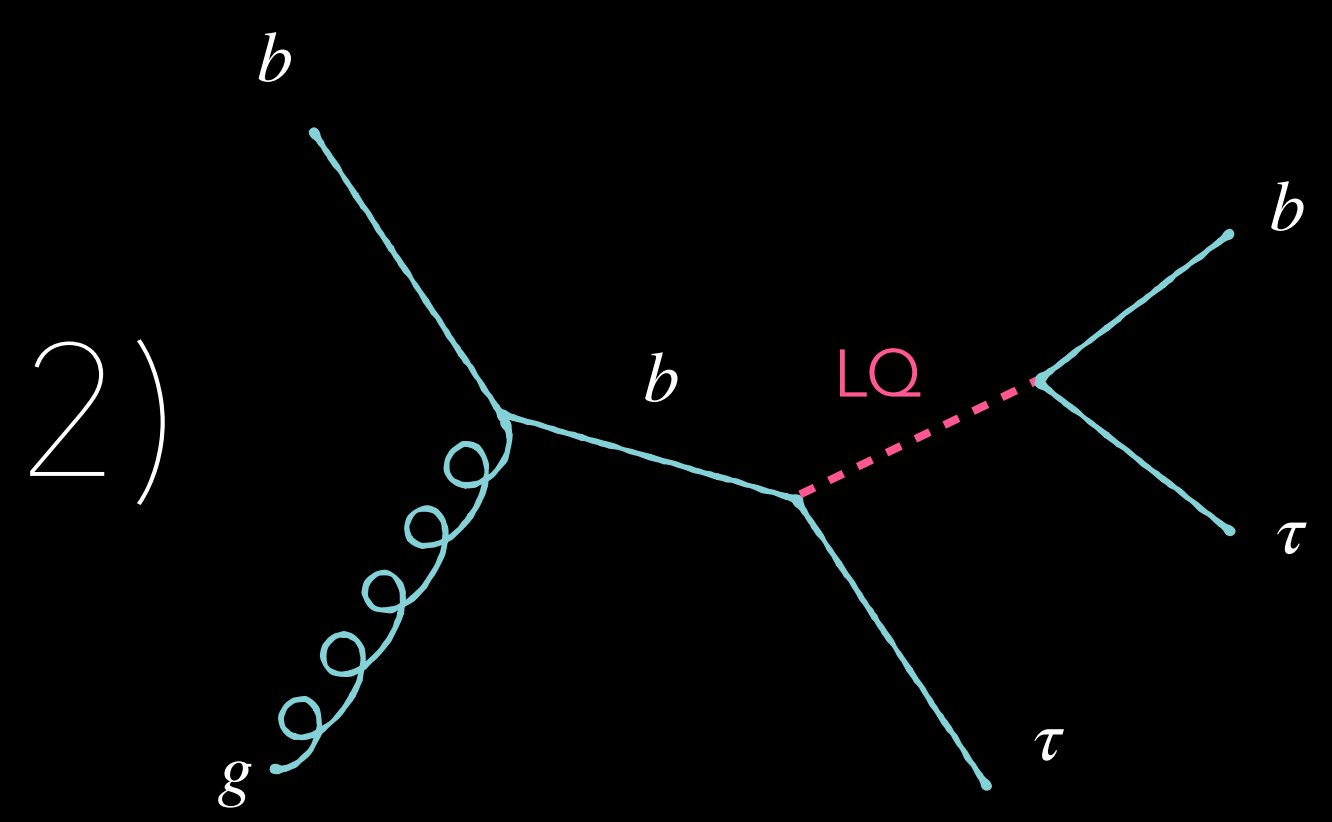
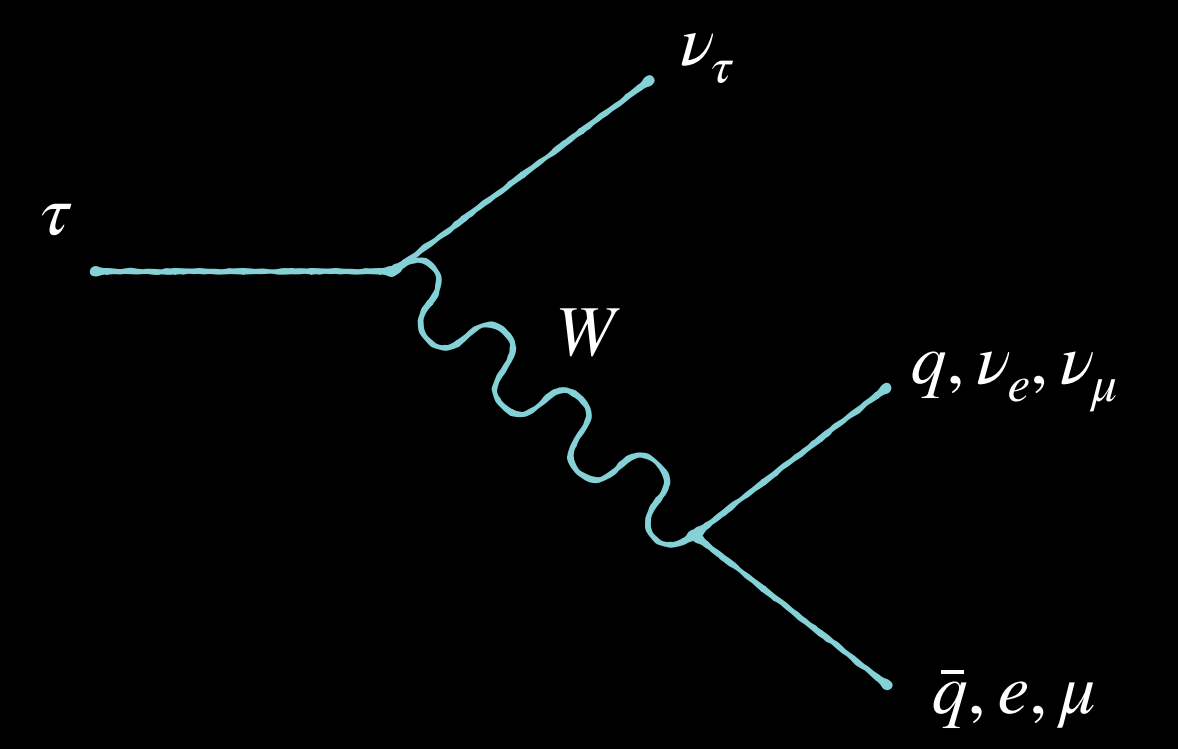
Both in  $\sqrt{s} = 13 \text{ TeV } pp$  collisions with  $L = 139 \text{ fb}^{-1}$



Search for pair production of third-generation leptiquarks decaying into a bottom quark and  $\tau$ -lepton with the ATLAS detector.

[[arXiv:2303.01294](https://arxiv.org/abs/2303.01294)]  
Submitted to: EPJC  
March 2023

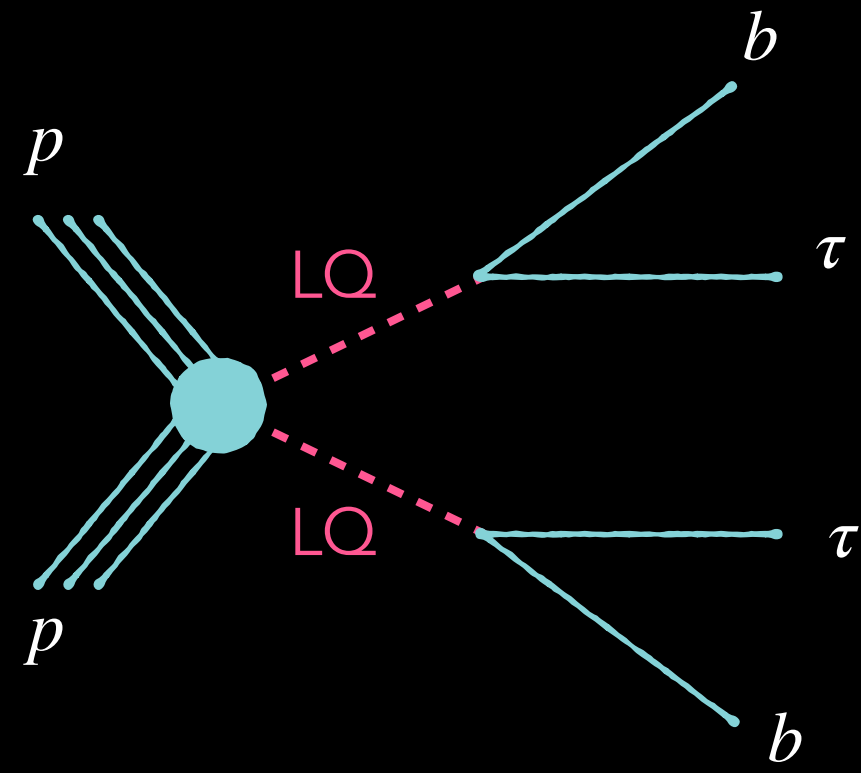
$\tau$  decays either hadronically or leptonically:



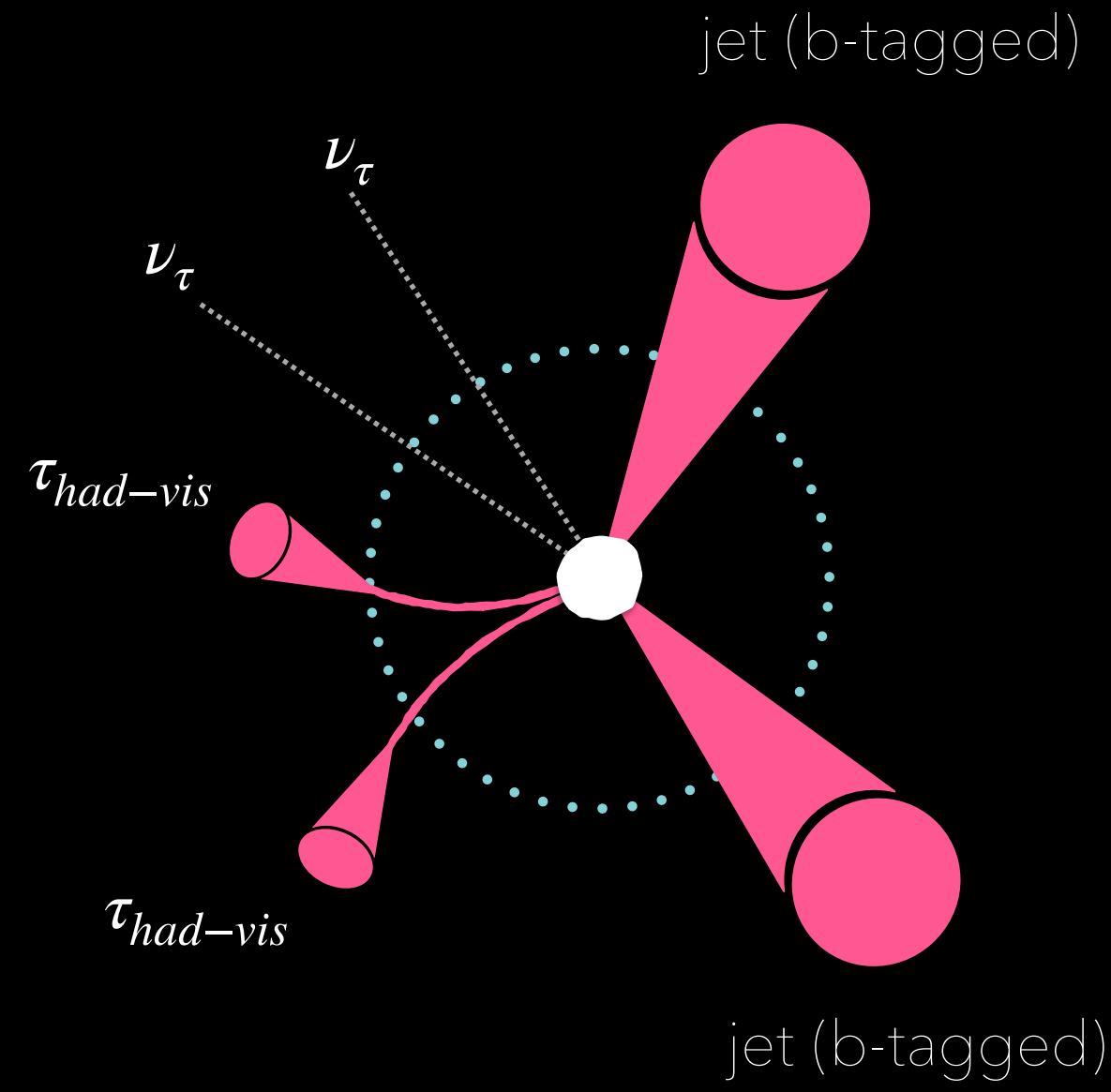
Search for leptiquarks decaying into the  $b\tau$  final state with the ATLAS detector.

[[arXiv:2305.15962](https://arxiv.org/abs/2305.15962)]  
Submitted to: JHEP  
May 2023

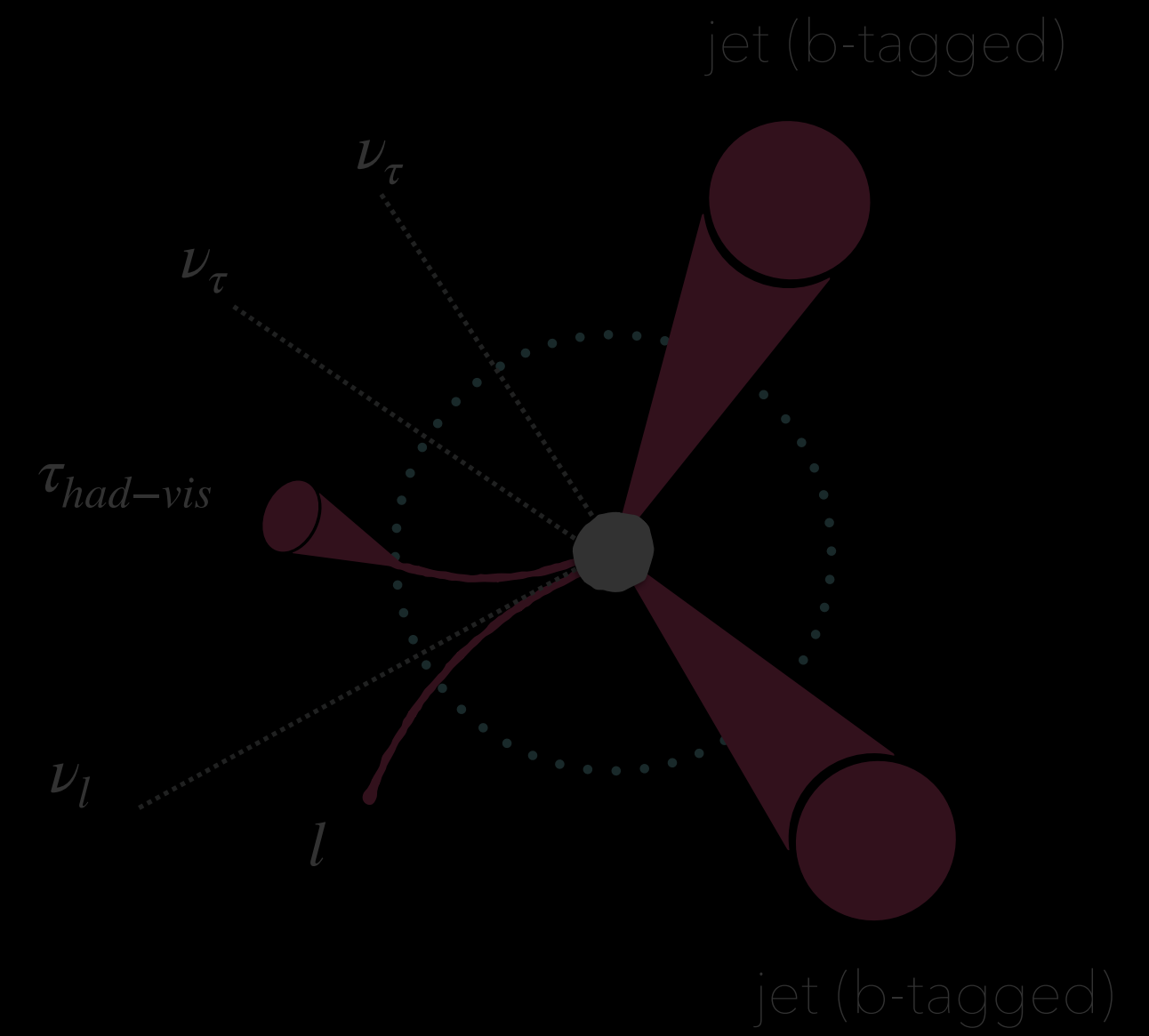
1)



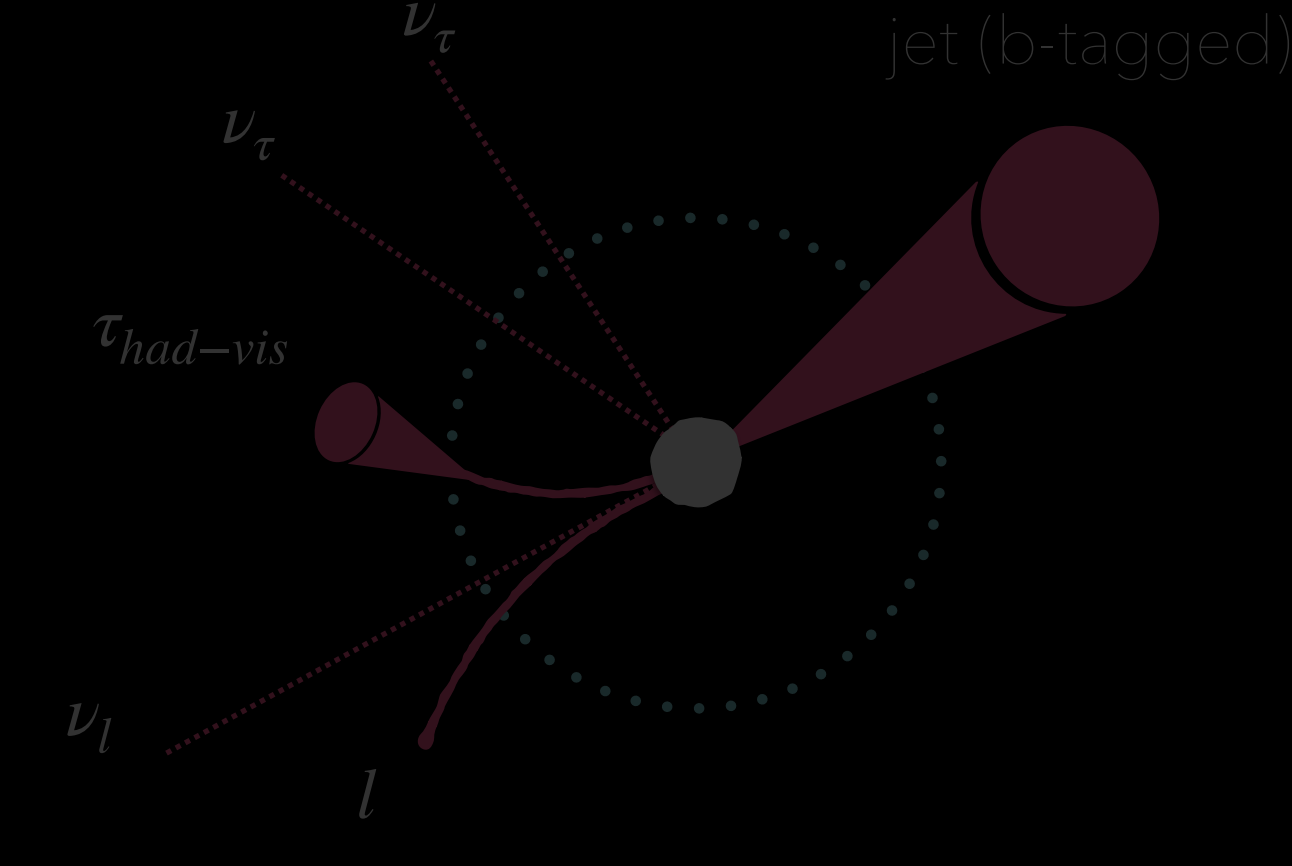
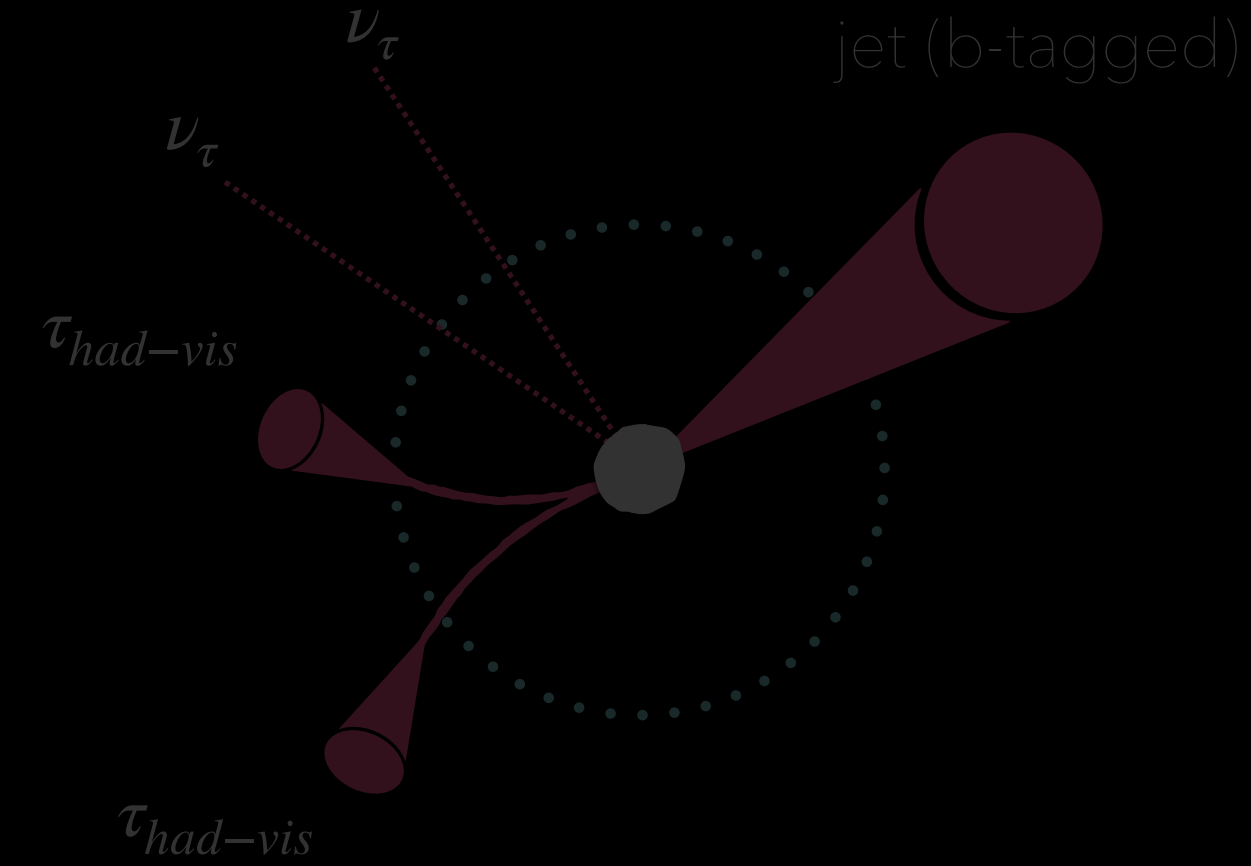
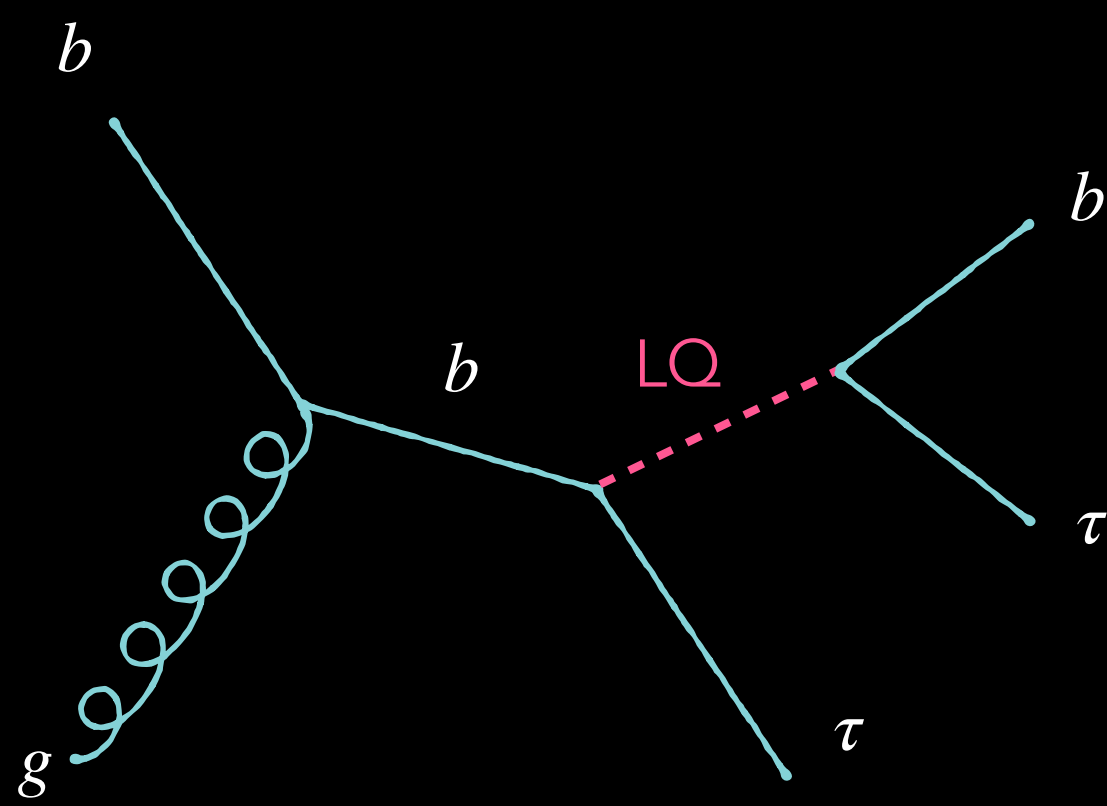
$\tau_{had}\tau_{had}$  channel



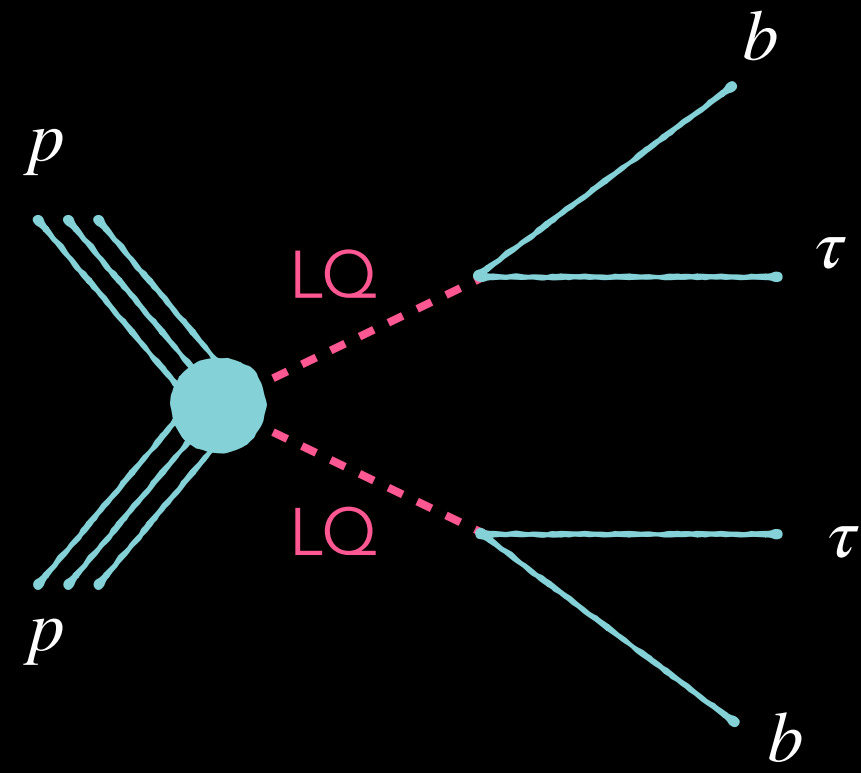
$\tau_{lep}\tau_{had}$  channel



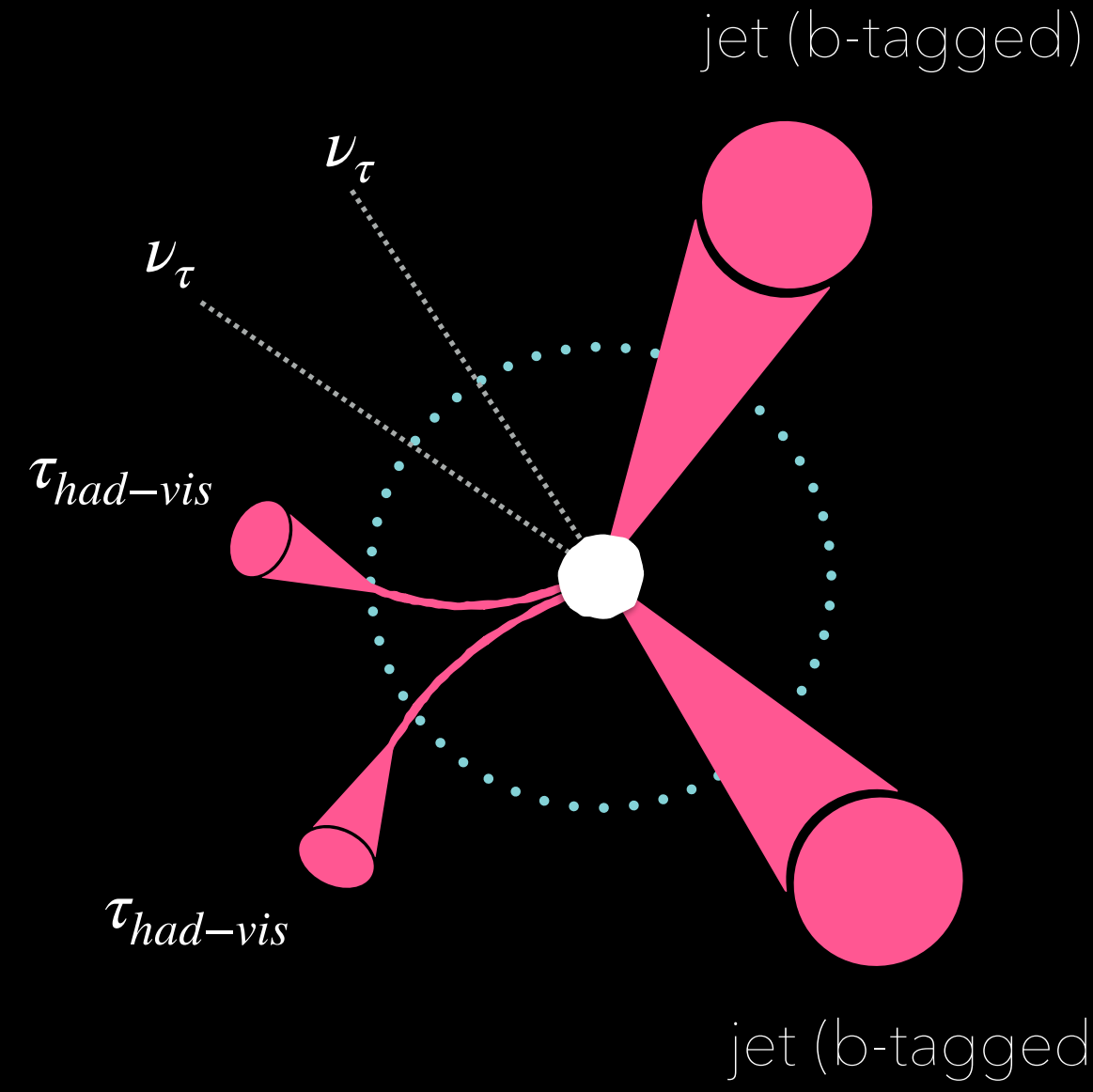
2)



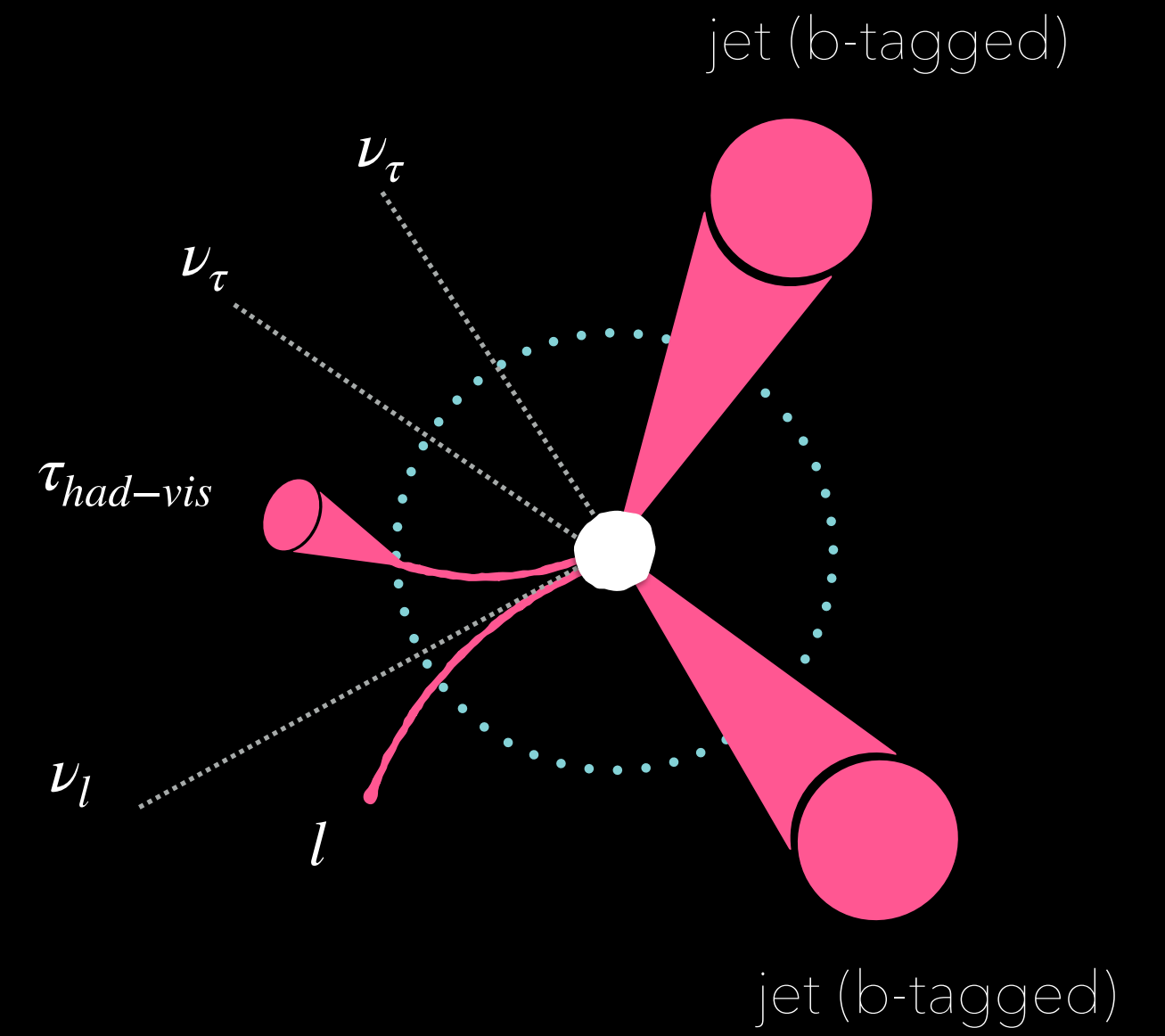
1)



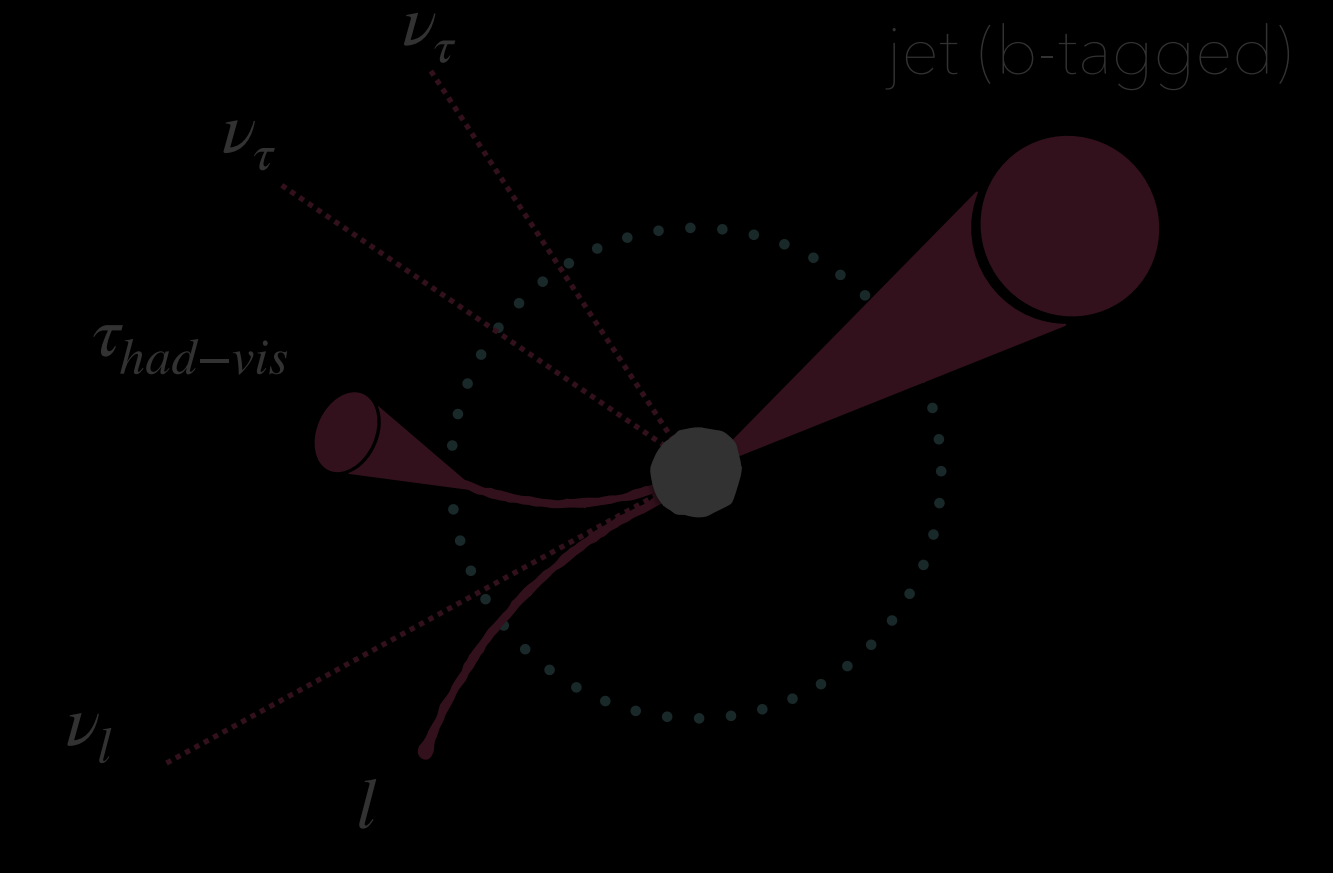
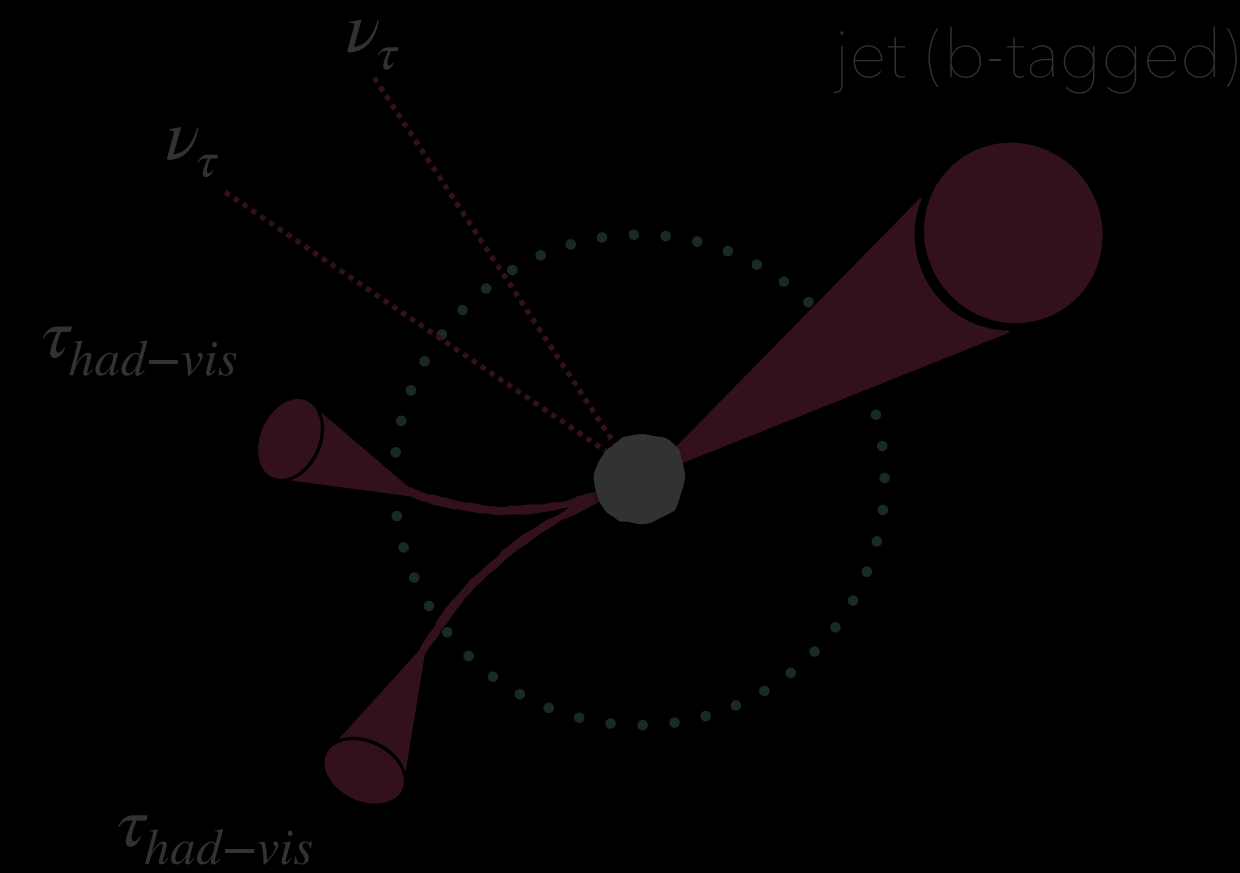
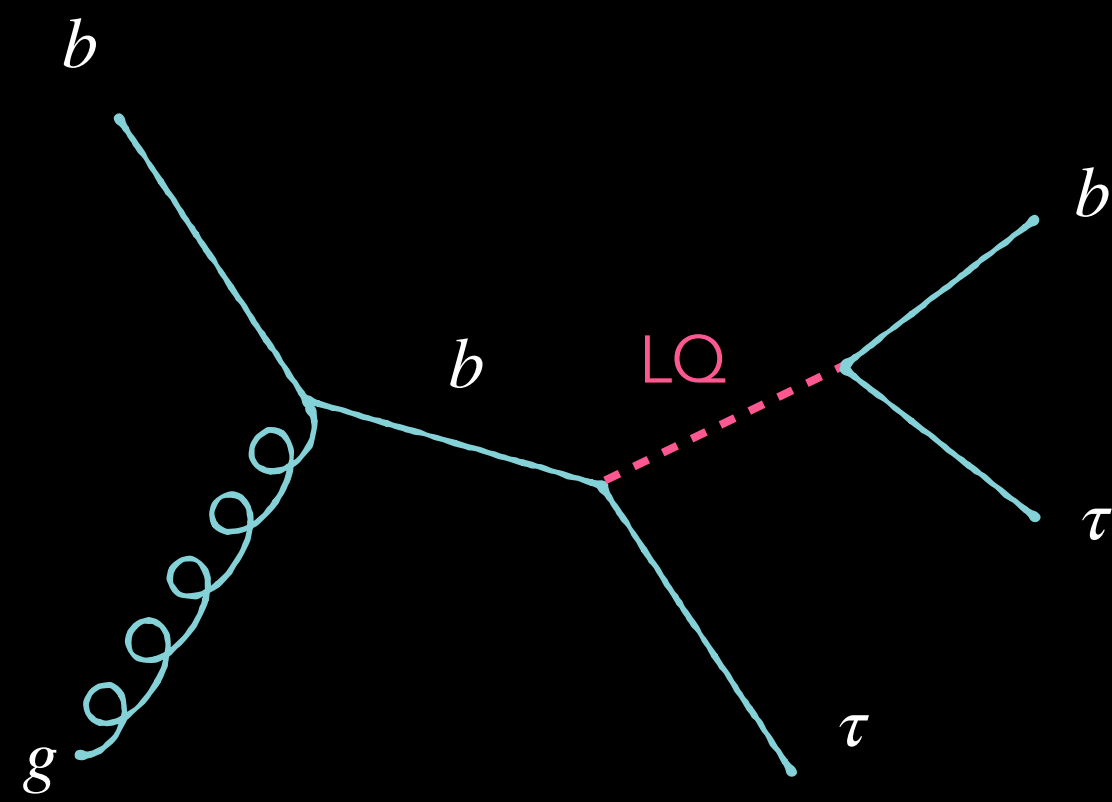
$\tau_{had}\tau_{had}$  channel



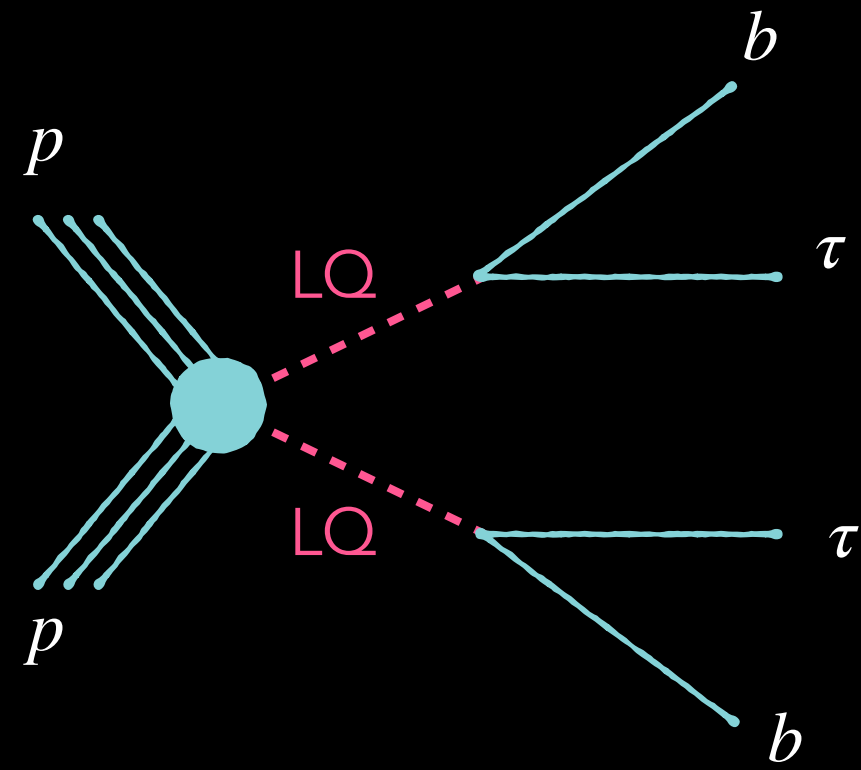
$\tau_{lep}\tau_{had}$  channel



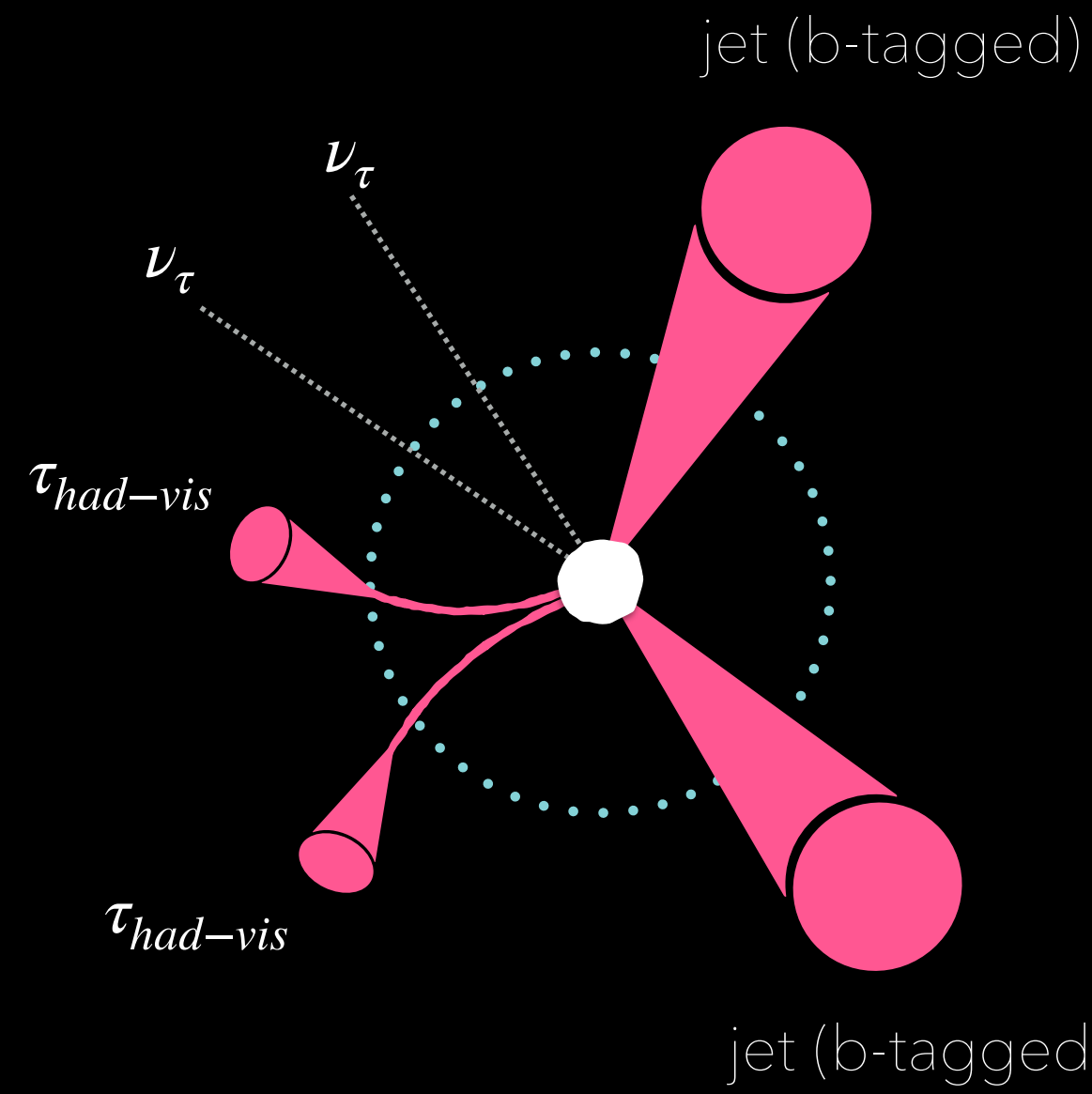
2)



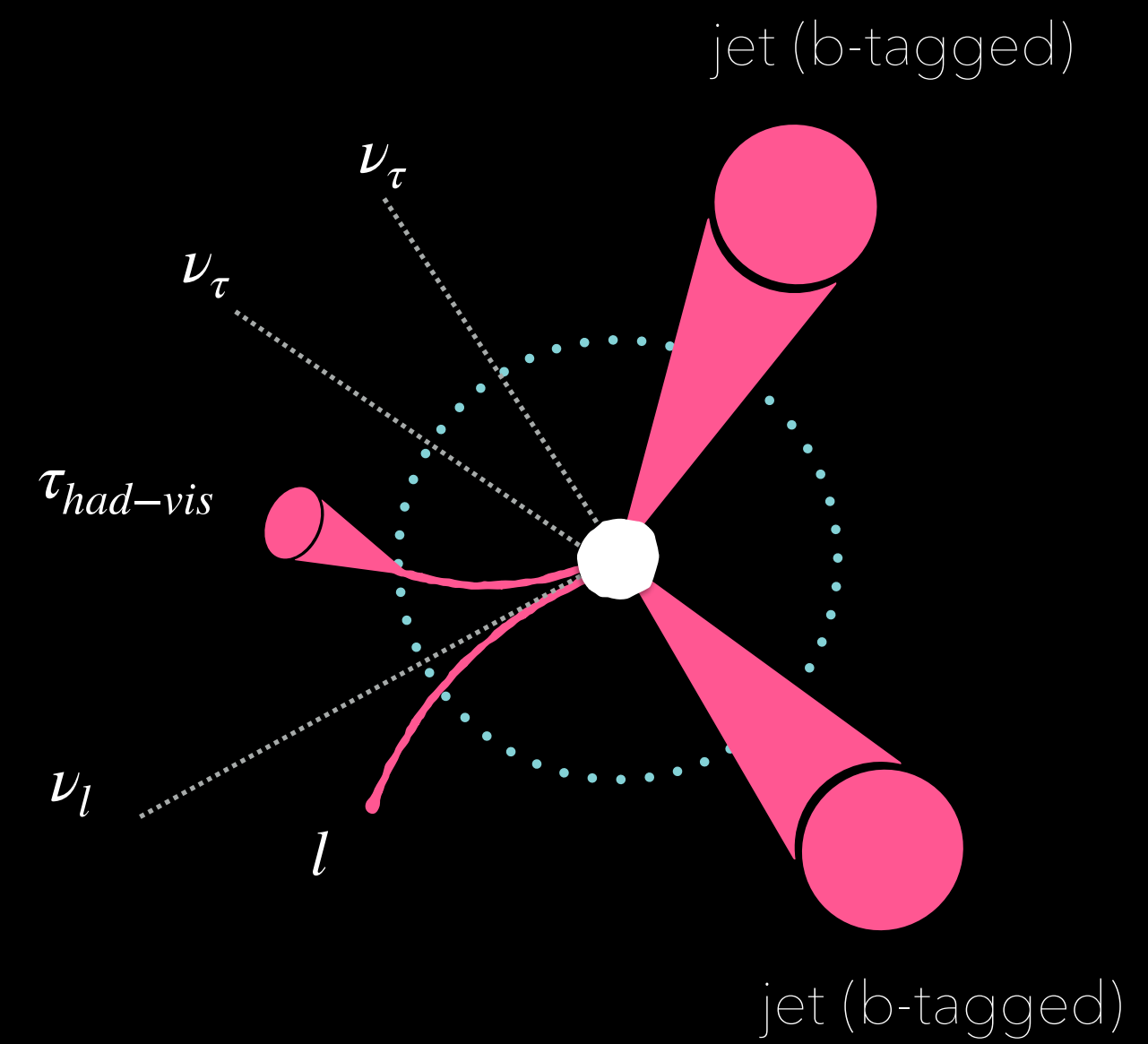
1)



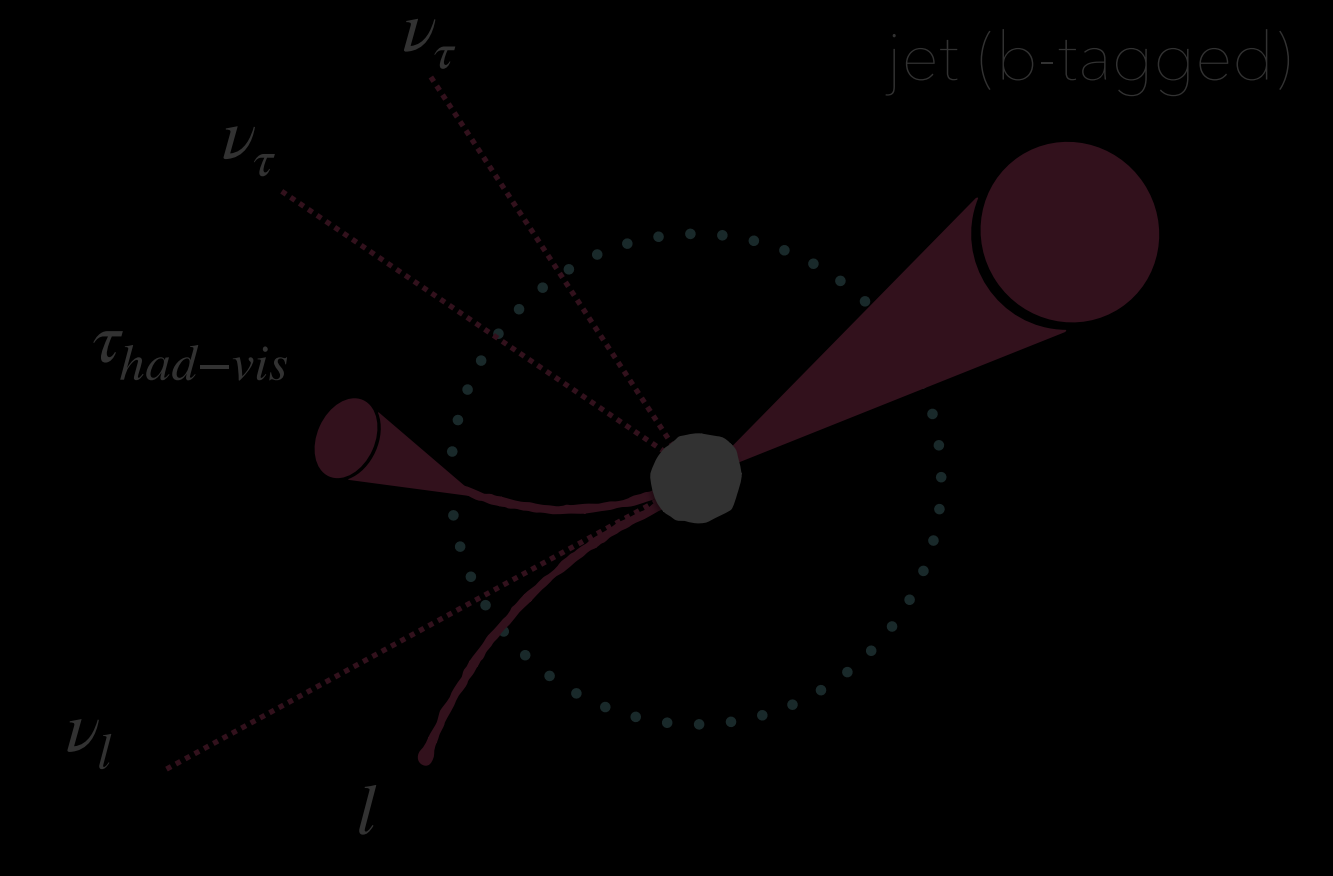
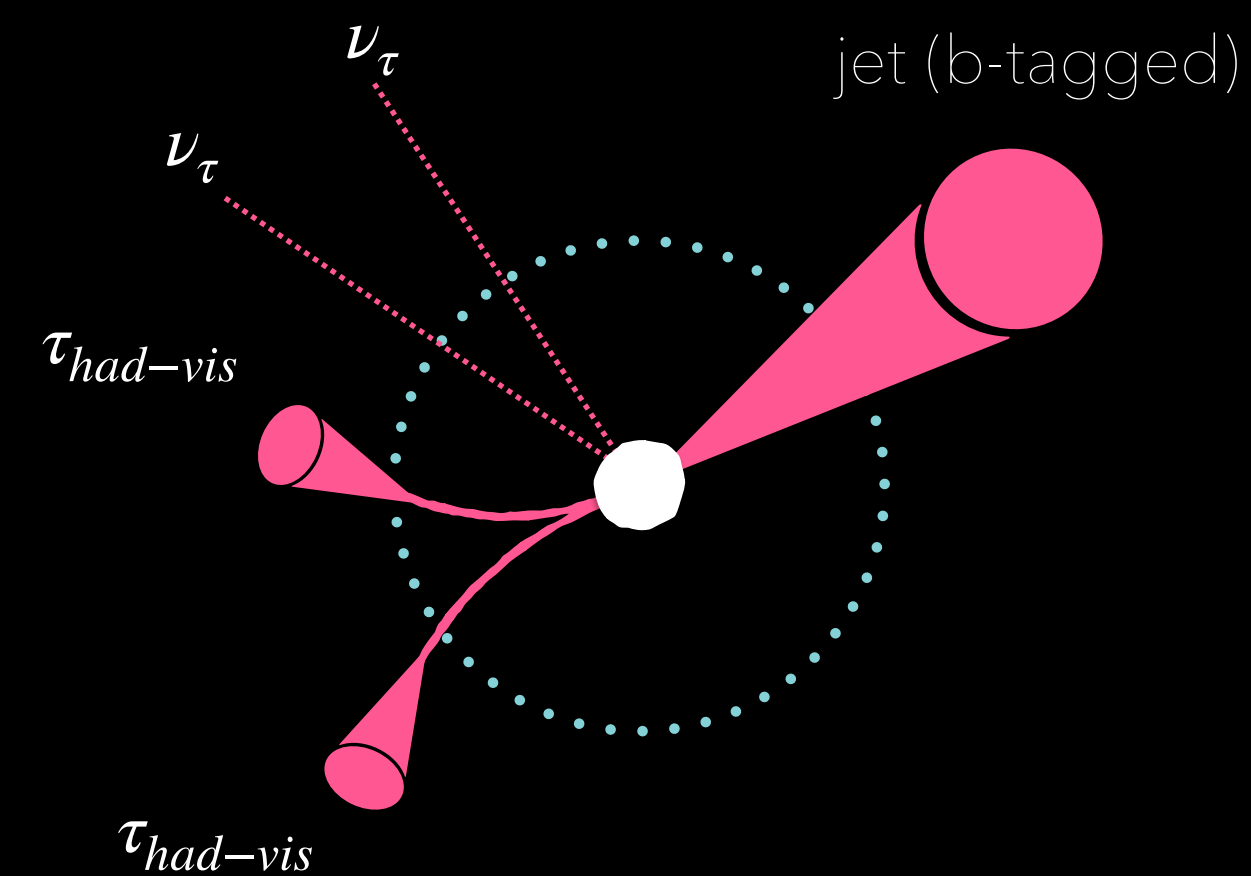
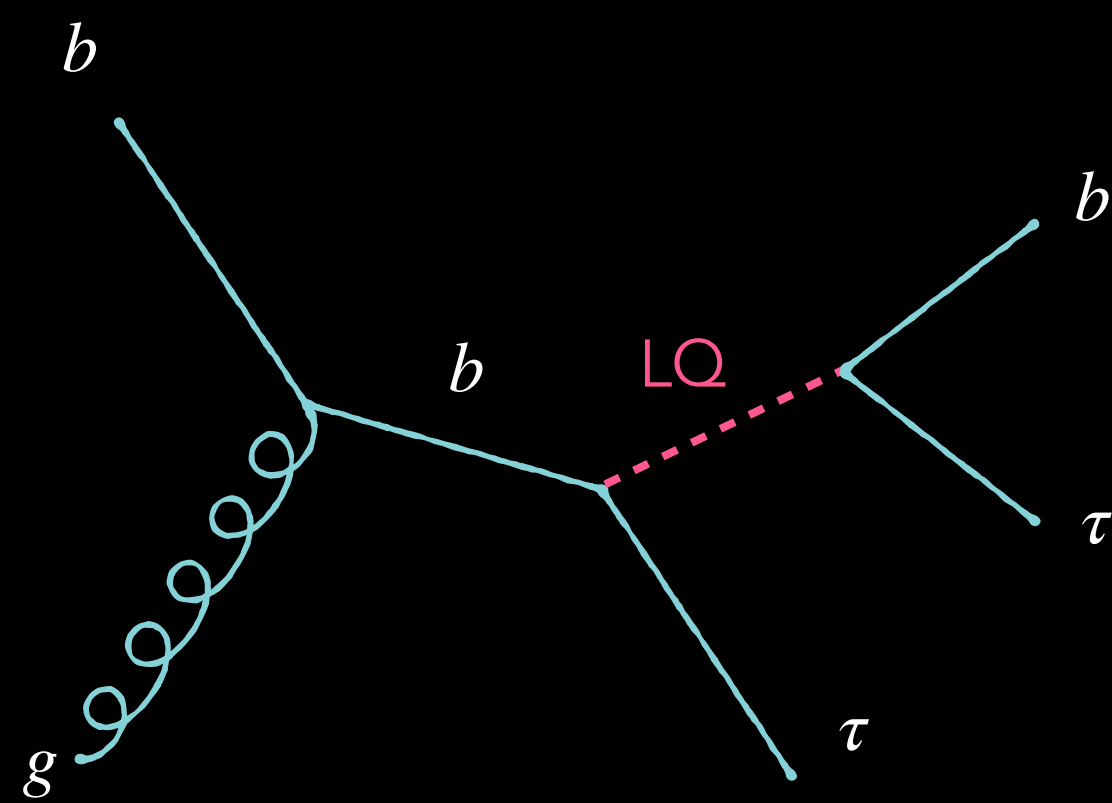
$\tau_{had}\tau_{had}$  channel



$\tau_{lep}\tau_{had}$  channel

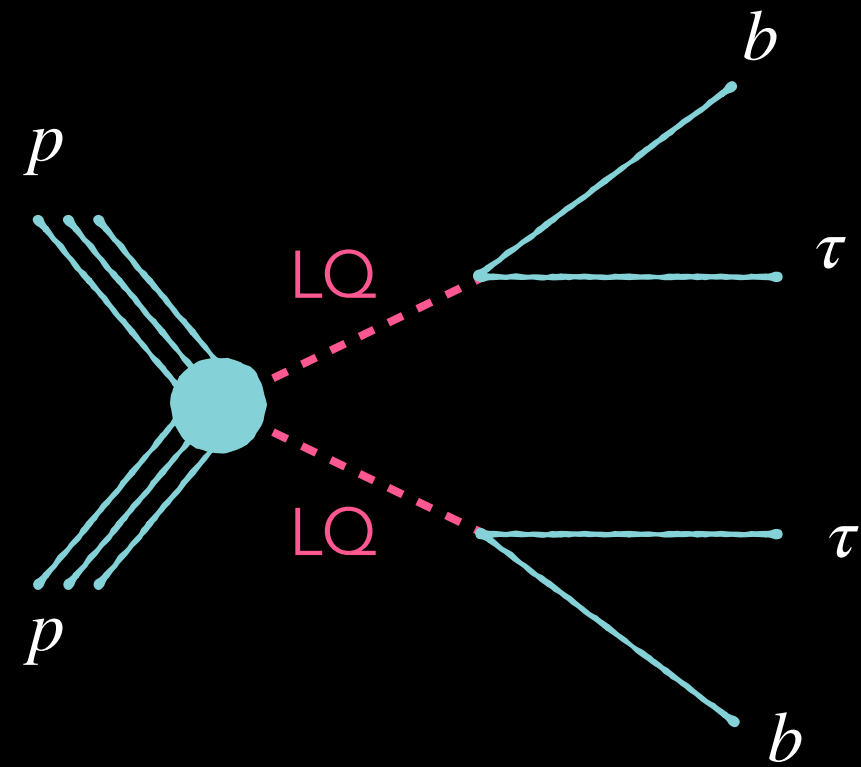


2)

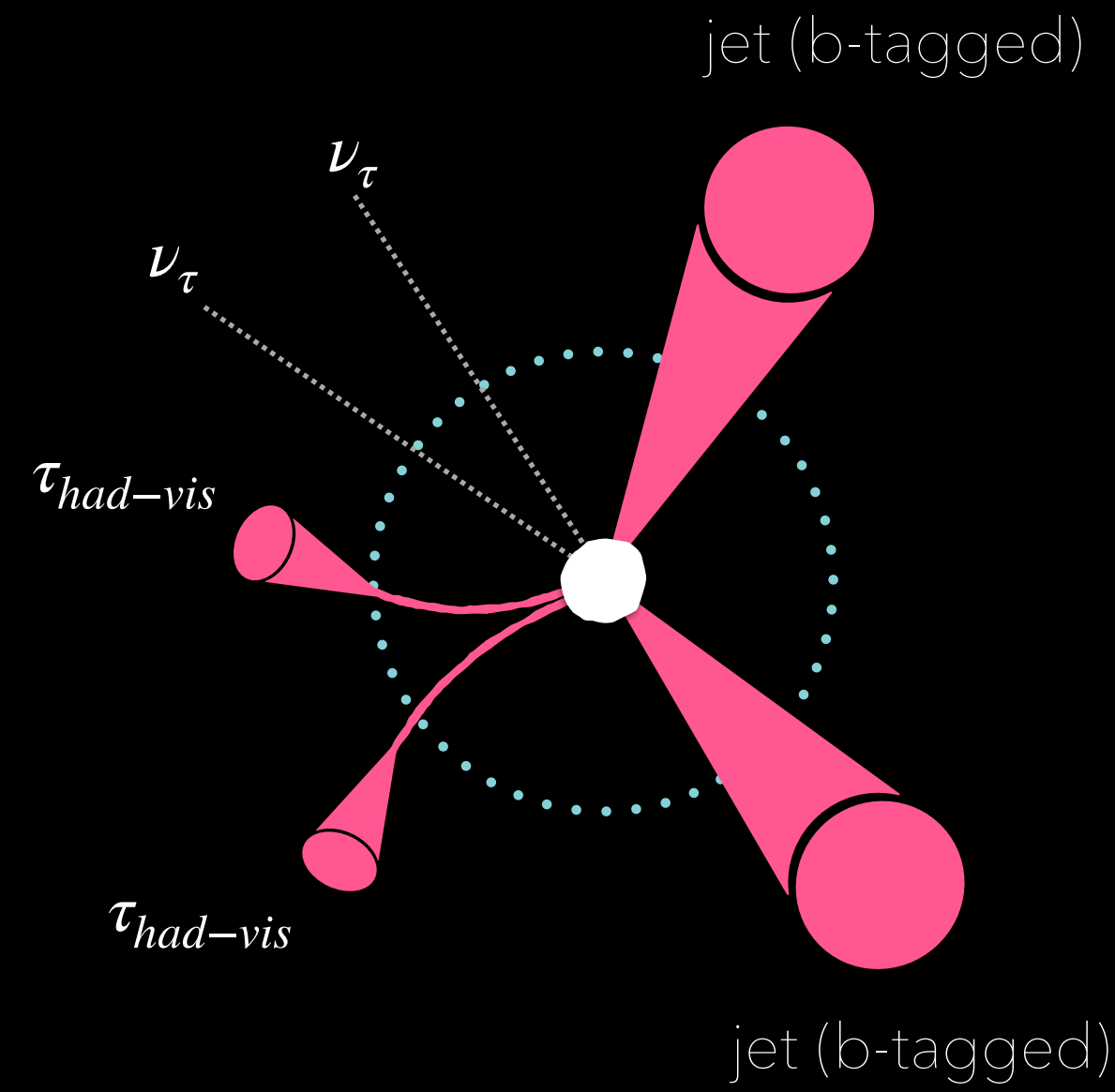




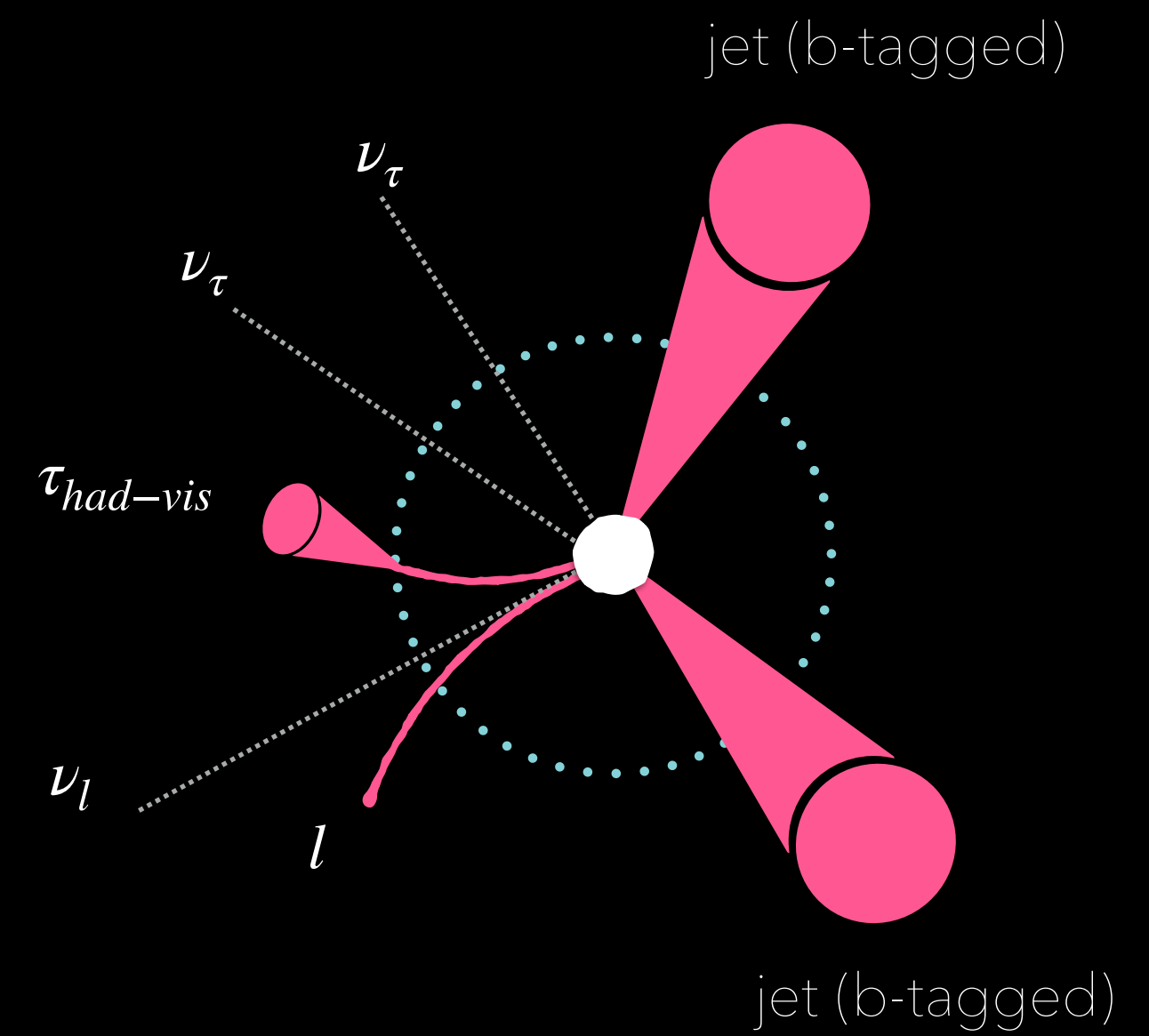
1)



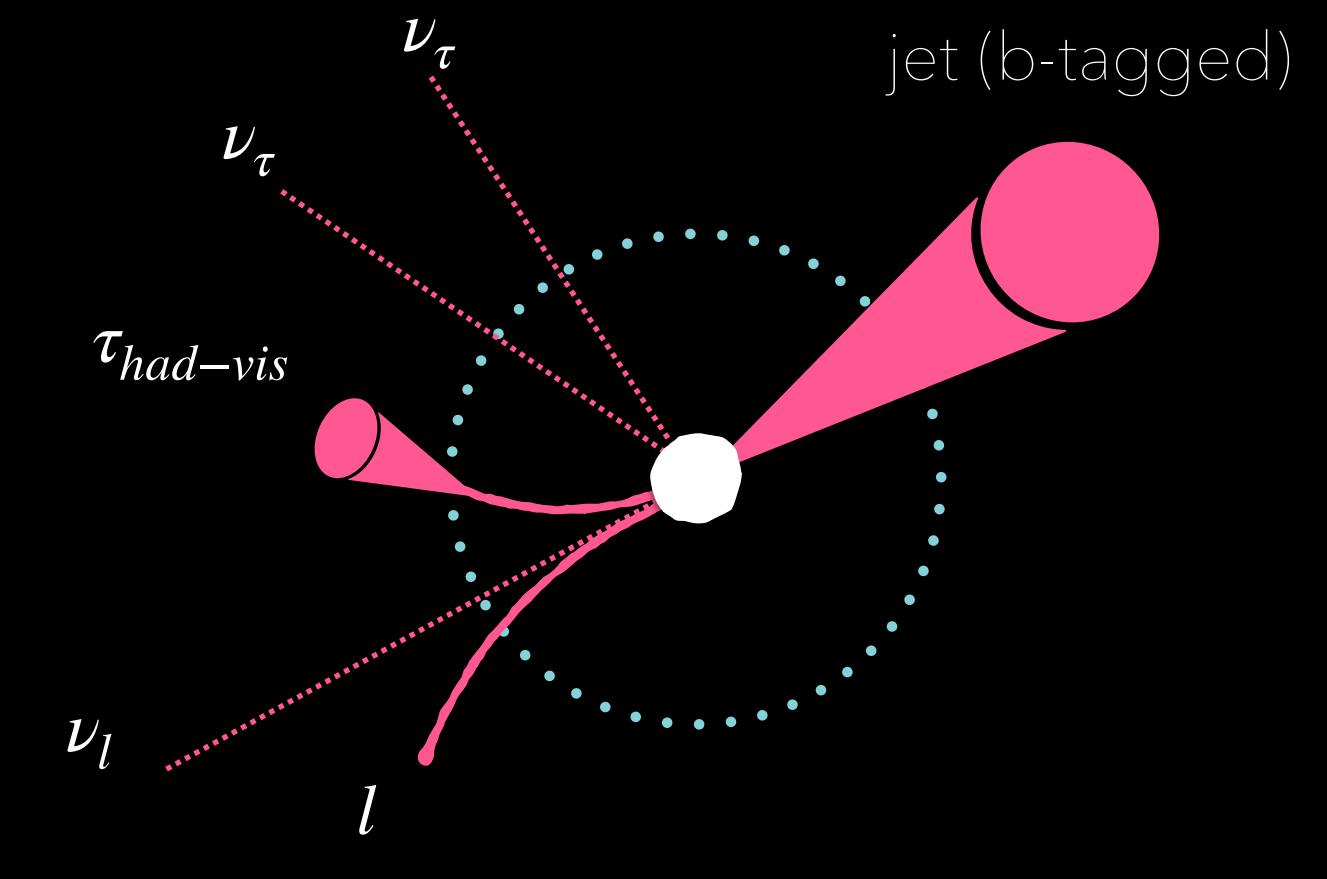
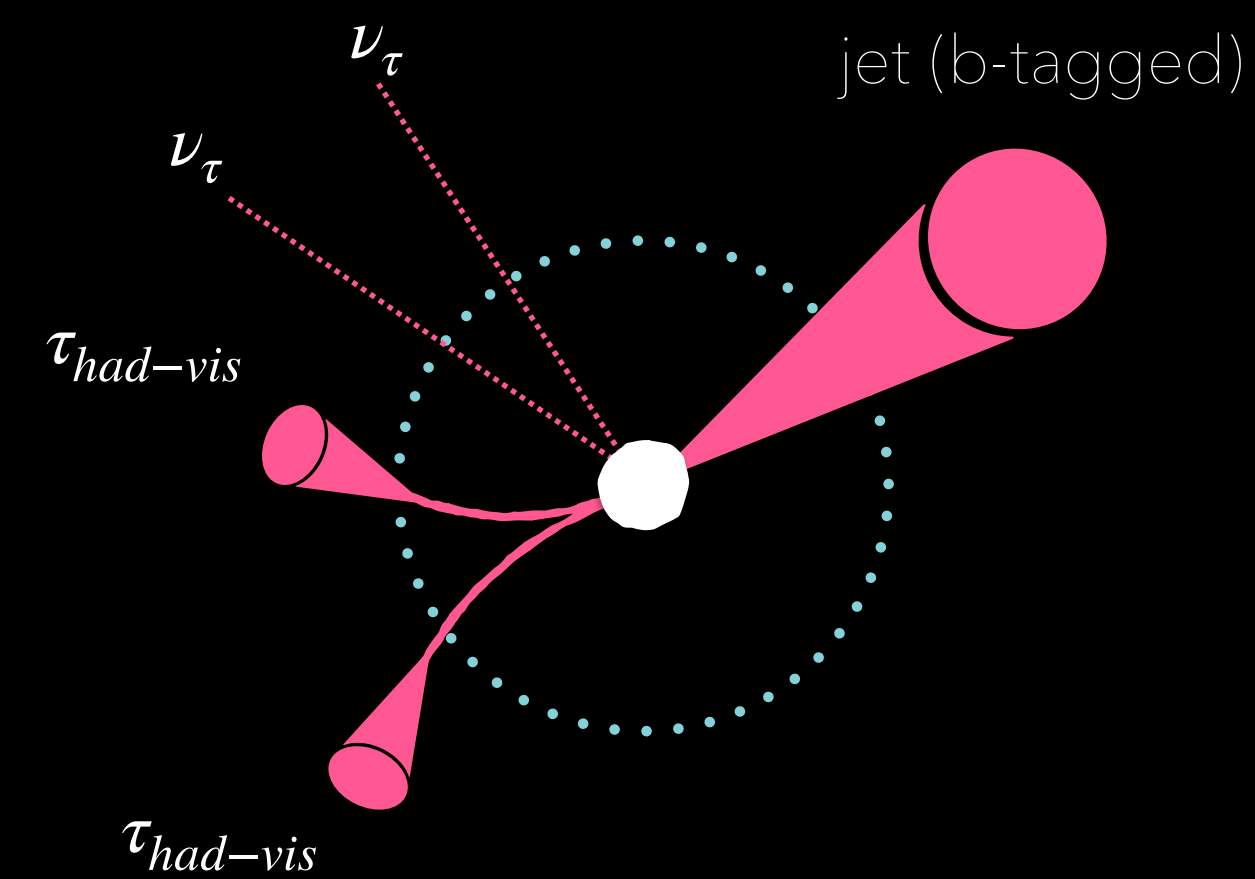
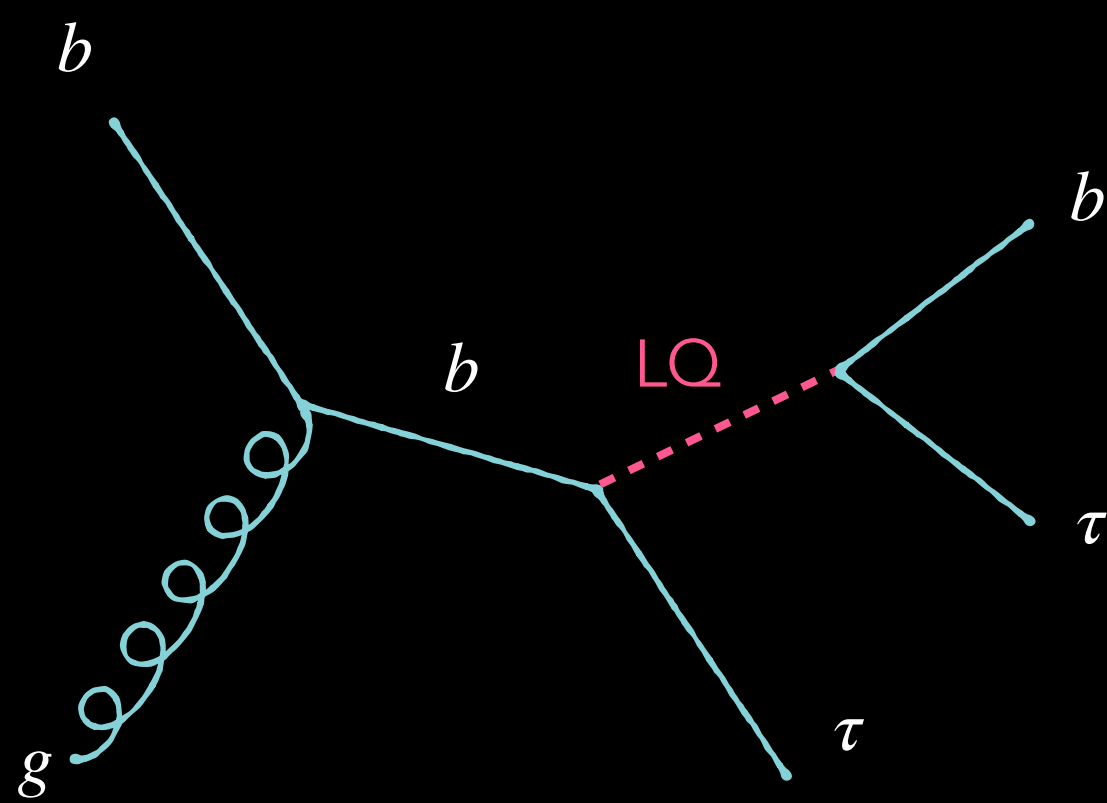
$\tau_{had}\tau_{had}$  channel



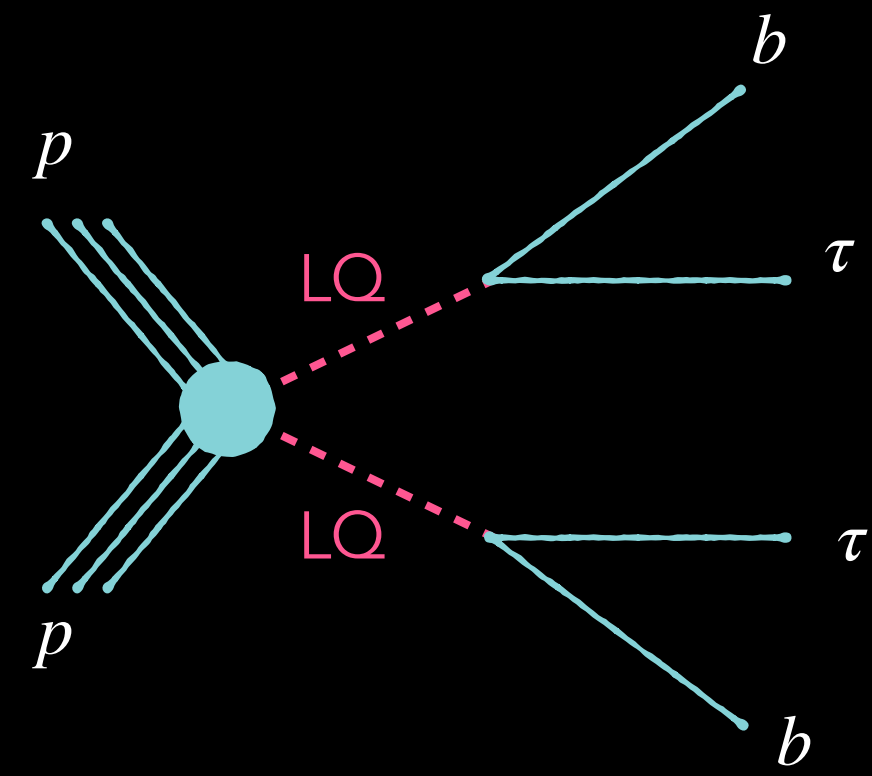
$\tau_{lep}\tau_{had}$  channel



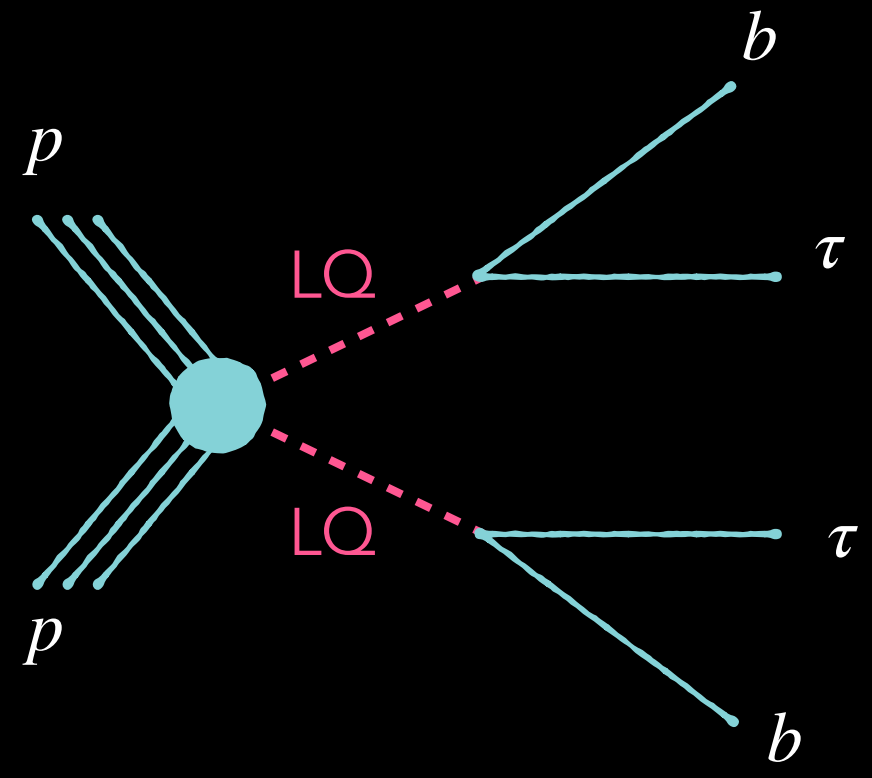
2)



1



# 1) LQ pair production analysis details



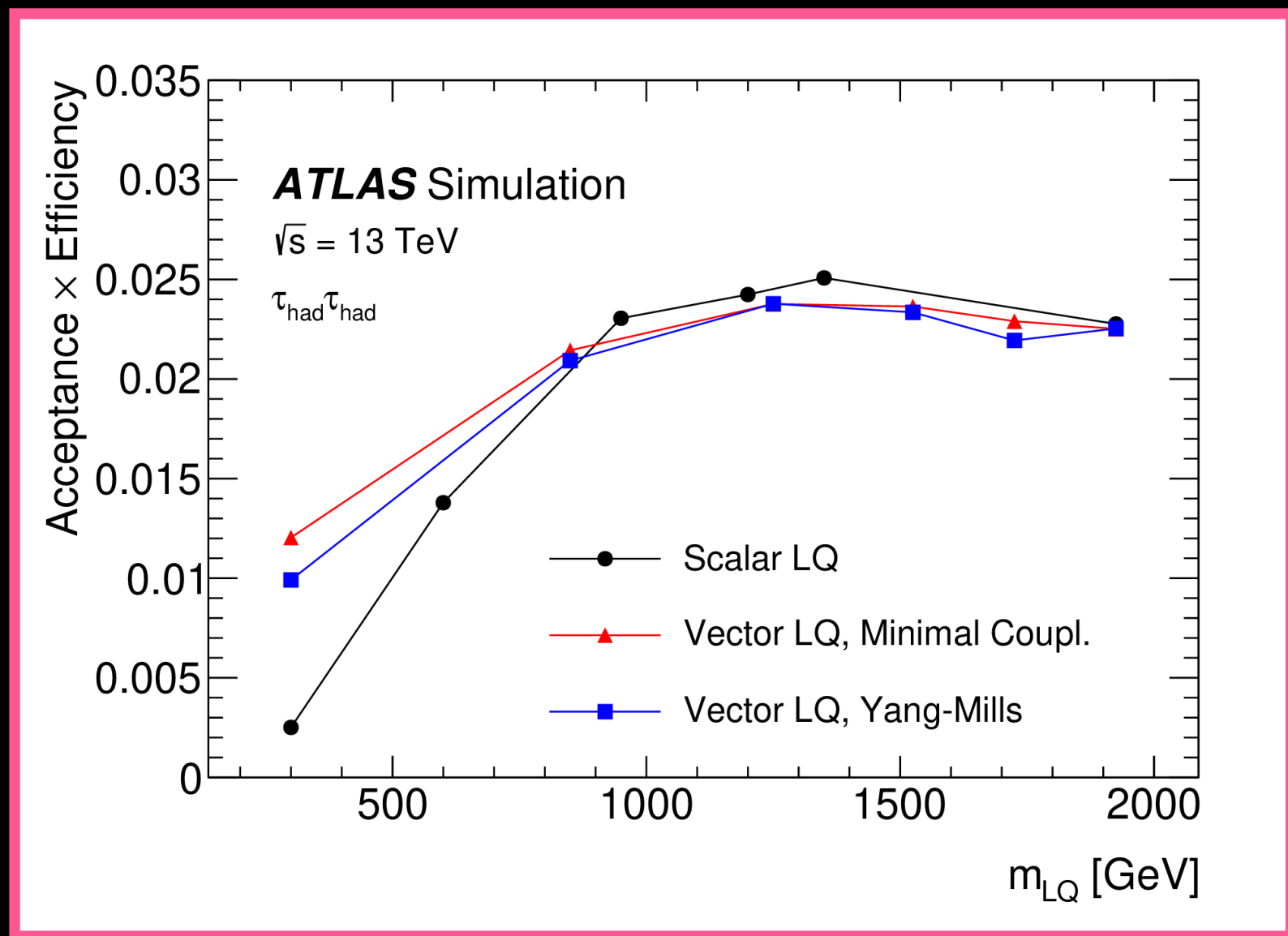
### Selection

	$\tau_{lep}\tau_{had}$ channel	$\tau_{had}\tau_{had}$ channel
$e/\mu$ selection	= 1 'signal' $e$ or $\mu$ $p_T^e > 25, 27$ GeV $p_T^\mu > 21, 27$ GeV	No 'veto' $e$ or $\mu$
$\tau_{had-vis}$ selection	= 1 $\tau_{had-vis}$ $p_T^\tau > 100$ GeV	= 2 $\tau_{had-vis}$ $p_T^\tau > 100, 140, 180$ (20) GeV
Jet selection	$\geq 2$ jets $p_T^{jet} > 45$ (20) GeV 1 or 2 $b$ -jets	
Additional selection	Opposite charge $e, \mu, \tau_{had}$ and $\tau_{had}$ $m_{\tau\tau}^{MMC} \notin 40 - 150$ GeV $E_T^{miss} > 100$ GeV $s_T > 600$ GeV	

### PNN input variables

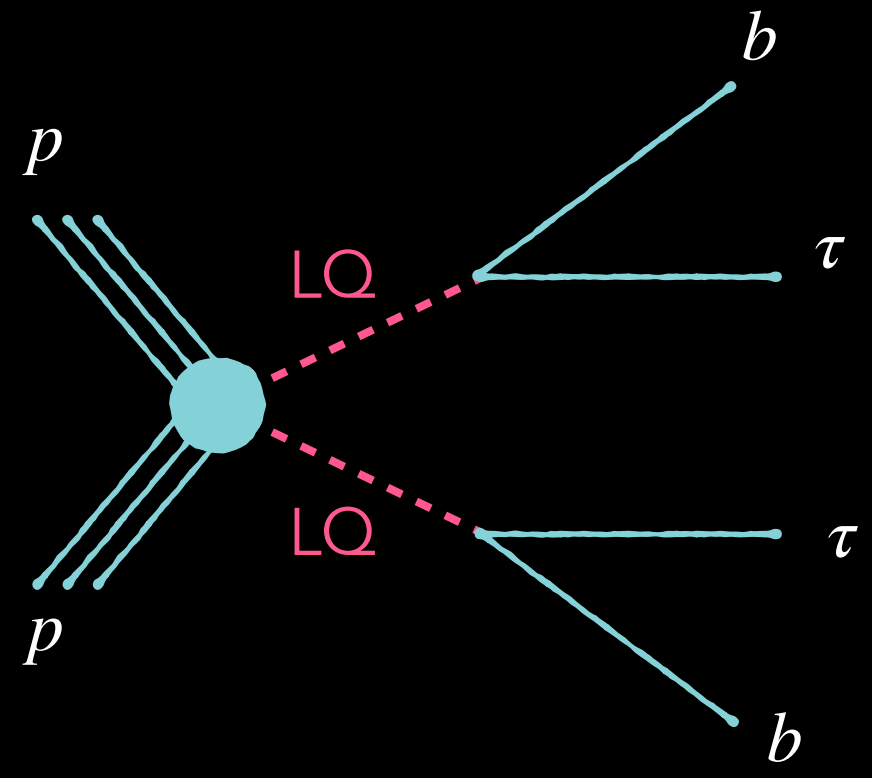
Variable	$\tau_{lep}\tau_{had}$ channel	$\tau_{had}\tau_{had}$ channel
$\tau_{had-vis} p_T^0$	✓	✓
$s_T$	✓	✓
$N_{b-jets}$	✓	✓
$m(\tau, jet)_{0,1}$		✓
$m(\ell, jet), m(\tau_{had}, jet)$	✓	
$\Delta R(\tau, jet)$	✓	✓
$\Delta\phi(\ell, E_T^{miss})$	✓	
$E_T^{miss} \phi$ centrality	✓	✓

PNN  
parameterised  
neural network  
in terms of  $m_{LQ}$



The search is optimised to probe high  $m_{LQ}$  values.

# 1) LQ pair production analysis details



### Selection

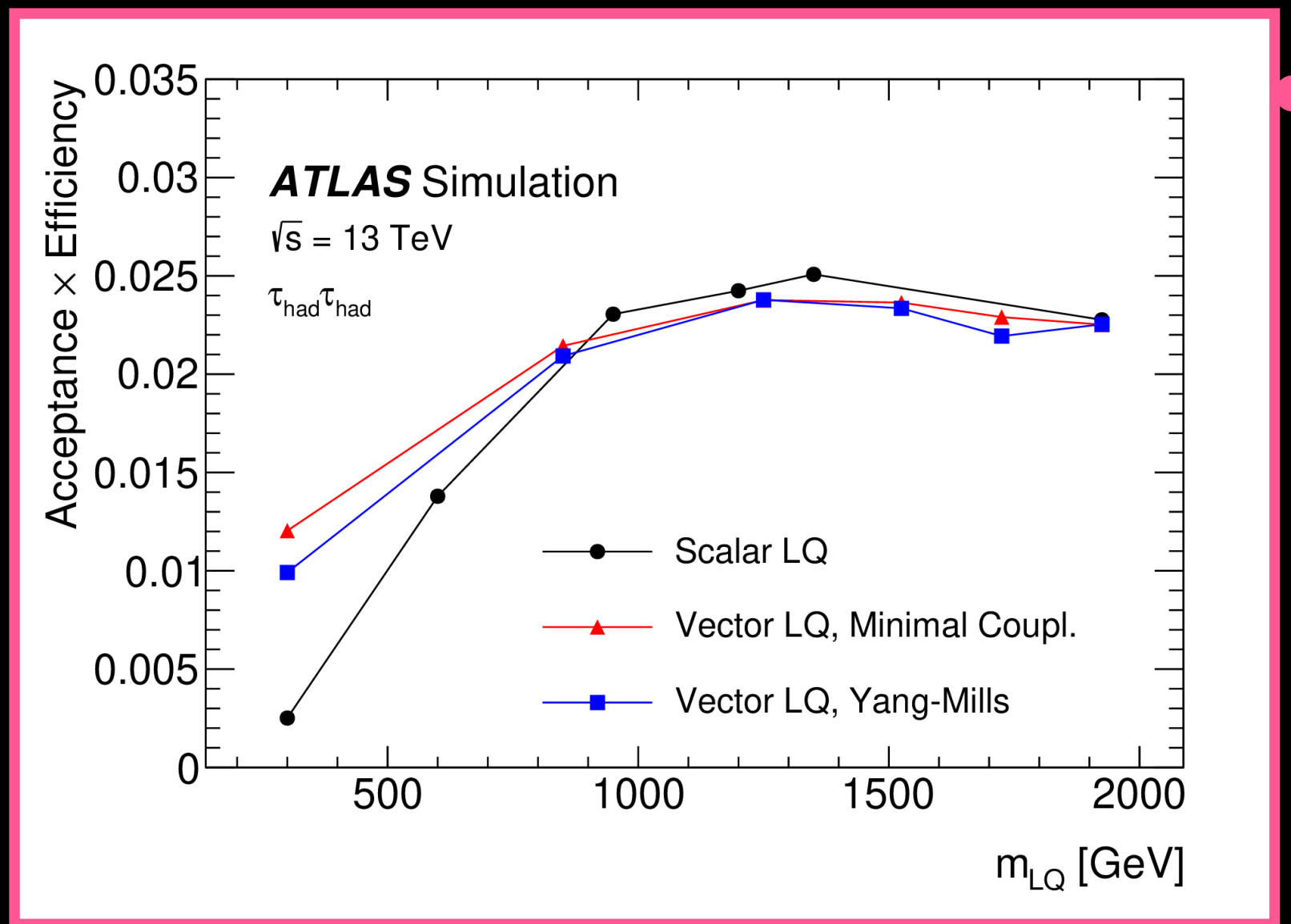
	$\tau_{lep}\tau_{had}$ channel	$\tau_{had}\tau_{had}$ channel
$e/\mu$ selection	= 1 'signal' $e$ or $\mu$ $p_T^e > 25, 27$ GeV $p_T^\mu > 21, 27$ GeV	No 'veto' $e$ or $\mu$
$\tau_{had-vis}$ selection	= 1 $\tau_{had-vis}$ $p_T^\tau > 100$ GeV	= 2 $\tau_{had-vis}$ $p_T^\tau > 100, 140, 180$ (20) GeV
Jet selection	$\geq 2$ jets $p_T^{jet} > 45$ (20) GeV 1 or 2 $b$ -jets	
Additional selection	Opposite charge $e, \mu, \tau_{had}$ and $\tau_{had}$ $m_{\tau\tau}^{MMC} \notin 40 - 150$ GeV $E_T^{miss} > 100$ GeV $s_T > 600$ GeV	

### PNN input variables

Variable	$\tau_{lep}\tau_{had}$ channel	$\tau_{had}\tau_{had}$ channel
$\tau_{had-vis} p_T^0$	✓	✓
$s_T$	✓	✓
$N_{b-jets}$	✓	✓
$m(\tau, jet)_{0,1}$		✓
$m(\ell, jet), m(\tau_{had}, jet)$	✓	
$\Delta R(\tau, jet)$	✓	✓
$\Delta\phi(\ell, E_T^{miss})$	✓	
$E_T^{miss} \phi$ centrality	✓	✓

PNN

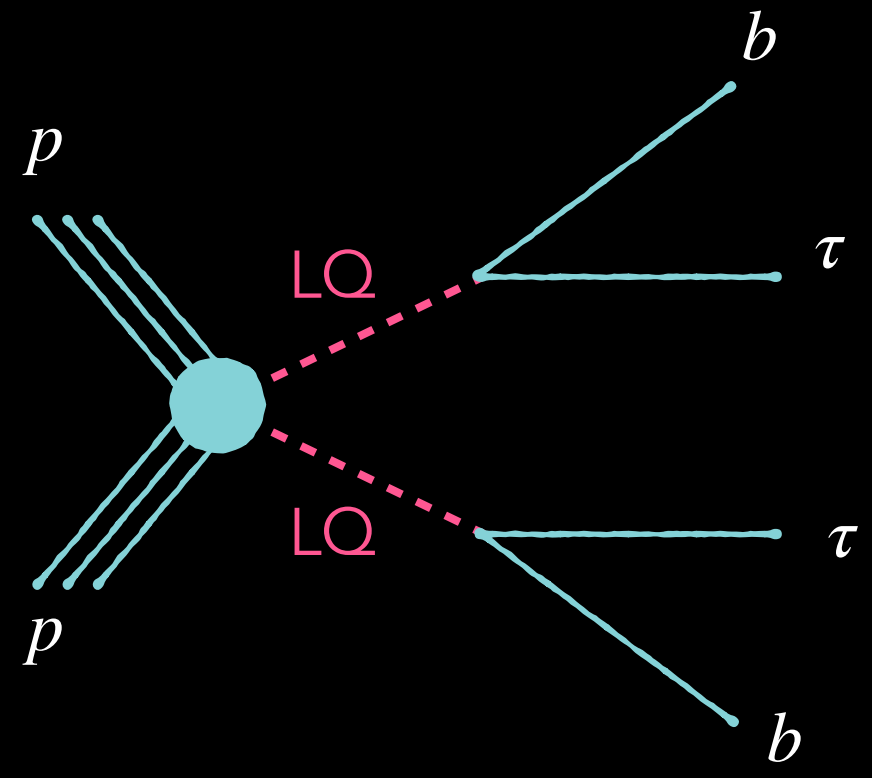
parameterised neural network in terms of  $m_{LQ}$



The search is optimised to probe high  $m_{LQ}$  values.



# 1) LQ pair production analysis details



### Selection

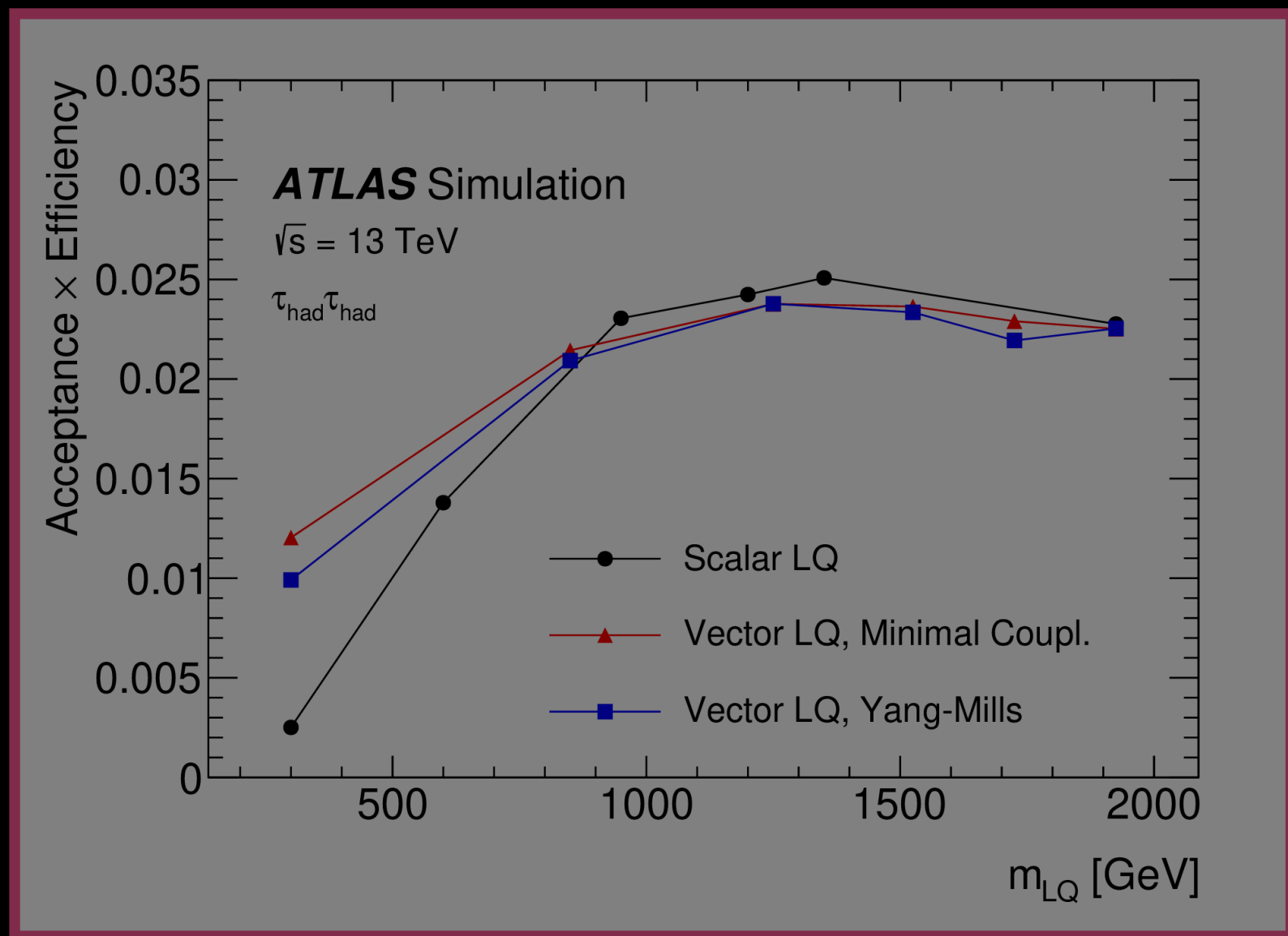
	$\tau_{lep}\tau_{had}$ channel	$\tau_{had}\tau_{had}$ channel
$e/\mu$ selection	= 1 'signal' $e$ or $\mu$ $p_T^e > 25, 27$ GeV $p_T^\mu > 21, 27$ GeV	No 'veto' $e$ or $\mu$
$\tau_{had-vis}$ selection	= 1 $\tau_{had-vis}$ $p_T^\tau > 100$ GeV	= 2 $\tau_{had-vis}$ $p_T^\tau > 100, 140, 180$ (20) GeV
Jet selection	$\geq 2$ jets $p_T^{jet} > 45$ (20) GeV 1 or 2 $b$ -jets	
Additional selection	Opposite charge $e, \mu, \tau_{had}$ and $\tau_{had}$ $m_{\tau\tau}^{MMC} \notin 40 - 150$ GeV $E_T^{miss} > 100$ GeV $s_T > 600$ GeV	

### PNN input variables

Variable	$\tau_{lep}\tau_{had}$ channel	$\tau_{had}\tau_{had}$ channel
$\tau_{had-vis} p_T^0$	✓	✓
$s_T$	✓	✓
$N_{b-jets}$	✓	✓
$m(\tau, jet)_{0,1}$		✓
$m(\ell, jet), m(\tau_{had}, jet)$	✓	✓
$\Delta R(\tau, jet)$	✓	✓
$\Delta\phi(\ell, E_T^{miss})$	✓	✓
$E_T^{miss} \phi$ centrality	✓	✓

PNN

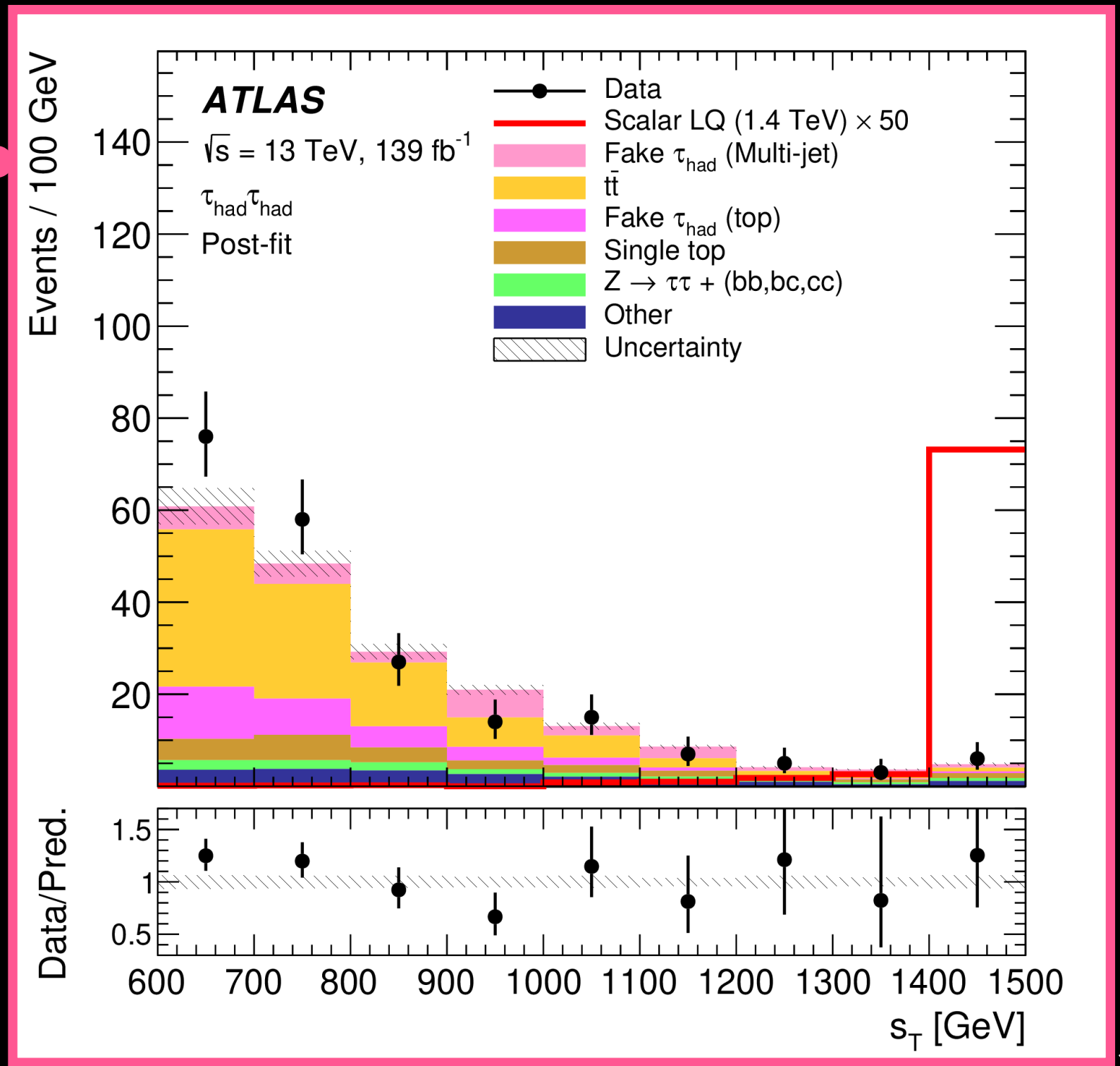
parameterised neural network in terms of  $m_{LQ}$



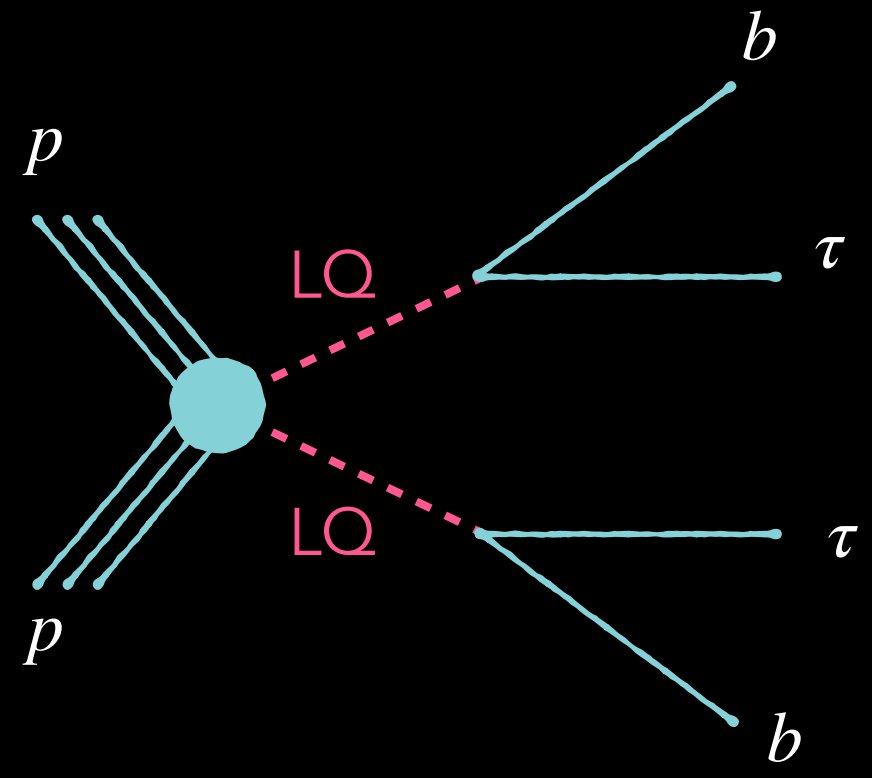
The search is optimised to probe high  $m_{LQ}$  values.

Here  $s_T$  is the scalar sum of transverse momenta ((light lepton) +  $\tau_{had-vis}$  + two leading jets +  $E_T^{miss}$ ).

$s_T$  is a powerful discriminator and is used in both channels.



# 1) LQ pair production analysis details



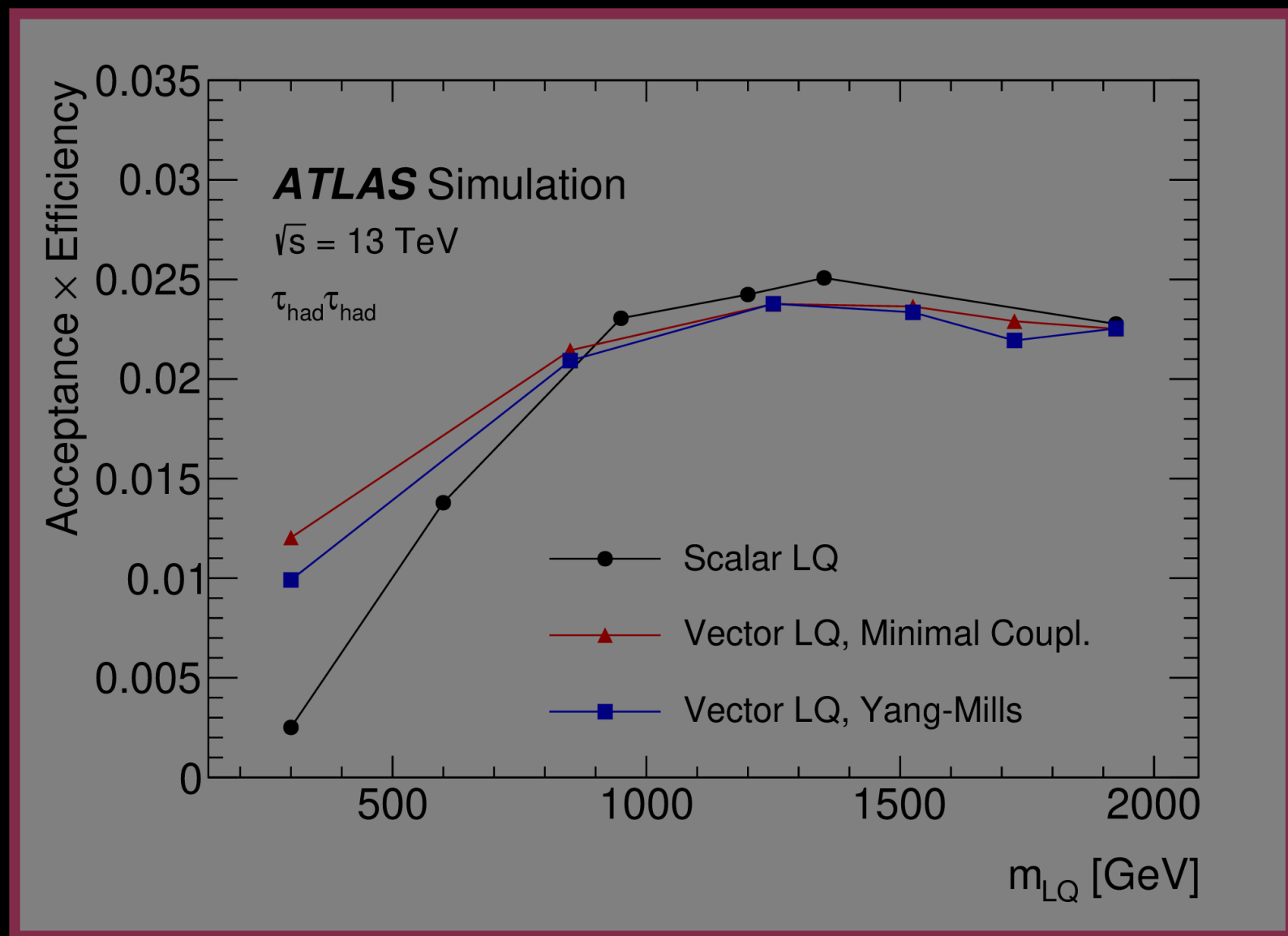
### Selection

	$\tau_{lep}\tau_{had}$ channel	$\tau_{had}\tau_{had}$ channel
$e/\mu$ selection	= 1 'signal' $e$ or $\mu$ $p_T^e > 25, 27$ GeV $p_T^\mu > 21, 27$ GeV	No 'veto' $e$ or $\mu$
$\tau_{had-vis}$ selection	= 1 $\tau_{had-vis}$ $p_T^\tau > 100$ GeV	= 2 $\tau_{had-vis}$ $p_T^\tau > 100, 140, 180$ (20) GeV
Jet selection	$\geq 2$ jets $p_T^{jet} > 45$ (20) GeV 1 or 2 $b$ -jets	
Additional selection	Opposite charge $e, \mu, \tau_{had}$ and $\tau_{had}$ $m_{\tau\tau}^{MMC} \notin 40 - 150$ GeV $E_T^{miss} > 100$ GeV $s_T > 600$ GeV	

### PNN input variables

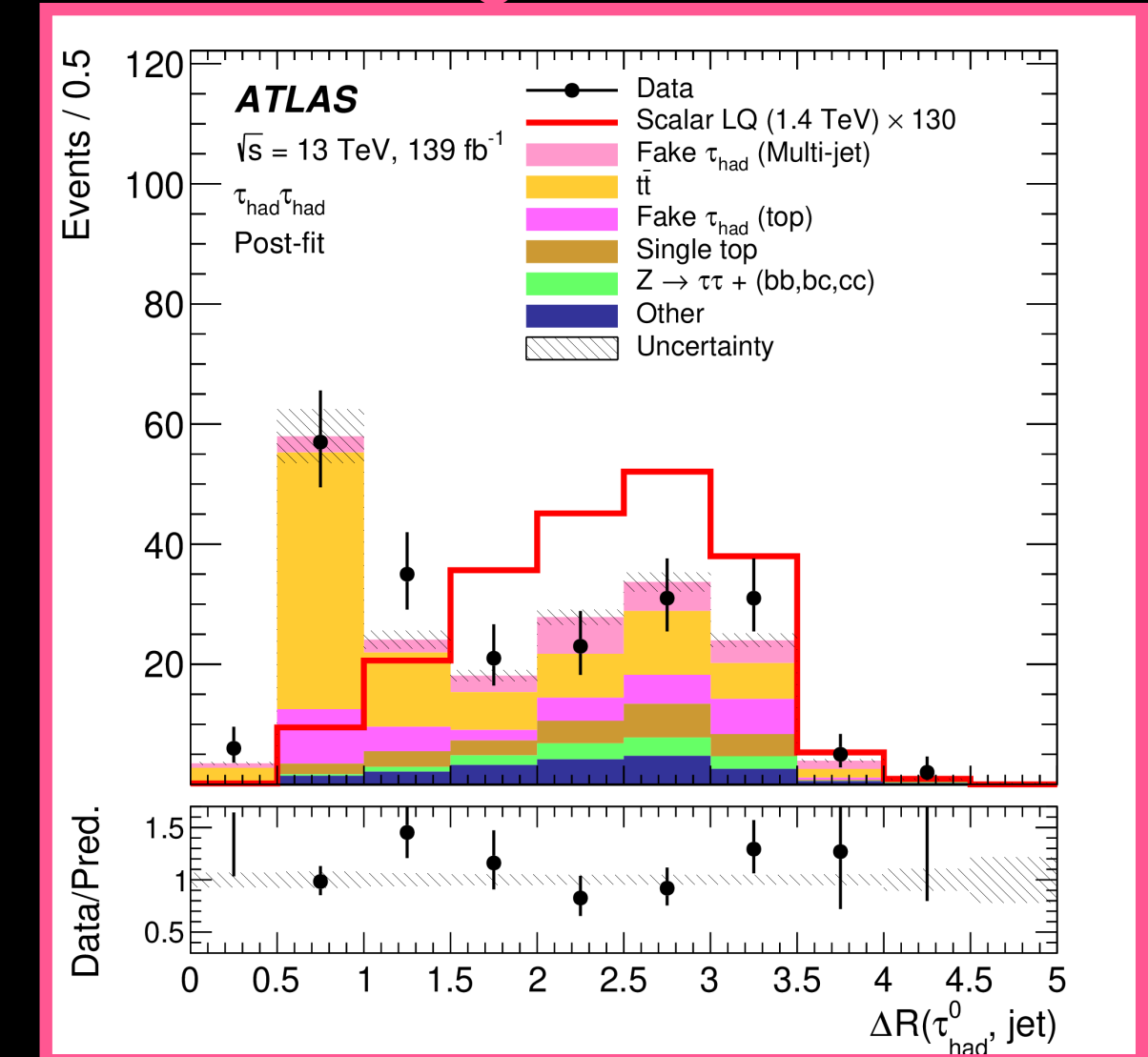
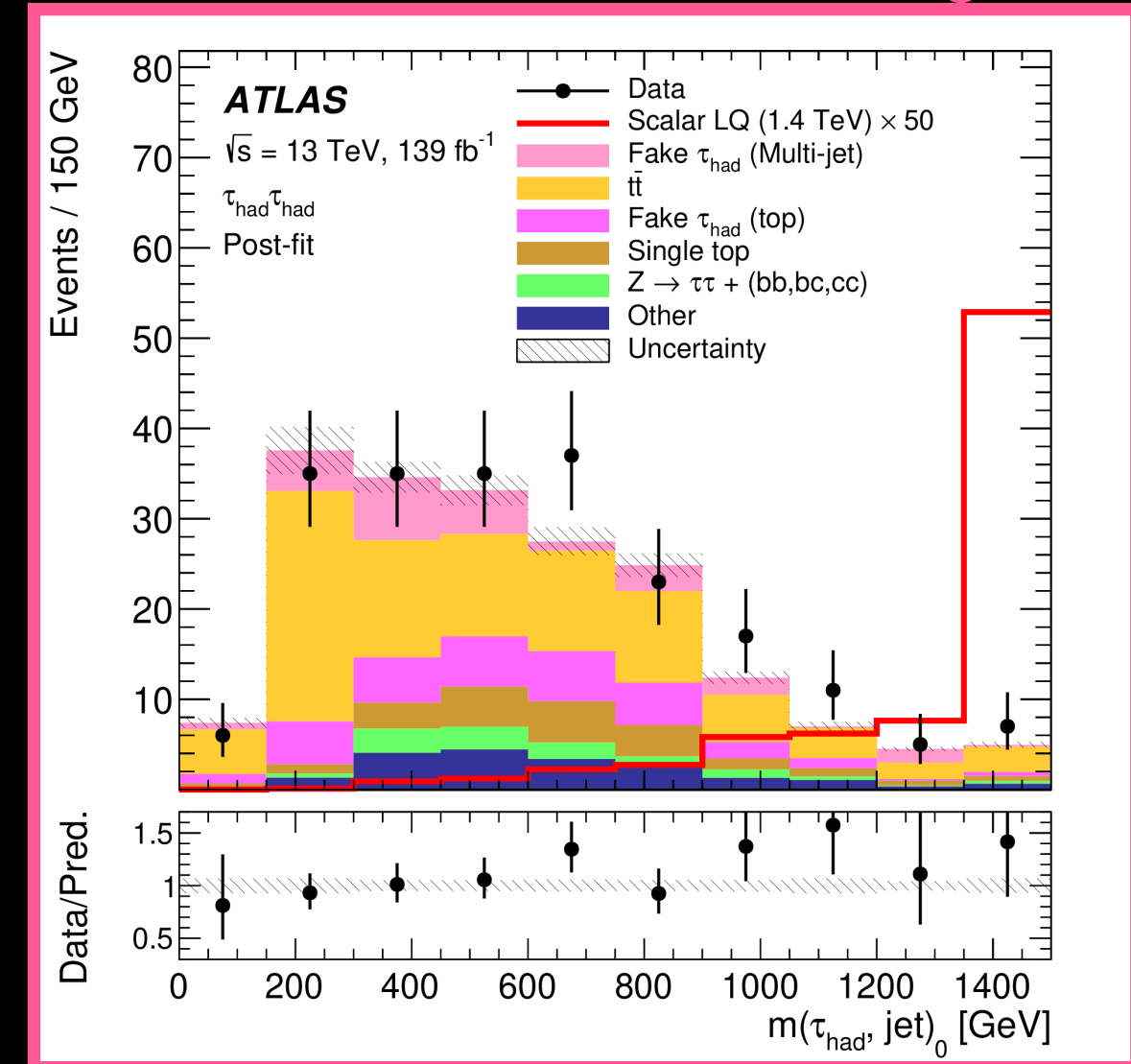
Variable	$\tau_{lep}\tau_{had}$ channel	$\tau_{had}\tau_{had}$ channel
$\tau_{had-vis} p_T^0$	✓	✓
$s_T$	✓	✓
$N_{b-jets}$	✓	✓
$m(\tau, jet)_{0,1}$		✓
$m(\ell, jet), m(\tau_{had}, jet)$	✓	
$\Delta R(\tau, jet)$	✓	✓
$\Delta\phi(\ell, E_T^{miss})$	✓	
$E_T^{miss} \phi$ centrality	✓	✓

PNN  
parameterised  
neural network  
in terms of  $m_{LQ}$



The search is optimised to probe high  $m_{LQ}$  values.

Invariant mass of  $\tau_{had-vis}$  and leading jet.

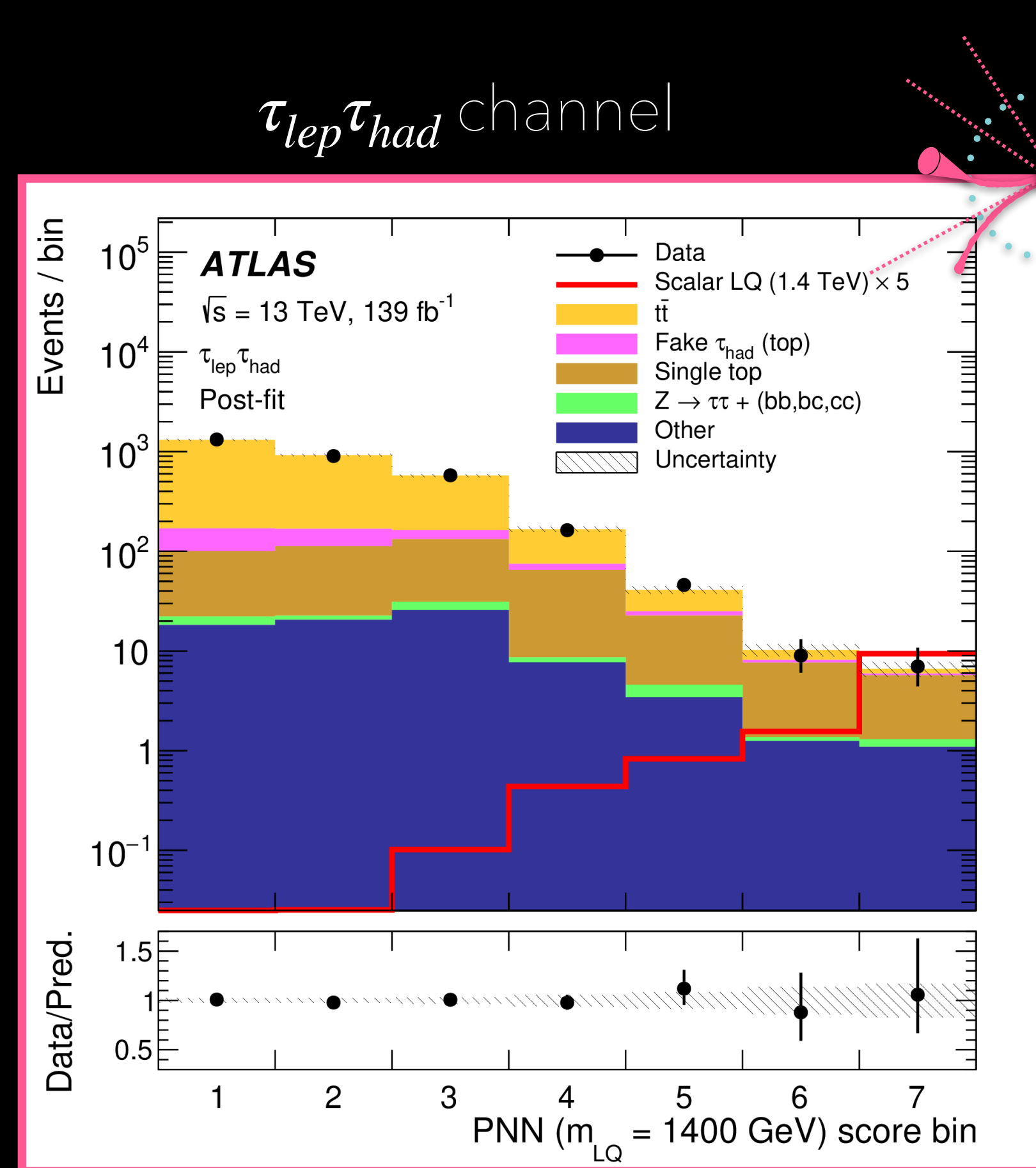
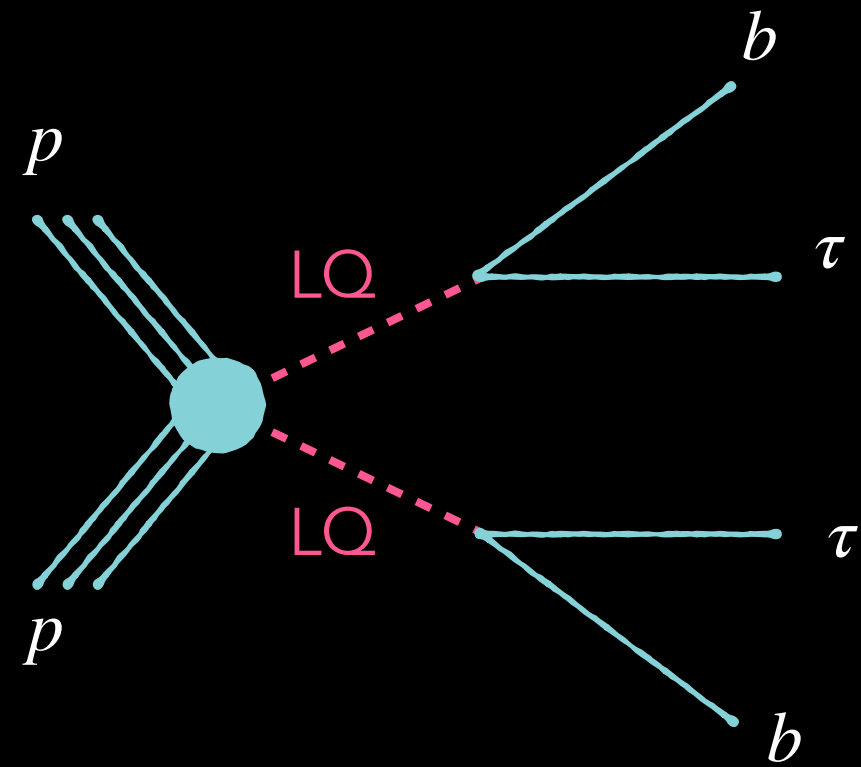


$\Delta R$  between leading  $\tau_{had-vis}$  and mass paired jet.

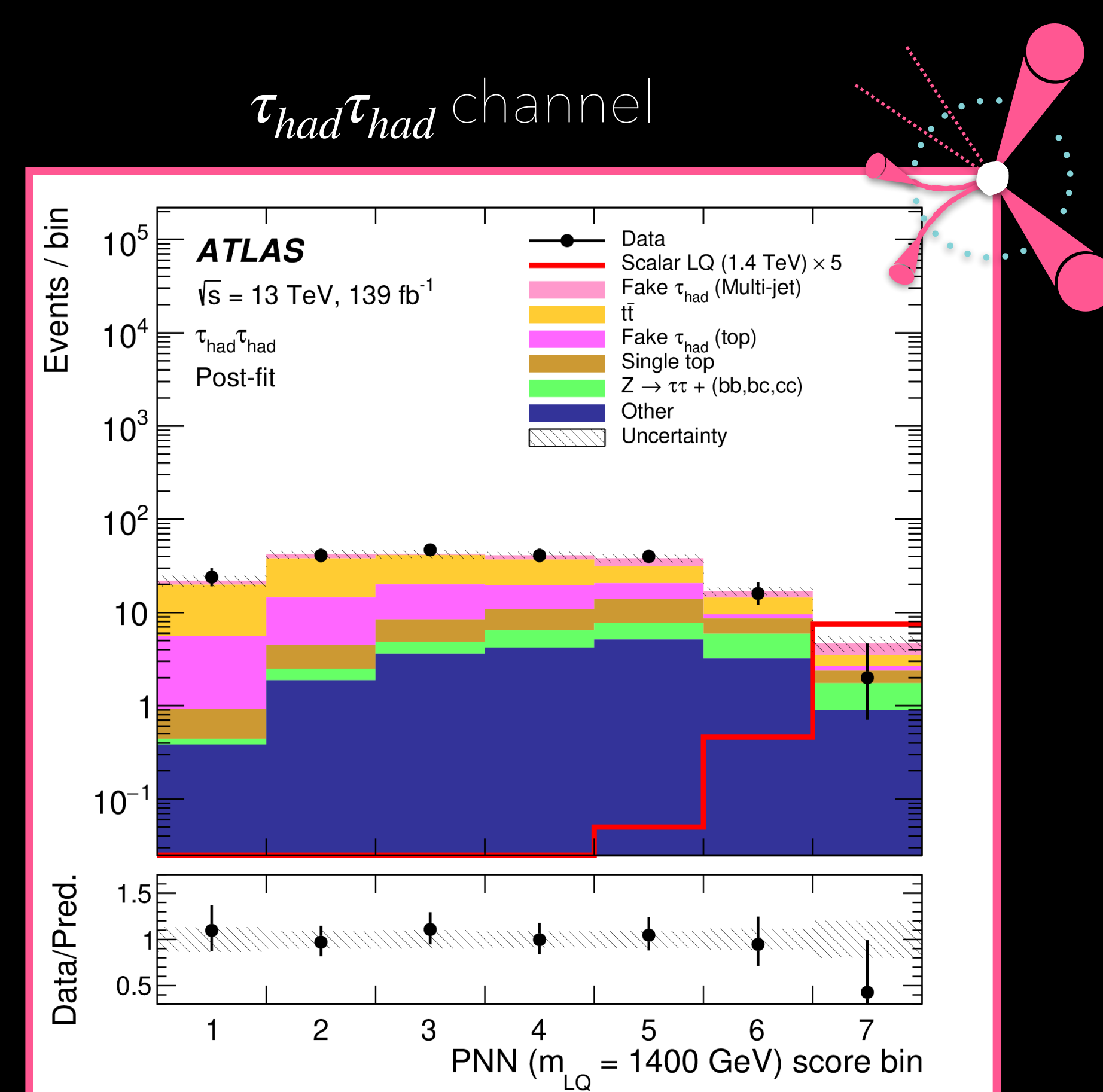
## 1) Final PNN scores

-> PNN binning is optimised for each LQ mass point.

-> A simultaneous binned maximum-likelihood fit is performed on the PNN score distributions for each LQ hypothesis.



At high values of the PNN score, top backgrounds dominate in the  $\tau_{lep}\tau_{had}$  channel.

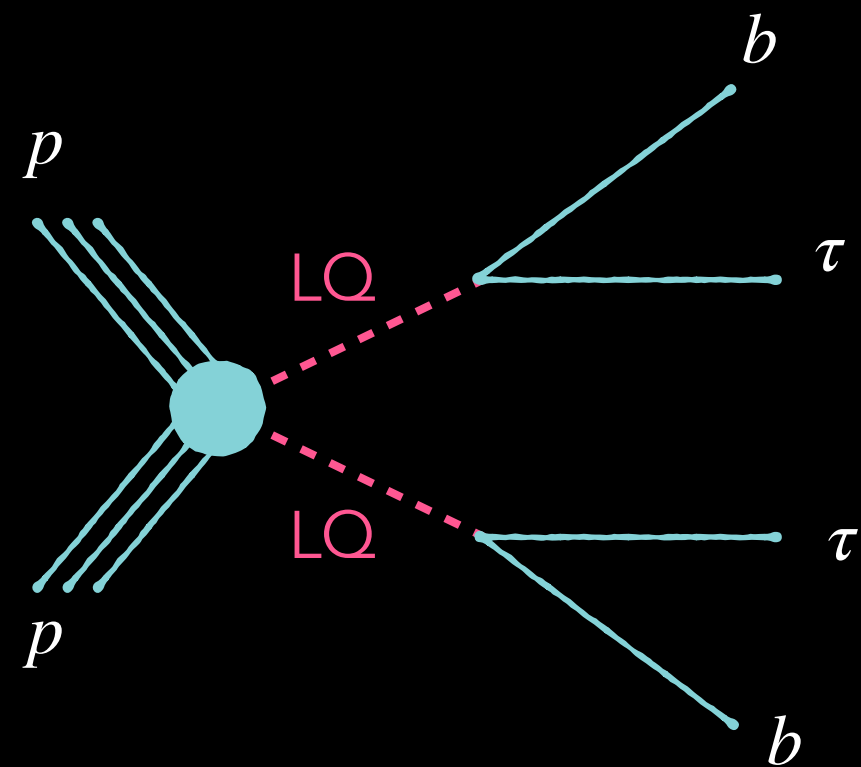


Slight deficit of data relative to the background prediction in the highest PNN score bin for the  $\tau_{had}\tau_{had}$  channel.



# 1) Results

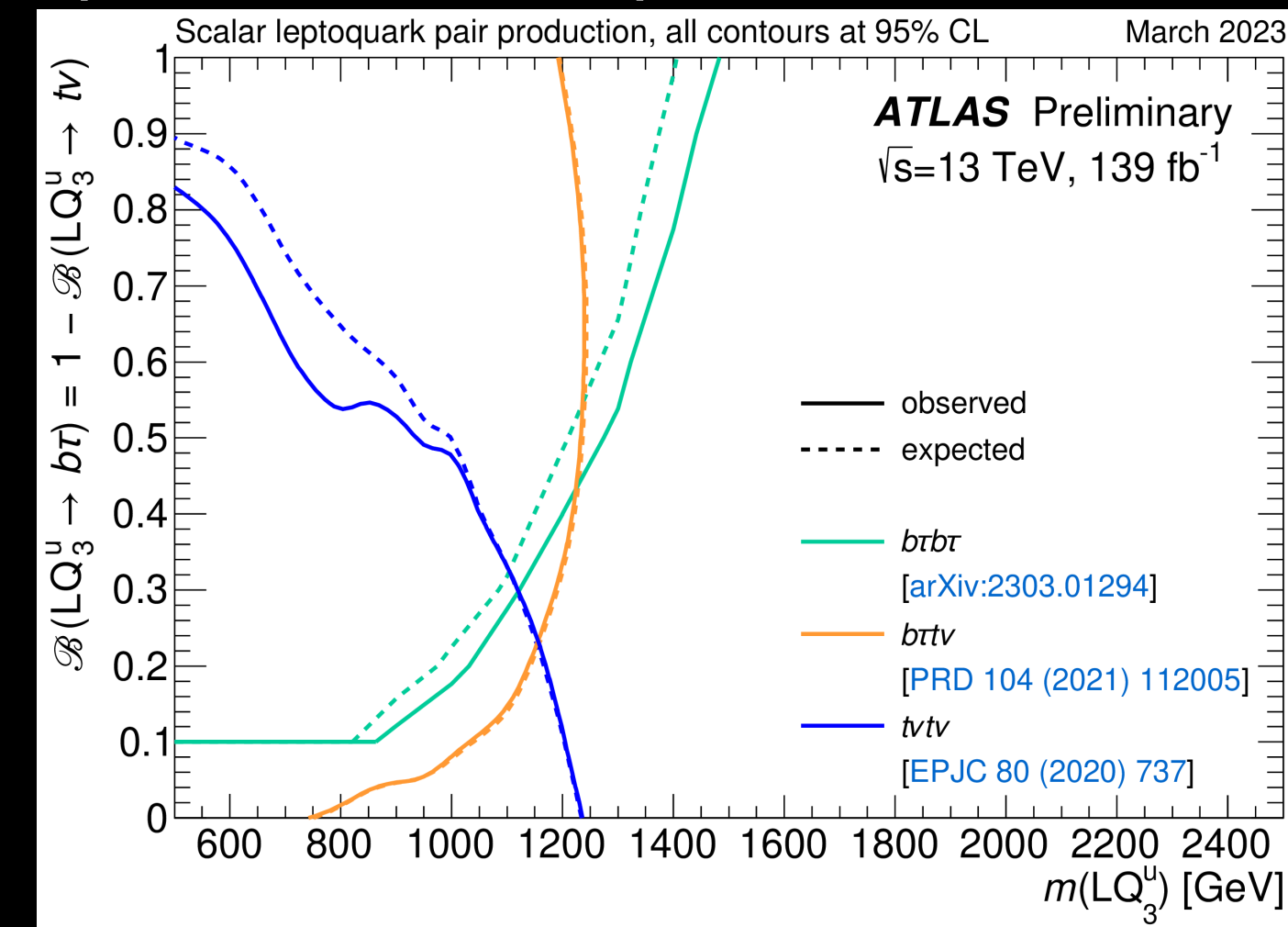
no significant excess above the SM prediction is observed



-> The improvement in the observed limit compared with the expectation is driven by the data deficit in the highest PNN bin for the  $\tau_{had}\tau_{had}$  channel.

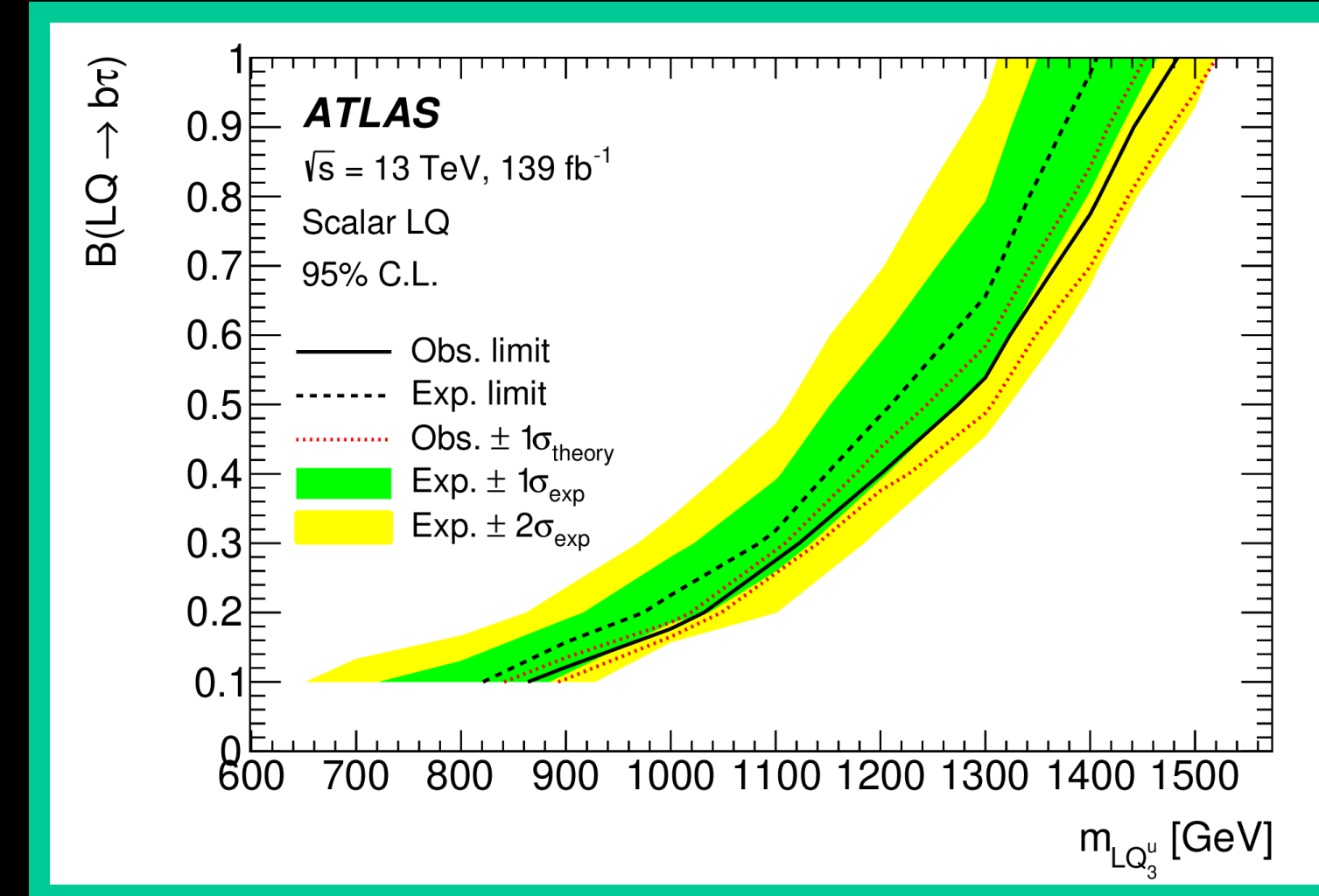
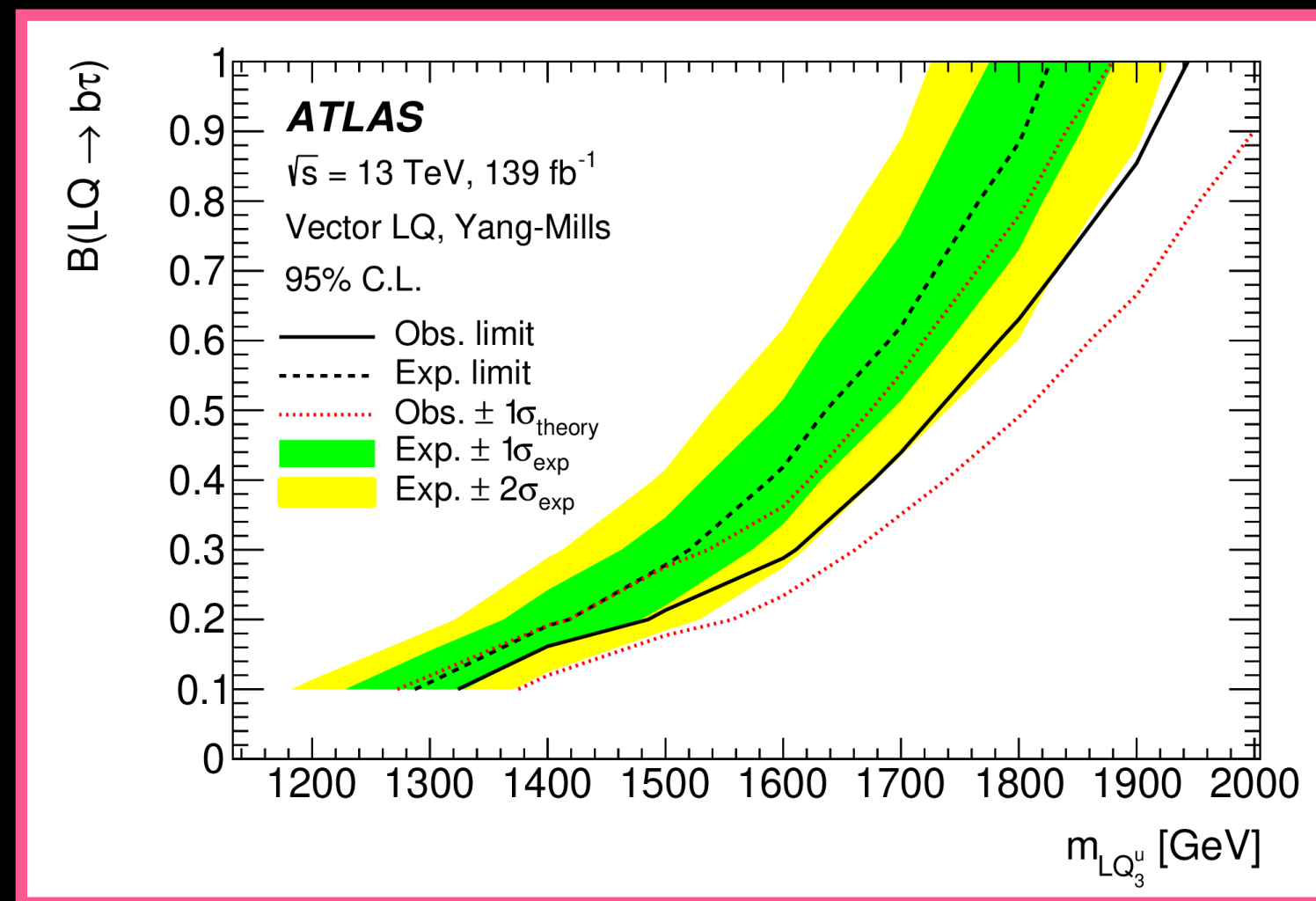
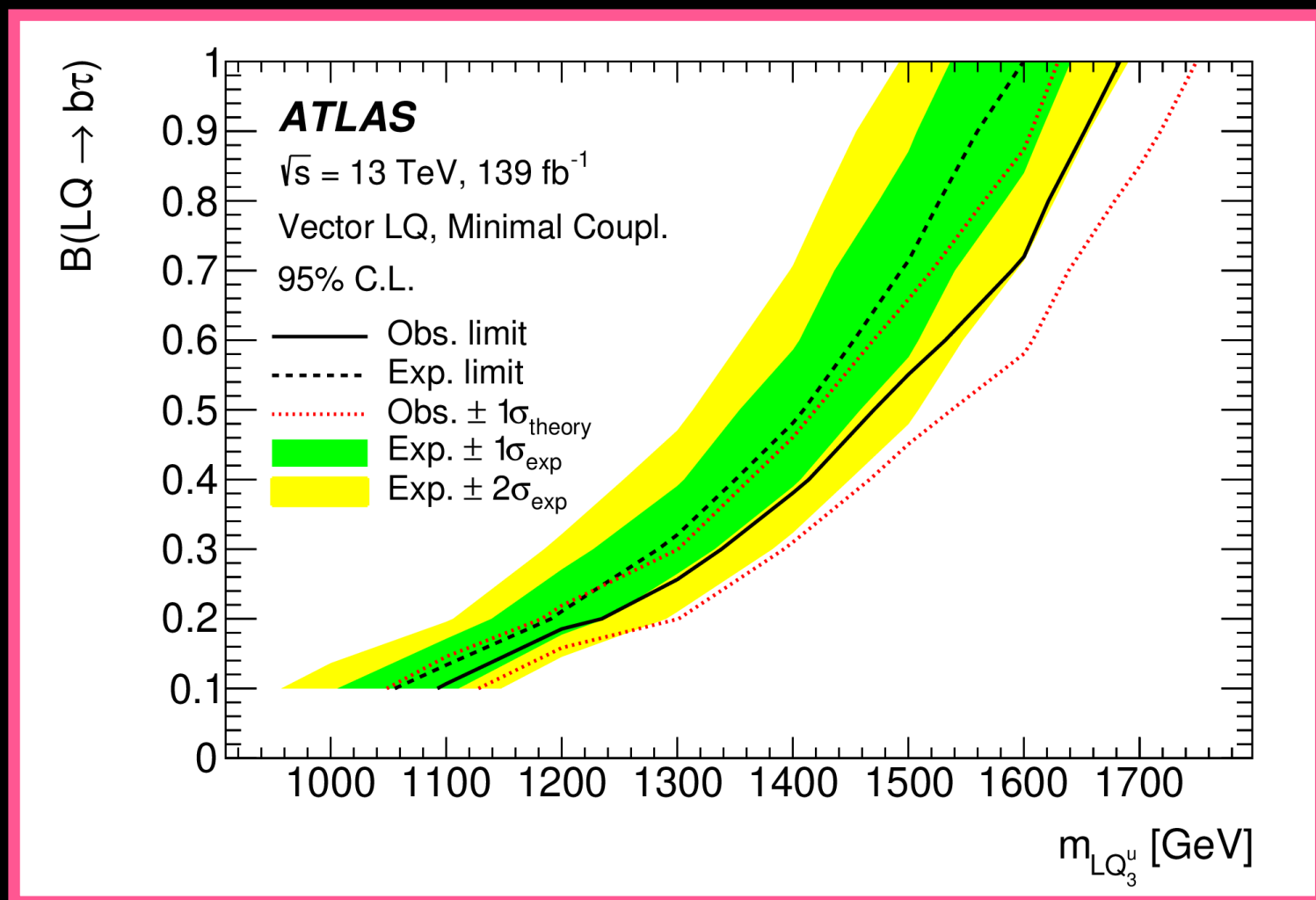
+ larger at high  $m_{LQ}$  because the signal becomes more localised at a high PNN score.

[ATL-PHYS-PUB-2023-006]



-> Extend the full Run 2 ATLAS reach for third-generation up-type LQs by around 200 GeV in all three models compared with the LQ LQ  $\rightarrow t\nu t\nu$  decay mode (see summary plot).

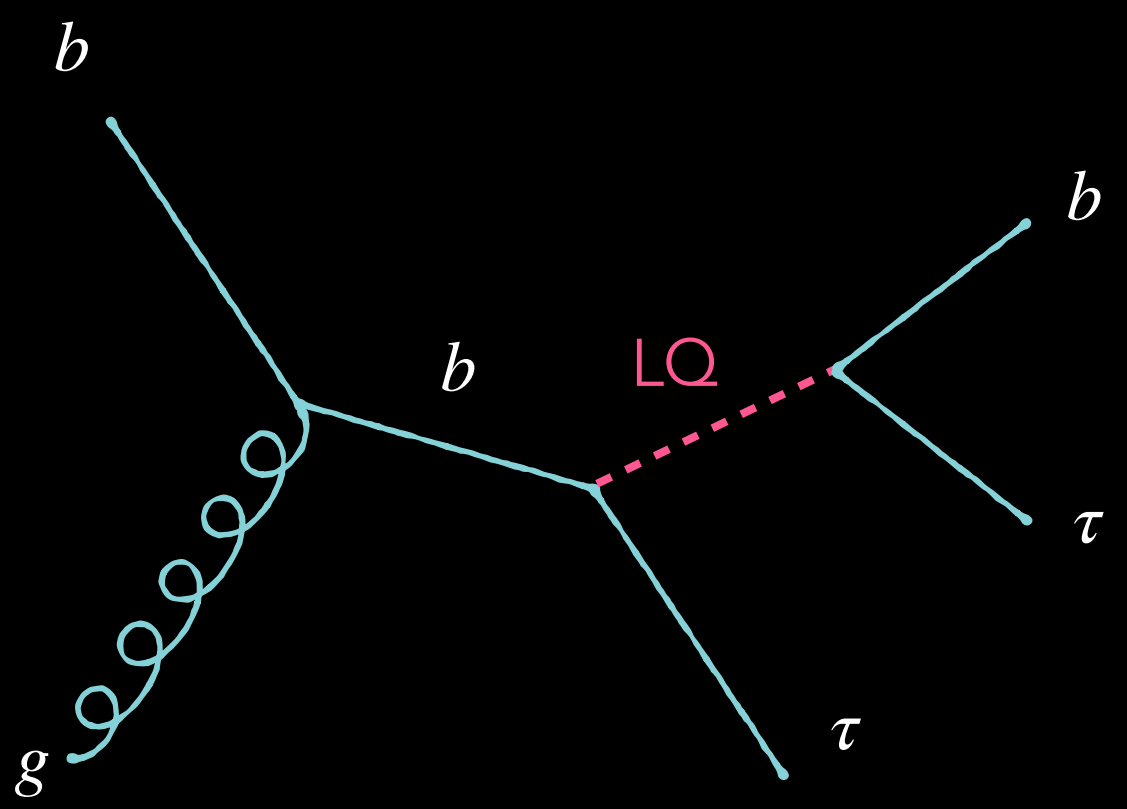
-> Improvement of 450 GeV compared to 36 fb<sup>-1</sup> result.







# 2) Singly produced LQs analysis details



## Selection

$\tau_{lep}\tau_{had}$

Signal Regions	Selection
Preselection	$\ell$ (trigger, isolated), $\tau_{had-vis}$ (medium $\tau_{had-ID}$ ), $q(\ell) \times q(\tau_{had-vis}) < 0$ , $\Delta\phi(\ell, E_T^{miss}) < 1.5$ , $m_{vis}(\ell, \tau_{had-vis}) > 100$ GeV, $S_T > 300$ GeV, <b>at least one <math>b</math>-jet</b>
High $b$ -jet $p_T$ SR	Leading $b$ -jet $p_T > 200$ GeV

$\tau_{had}\tau_{had}$

Signal Regions	Selection
Preselection	$\tau_{had,1}$ (trigger, medium $\tau_{had-ID}$ ), $\tau_2$ (loose $\tau_{had-ID}$ ), $q(\tau_1) \times q(\tau_2) < 0$ , $m_{vis}(\tau_1, \tau_2) > 100$ GeV, $S_T > 300$ GeV, <b>at least one <math>b</math>-jet</b>
High $b$ -jet $p_T$ SR	Leading $b$ -jet $p_T > 200$ GeV

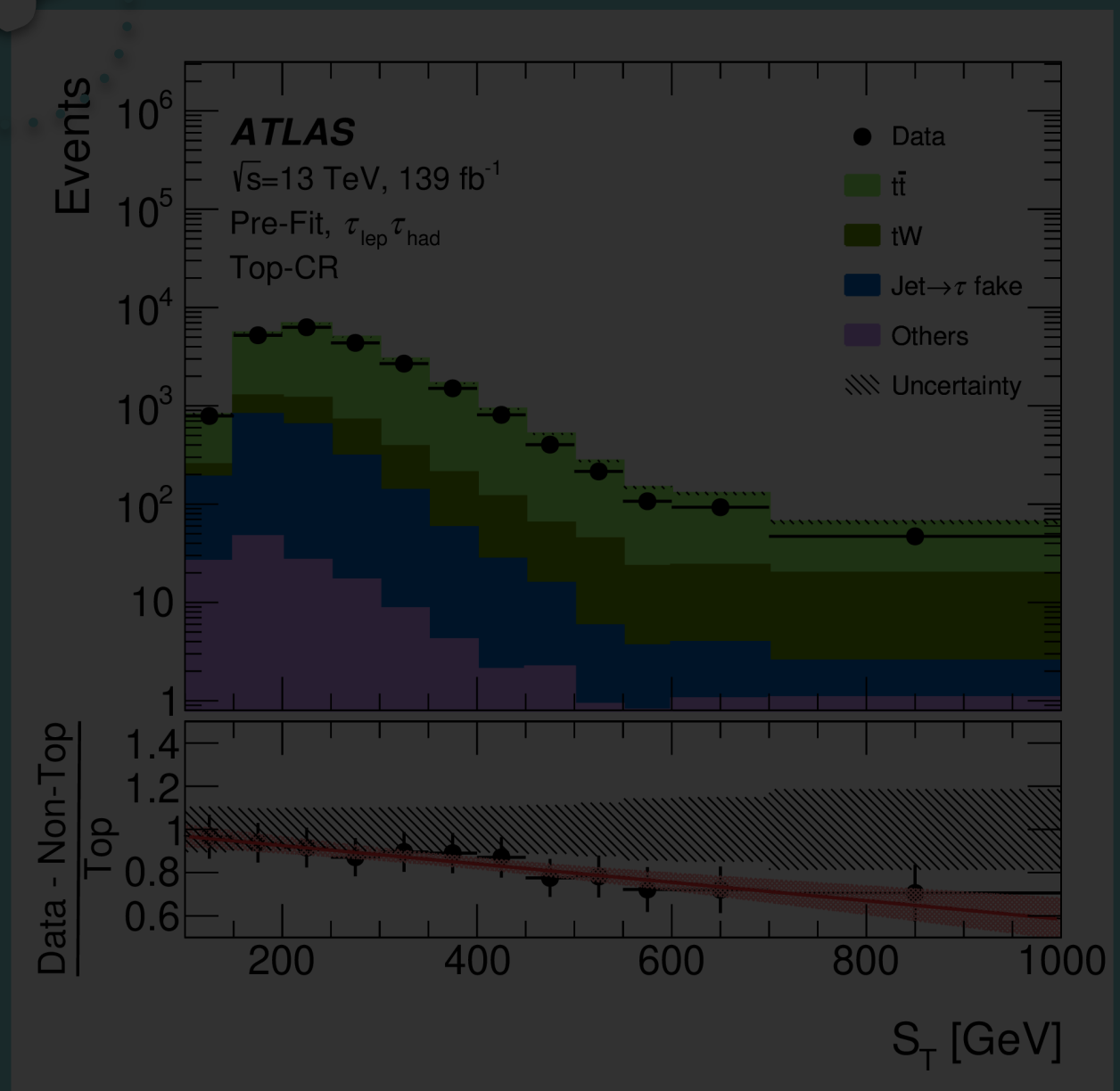
\*tables shortened, full list of CR selections in [arXiv:2305.15962]

## Top-CR

Satisfy SR except

- $\Delta\phi(\ell, E_T^{miss}) > 2.5$
- no  $S_T$  and leading  $b$ -jet  $p_T$  requirement

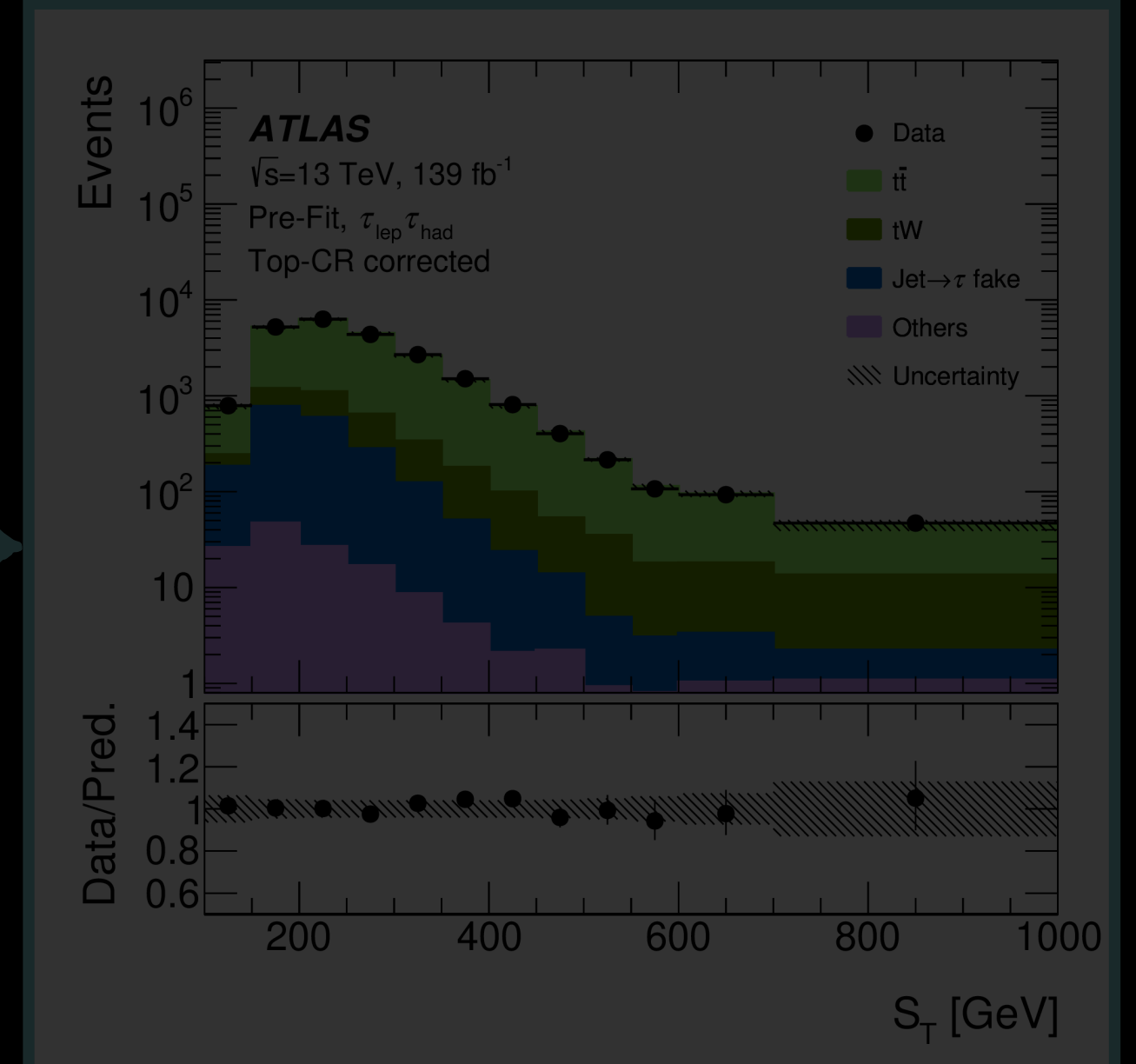
-> Ensure the background is accurately modelled



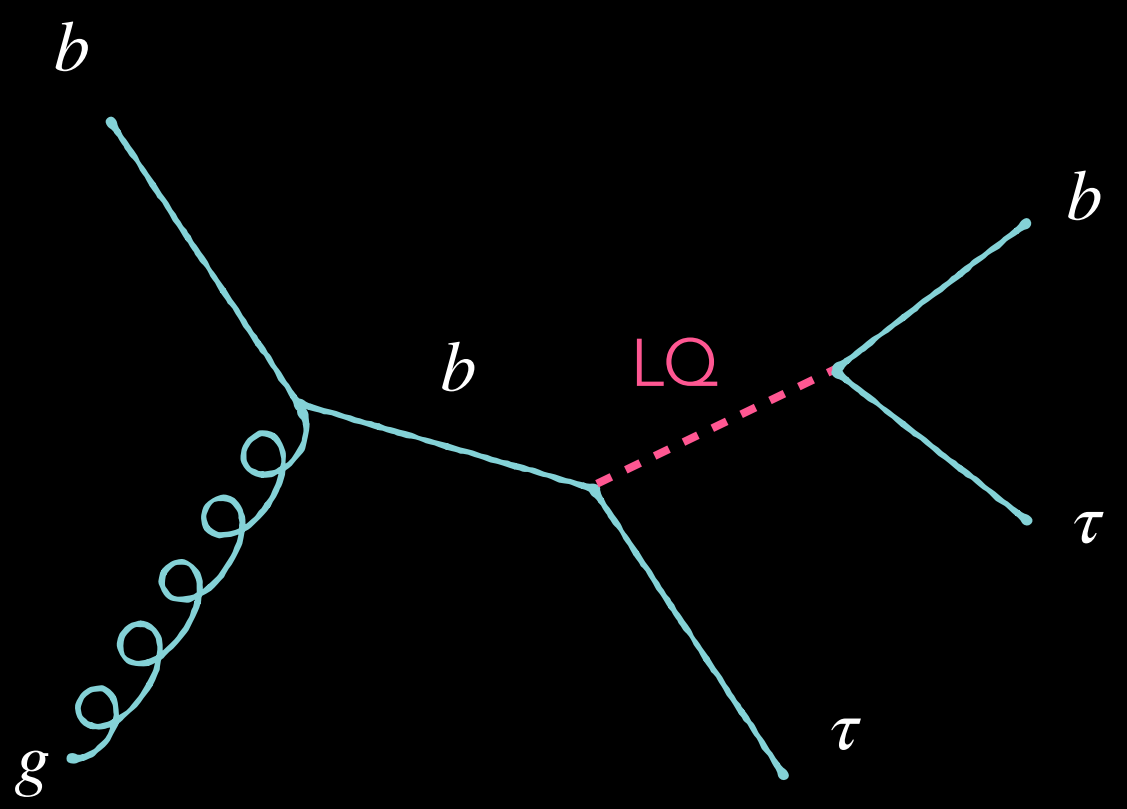
Current simulations of  $t\bar{t}$  processes overestimate the upper tail of the top-quark  $p_T$  spectrum. [1908.0735]

apply correction

$$SF_{Top}(S_T) = \frac{(N_{data} - N_{non-Top})(S_T)}{N_{Top}(S_T)}$$



# 2) Singly produced LQs analysis details



## Selection

$\tau_{lep}\tau_{had}$

Signal Regions	Selection
Preselection	$\ell$ (trigger, isolated), $\tau_{had-vis}$ (medium $\tau_{had-ID}$ ), $q(\ell) \times q(\tau_{had-vis}) < 0$ , $\Delta\phi(\ell, E_T^{miss}) < 1.5$ , $m_{vis}(\ell, \tau_{had-vis}) > 100$ GeV, $S_T > 300$ GeV, <b>at least one <math>b</math>-jet</b>
High $b$ -jet $p_T$ SR	Leading $b$ -jet $p_T > 200$ GeV

$\tau_{had}\tau_{had}$

Signal Regions	Selection
Preselection	$\tau_{had,1}$ (trigger, medium $\tau_{had-ID}$ ), $\tau_2$ (loose $\tau_{had-ID}$ ), $q(\tau_1) \times q(\tau_2) < 0$ , $m_{vis}(\tau_1, \tau_2) > 100$ GeV, $S_T > 300$ GeV, <b>at least one <math>b</math>-jet</b>
High $b$ -jet $p_T$ SR	Leading $b$ -jet $p_T > 200$ GeV

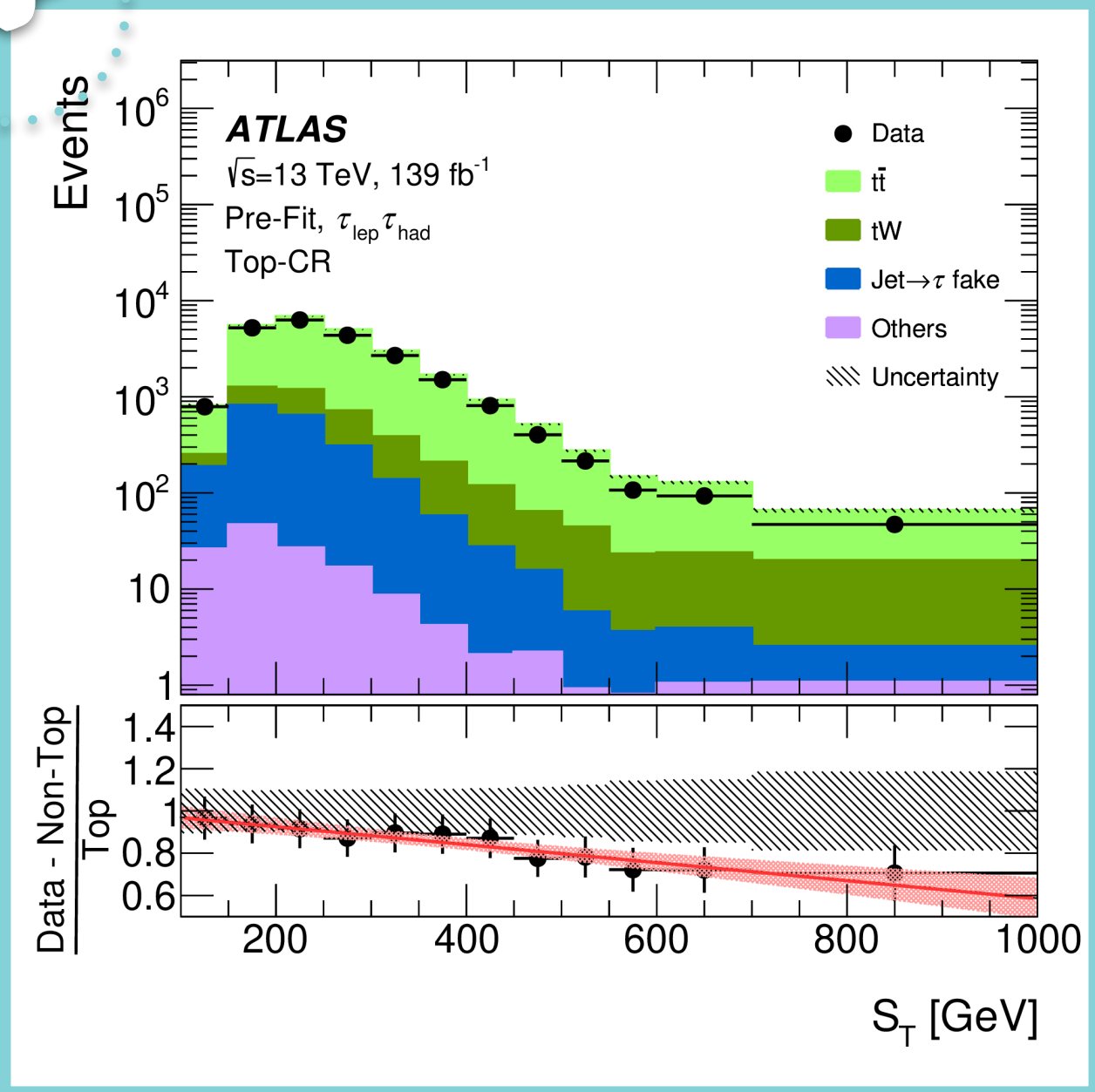
\*tables shortened, full list of CR selections in [arXiv:2305.15962]

## Top-CR

Satisfy SR except

- ⊙  $\Delta\phi(\ell, E_T^{miss}) > 2.5$
- ⊙ no  $S_T$  and leading  $b$ -jet  $p_T$  requirement

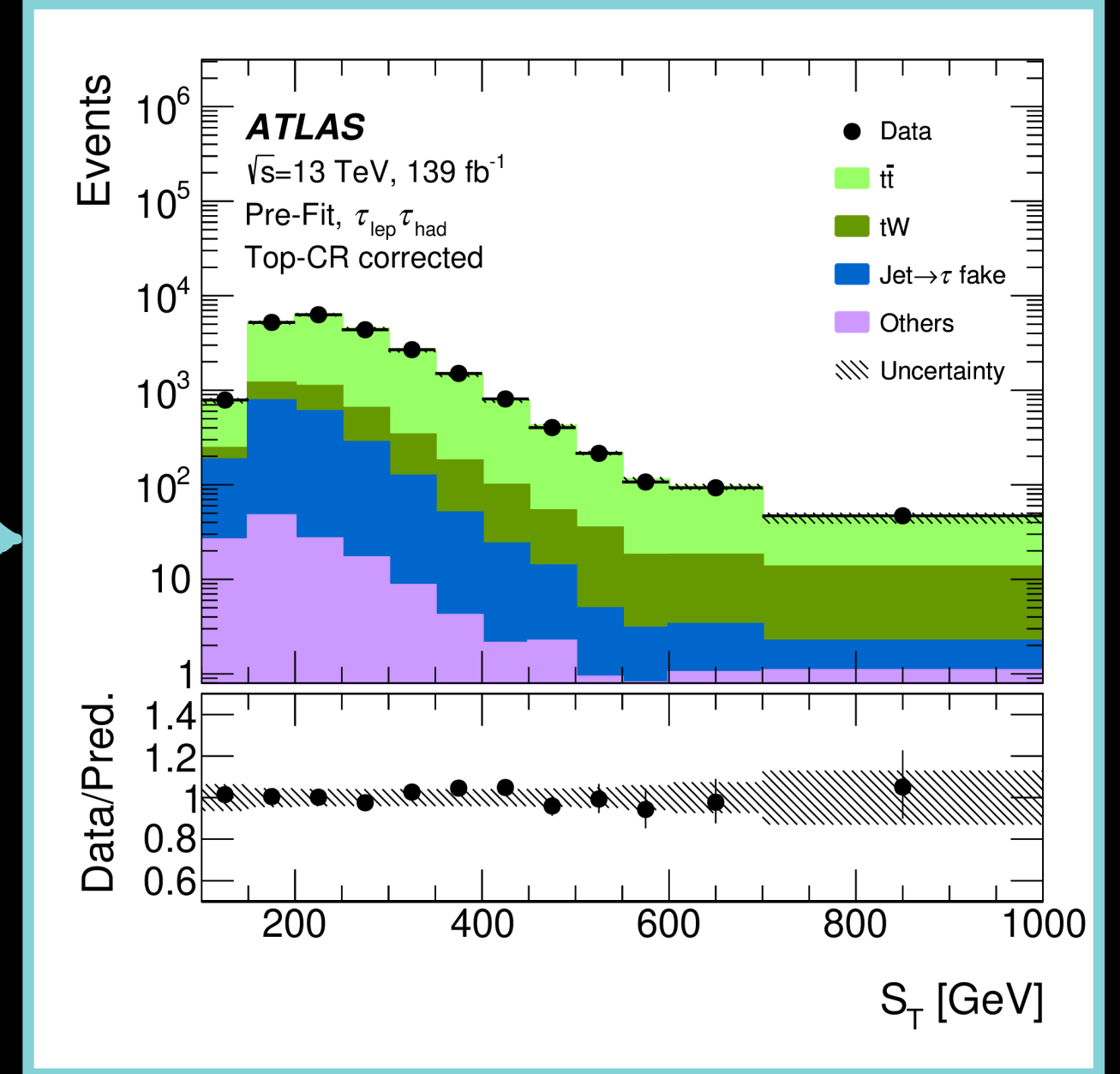
-> Ensure the background is accurately modelled



Current simulations of  $t\bar{t}$  processes overestimate the upper tail of the top-quark  $p_T$  spectrum. [1908.0735]

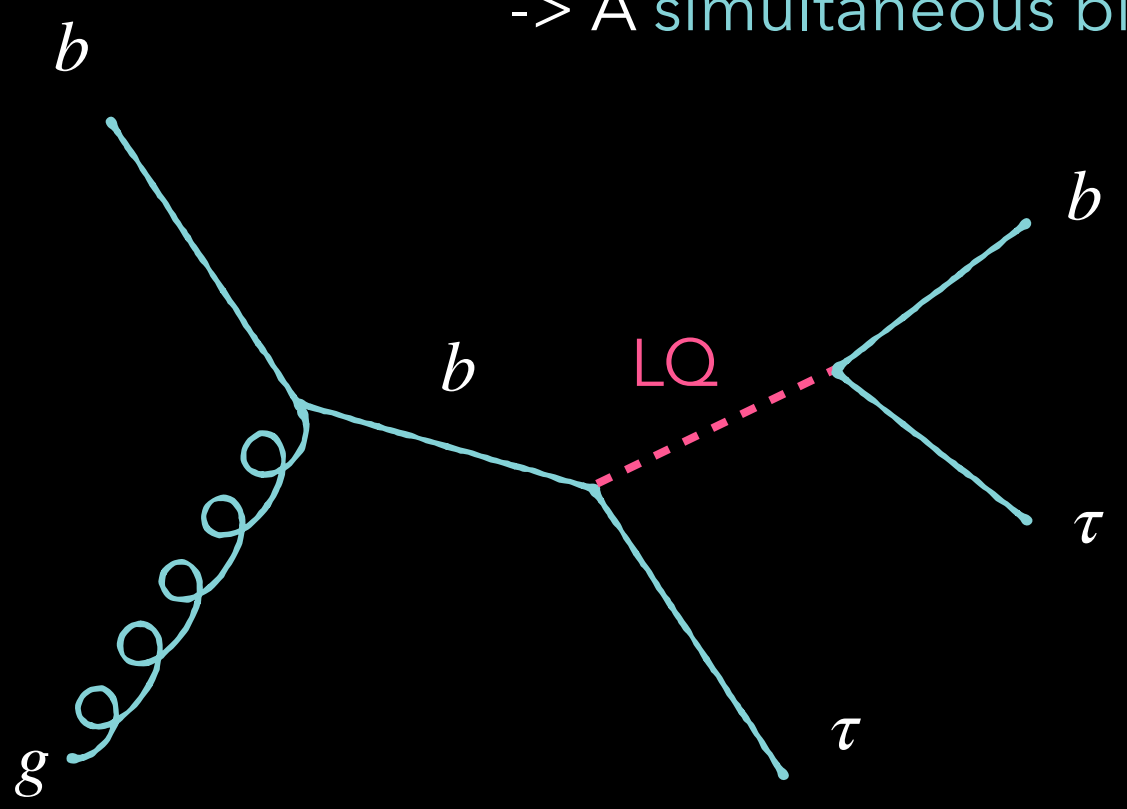
apply correction

$$SF_{Top}(S_T) = \frac{(N_{data-} - N_{non-Top})(S_T)}{N_{Top}(S_T)}$$



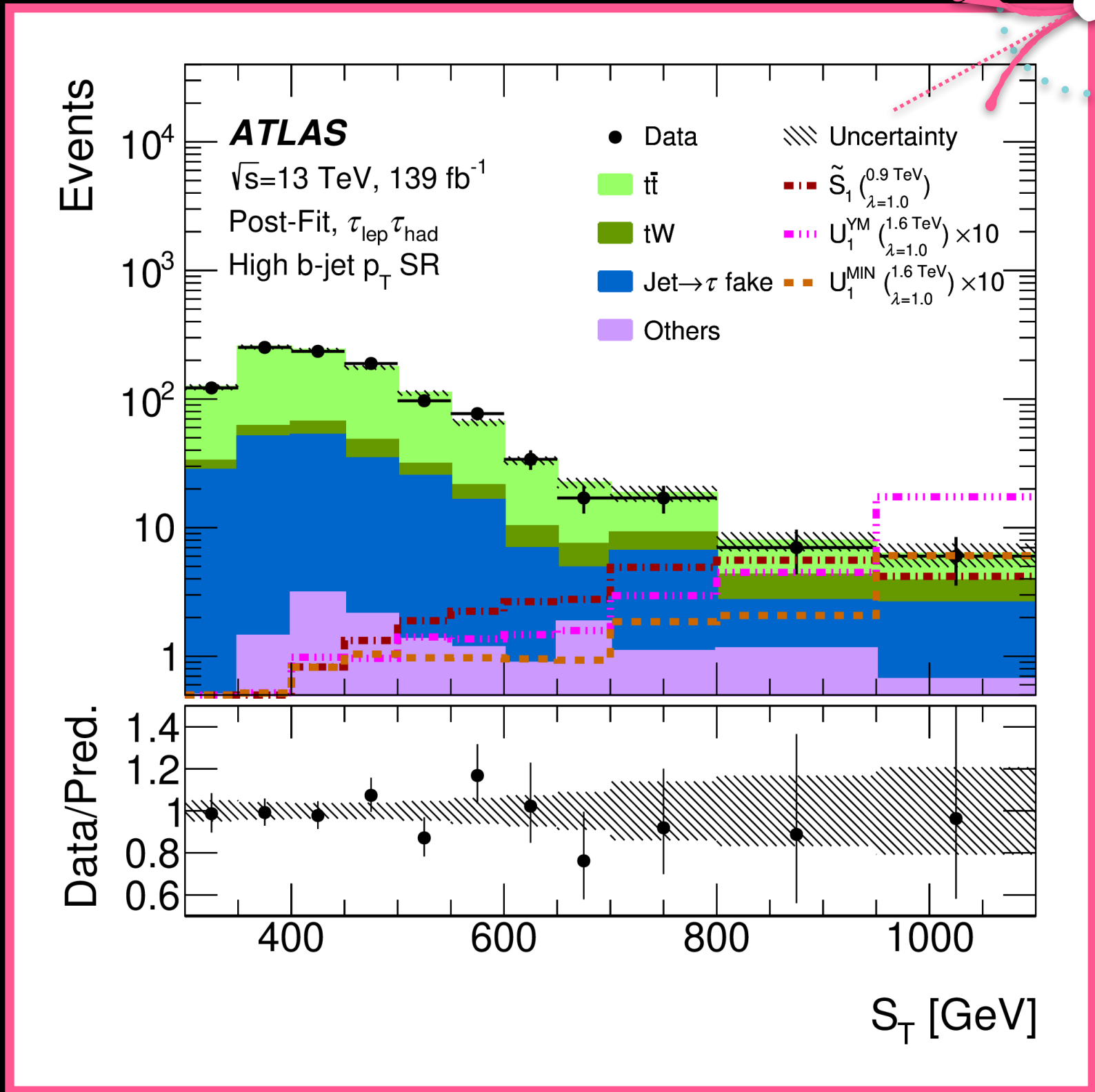
# 2) Discriminating variable

-> A simultaneous binned maximum-likelihood fit is performed on the  $S_T$  distributions for each LQ hypothesis.

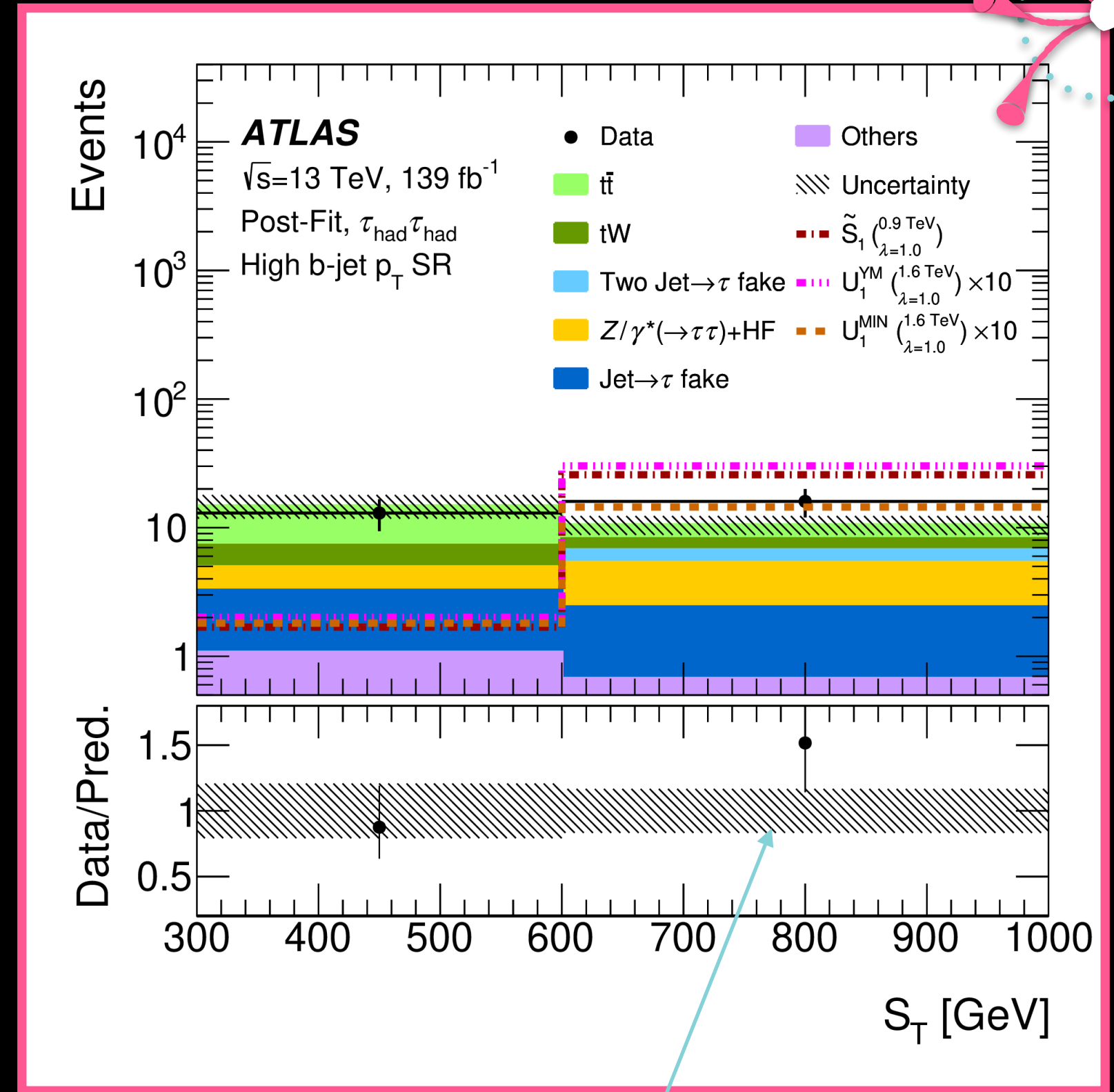


-> more sensitive due to larger signal/background ratio in the last  $S_T$  bin

$\tau_{lep}\tau_{had}$  channel



$\tau_{had}\tau_{had}$  channel



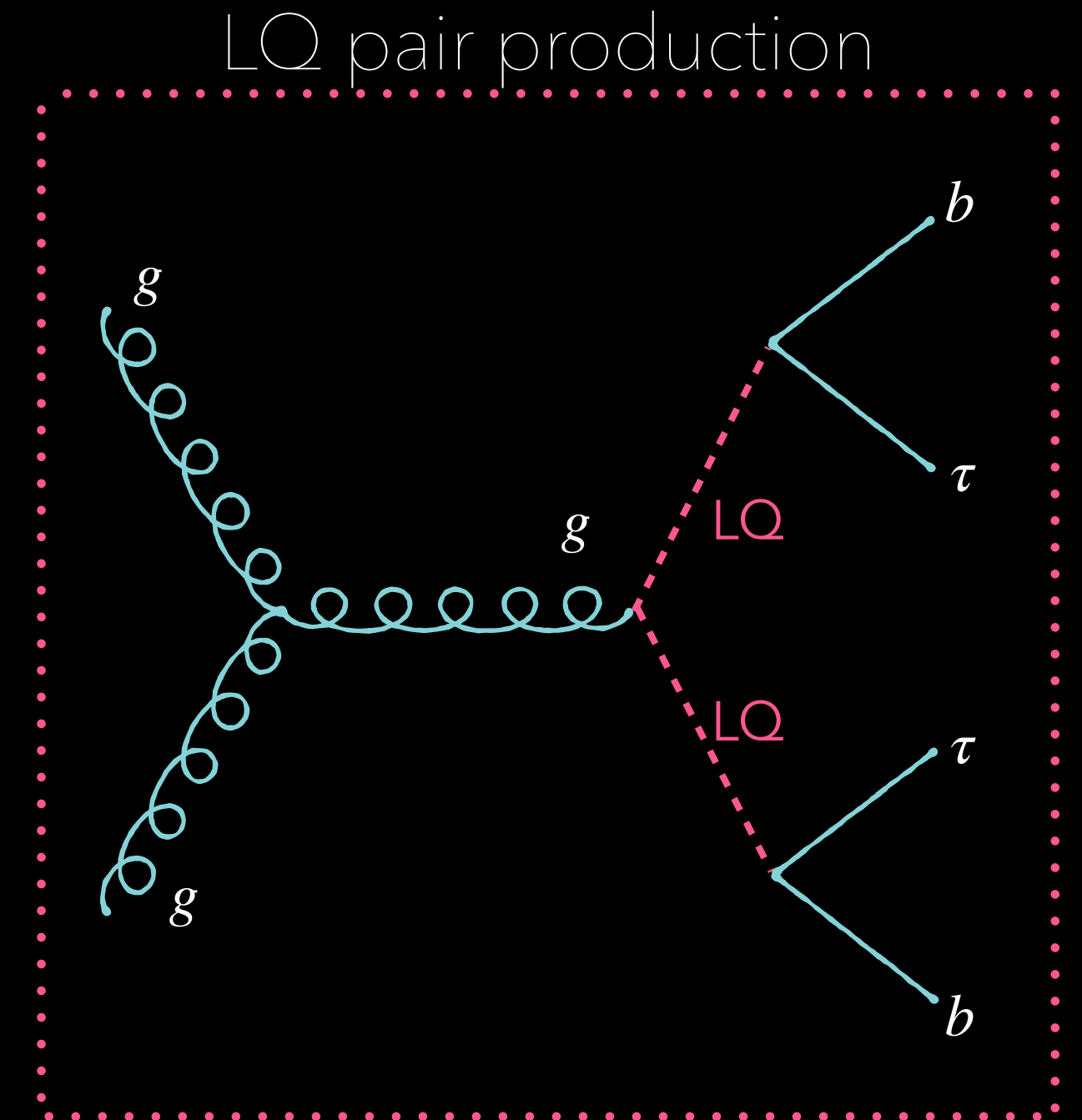
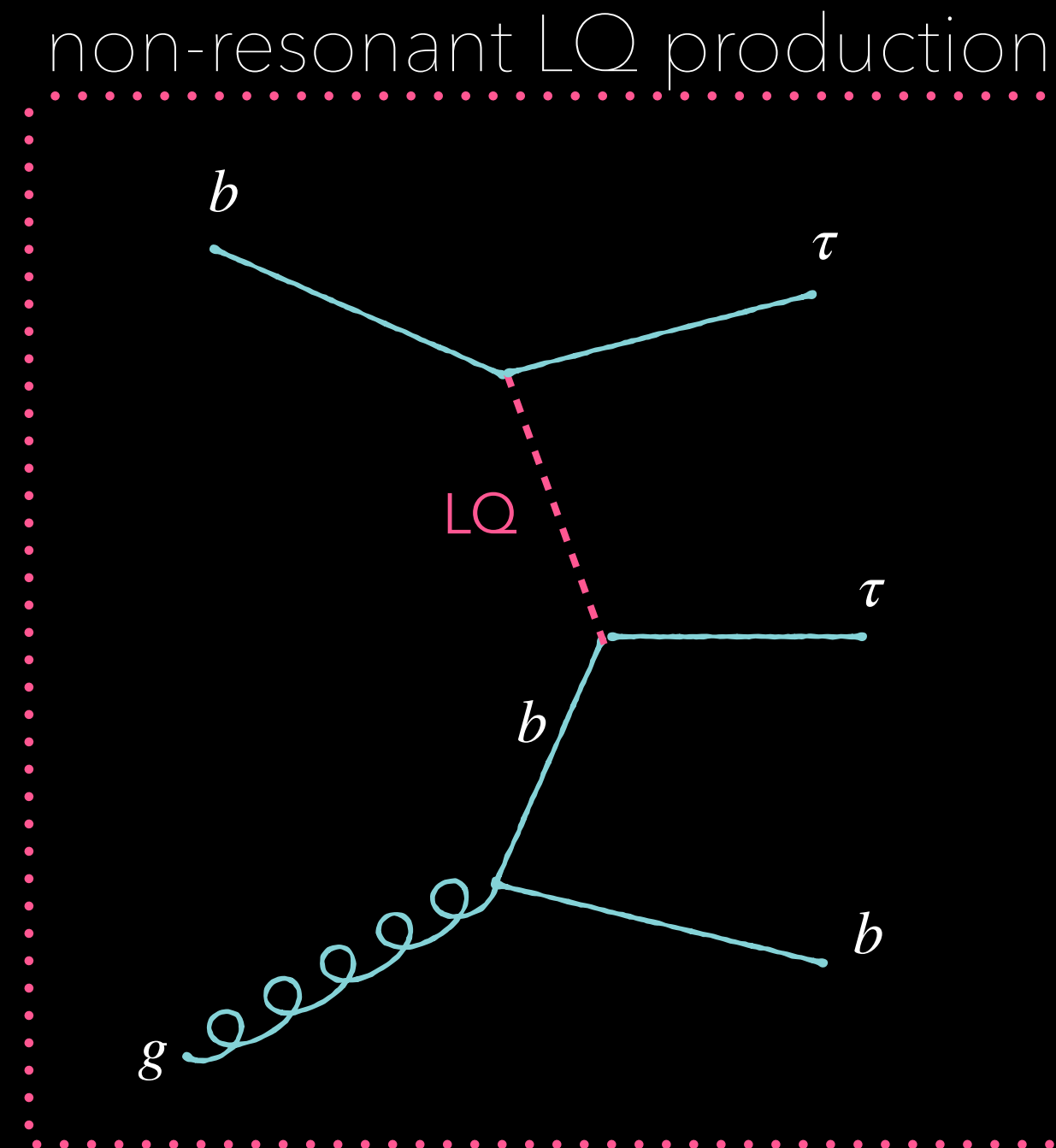
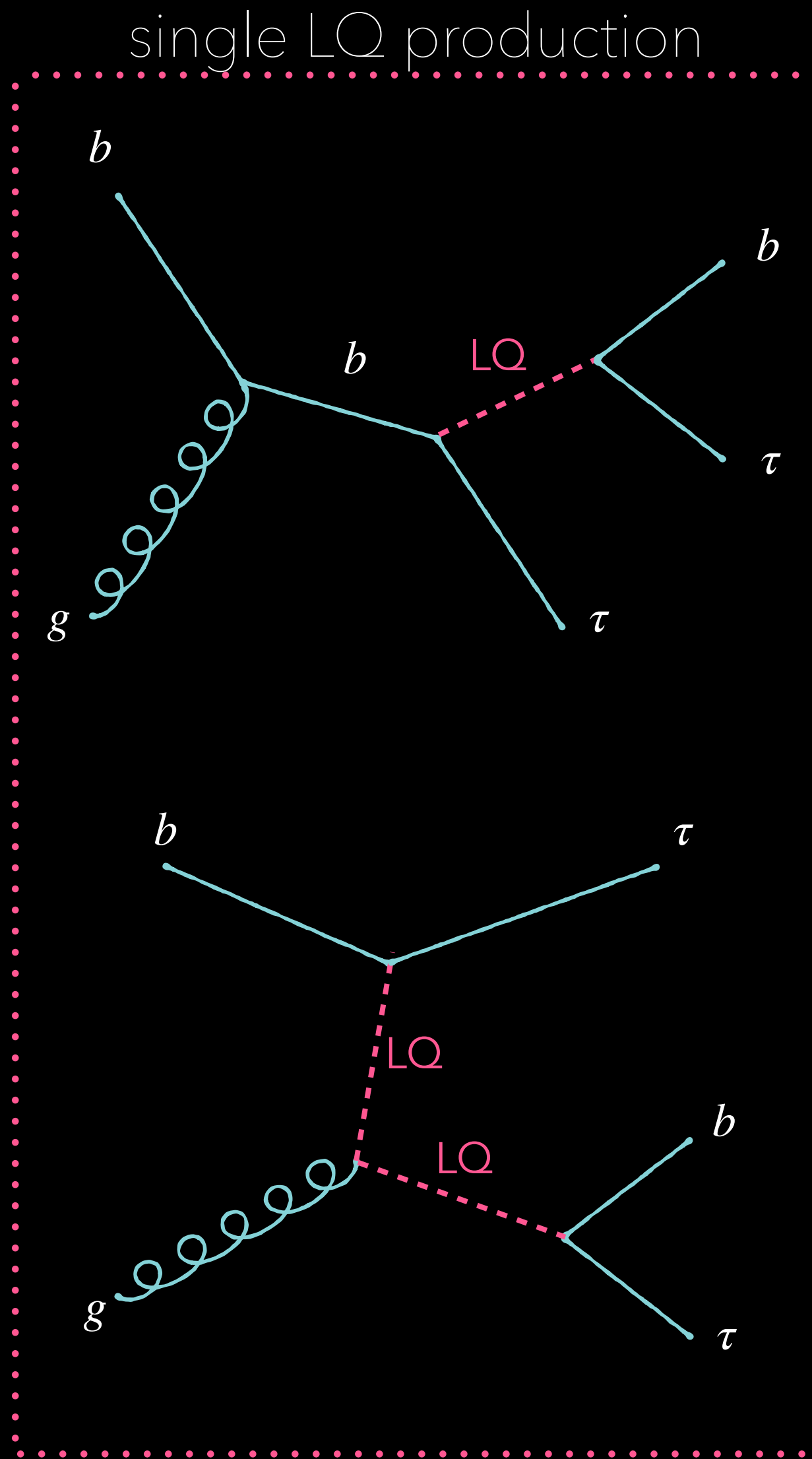
Keep this in mind for the next (next) slide.





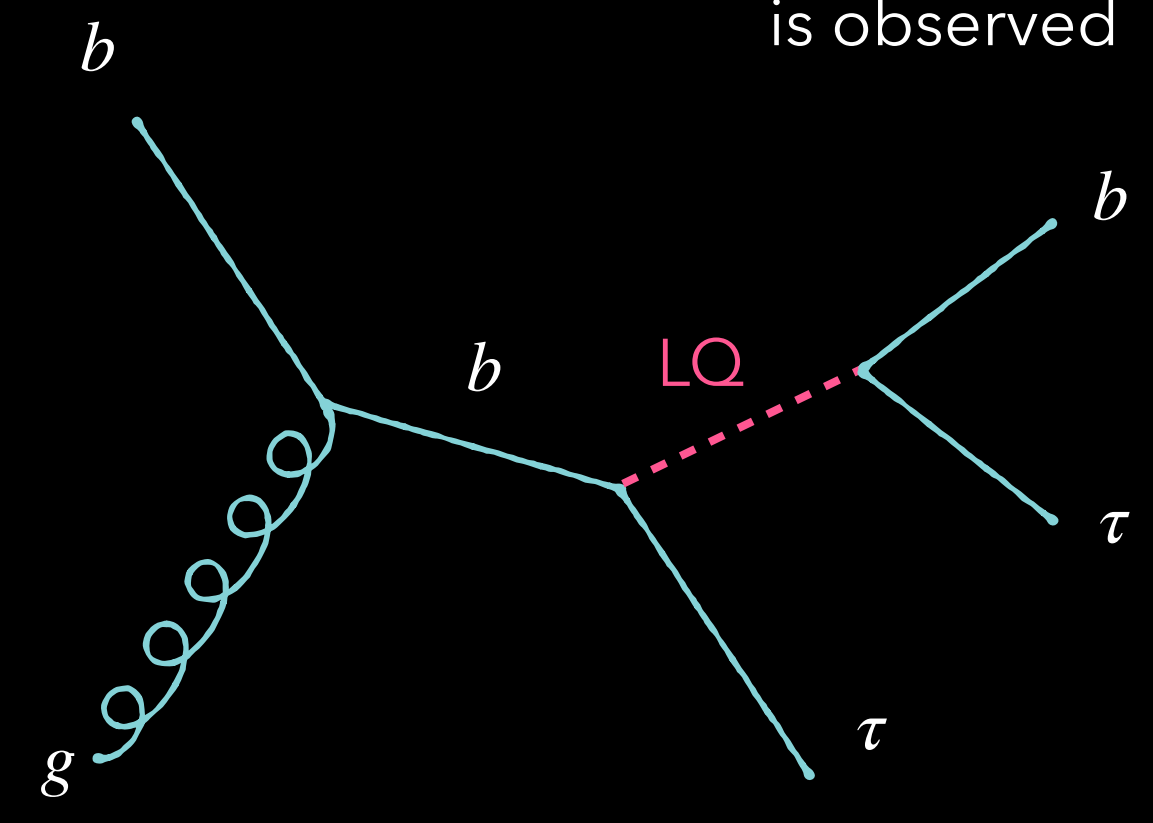


2) What I need to say before the next slide...

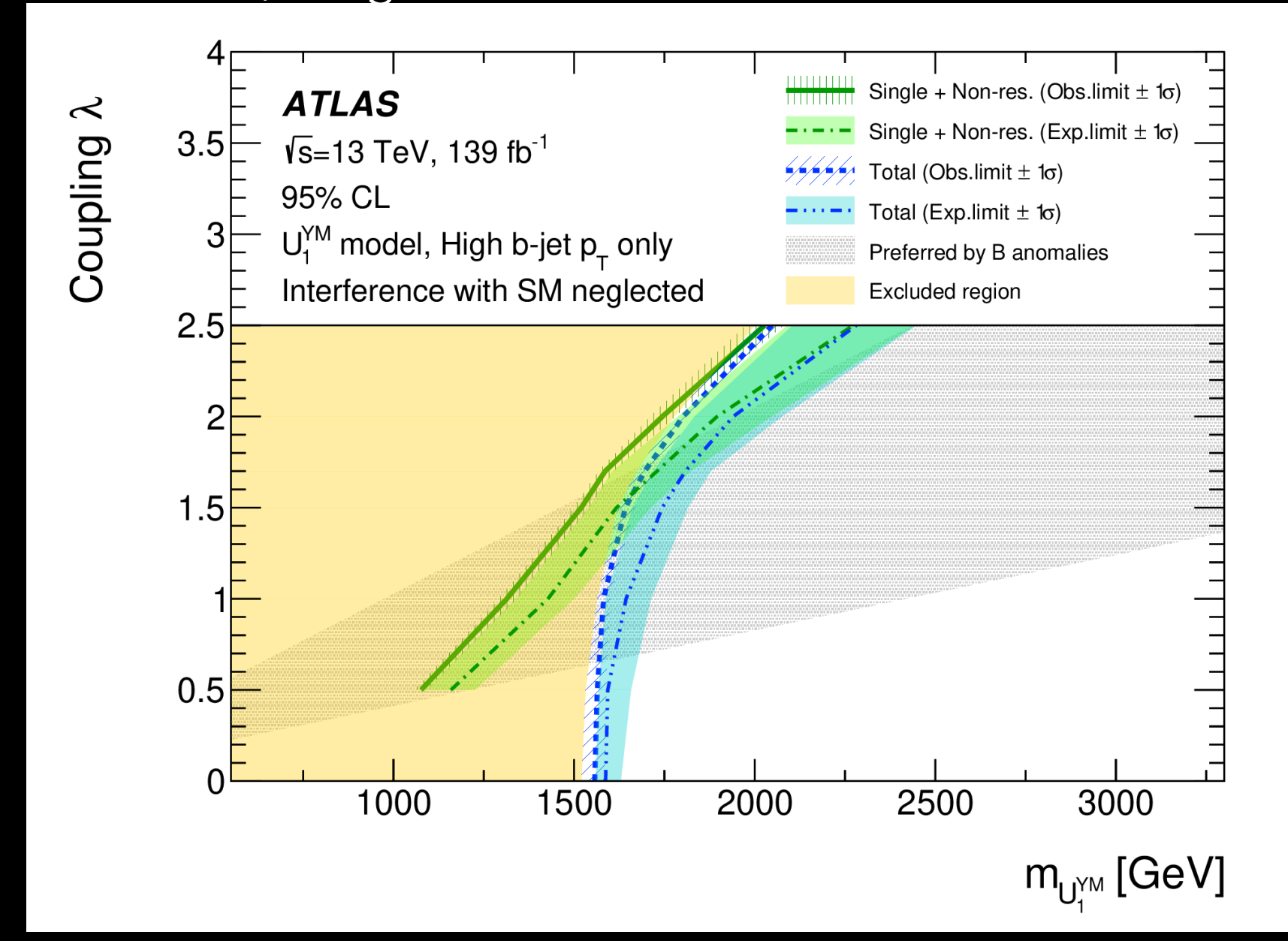


# 2) Results

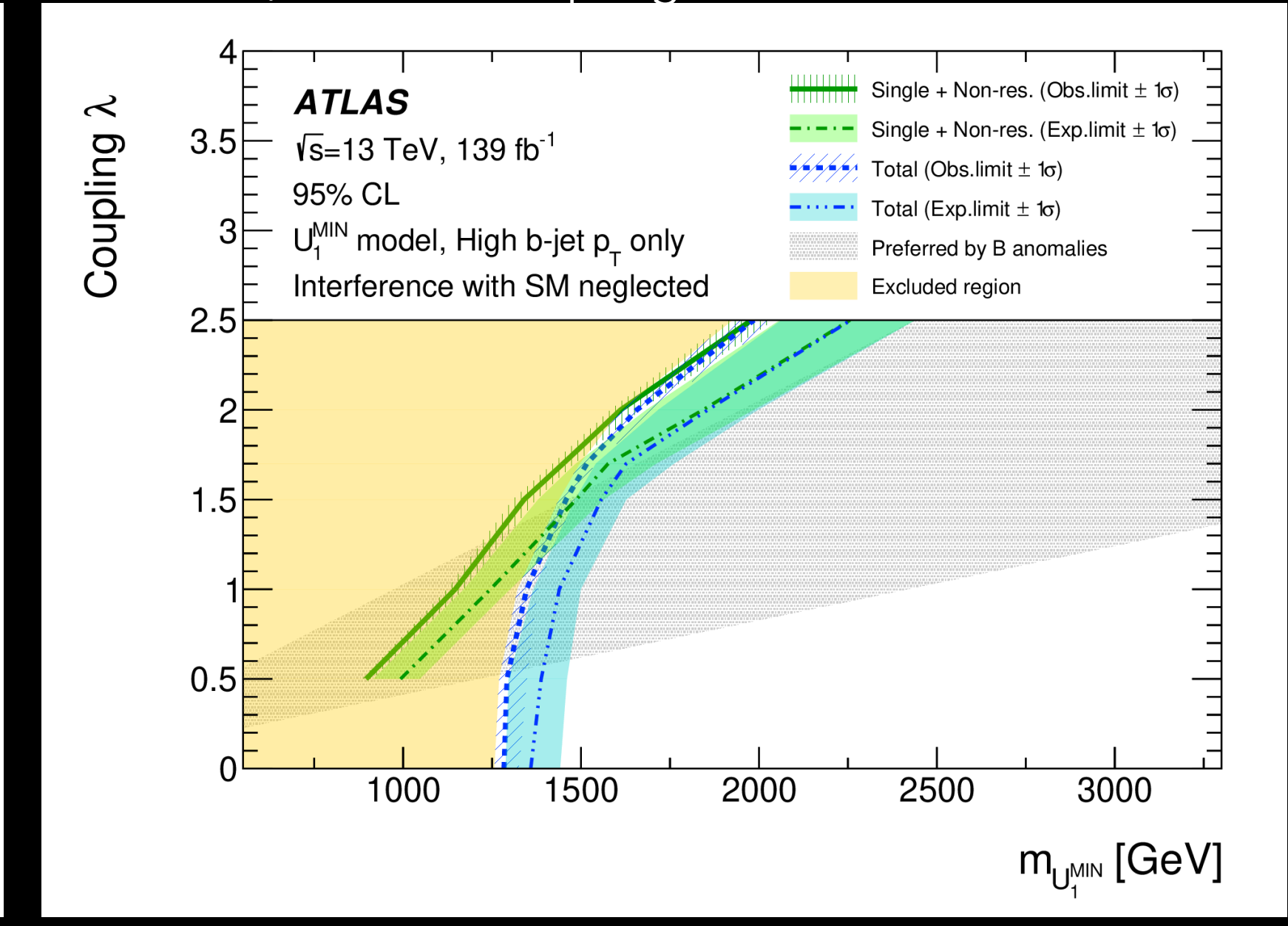
no significant excess above the SM prediction is observed



Vector LQs, Yang-Mills model



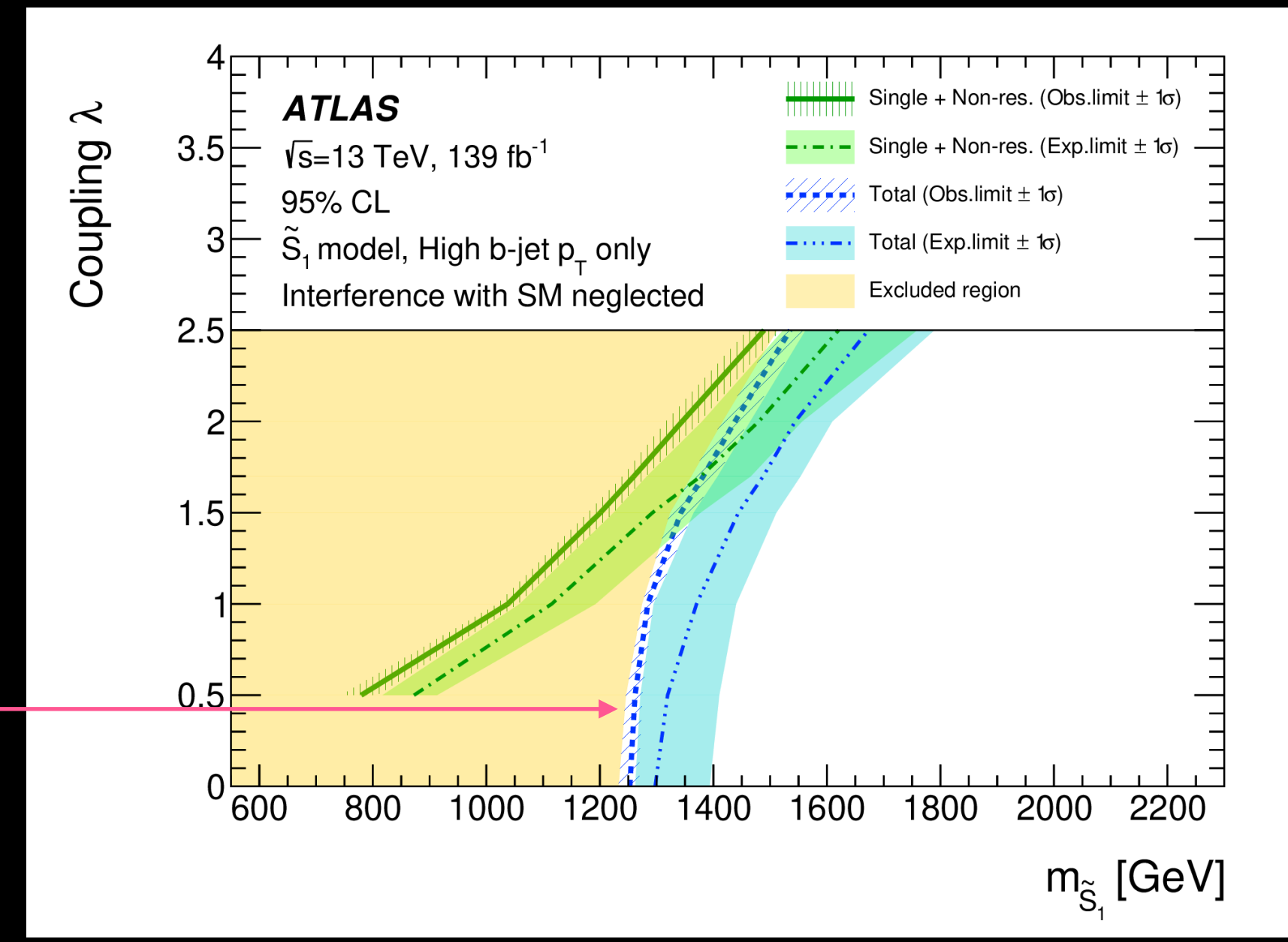
Vector LQs, Minimal coupling model



Measurement excludes part of the  $\lambda(m_{U_1})$  space that is preferred by  $B$  anomalies!

[[Eur. Phys. J. C 83 \(2023\) 153](#)]

Scalar LQs



total := single + non-resonant + pair LQ

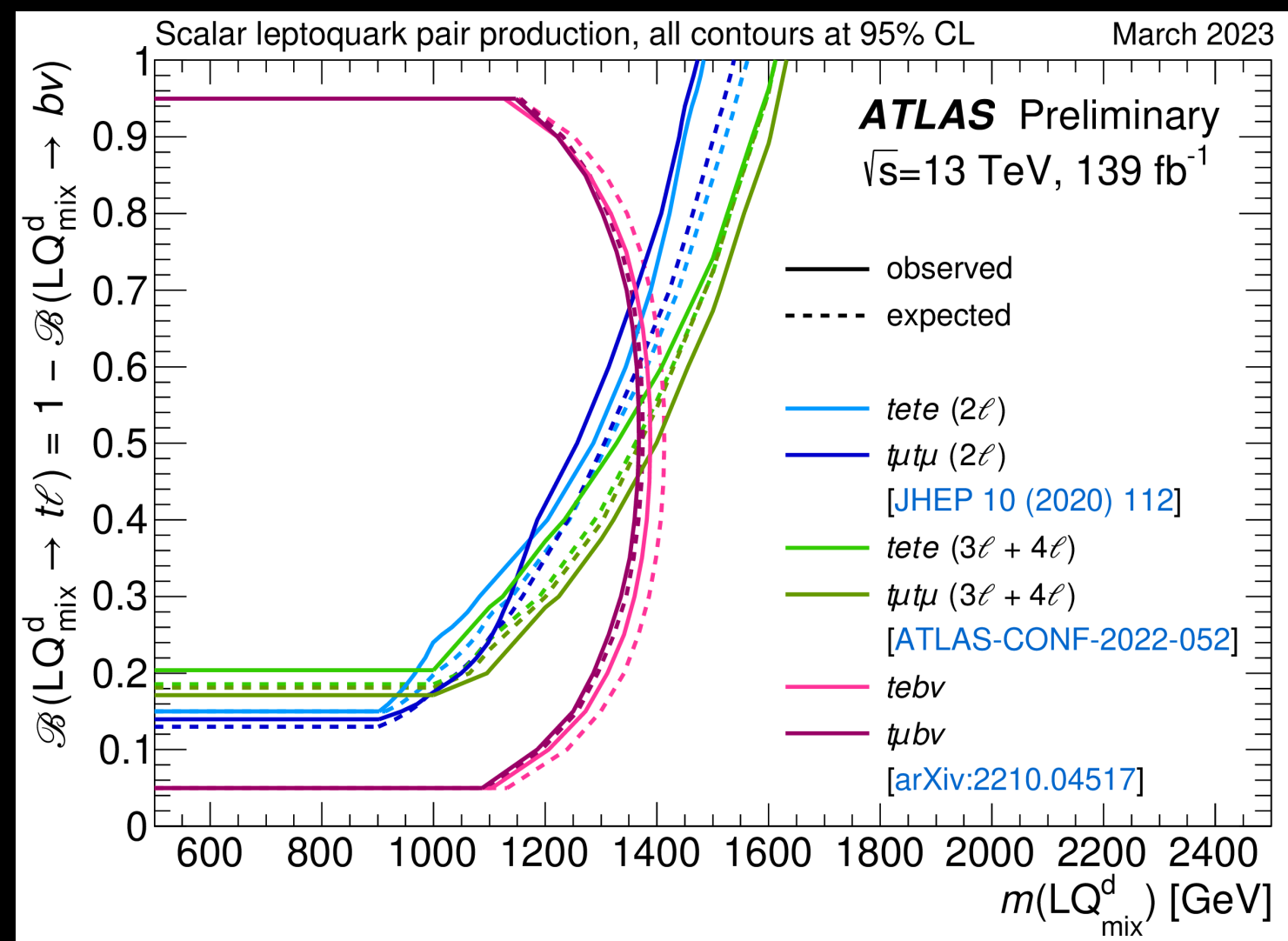
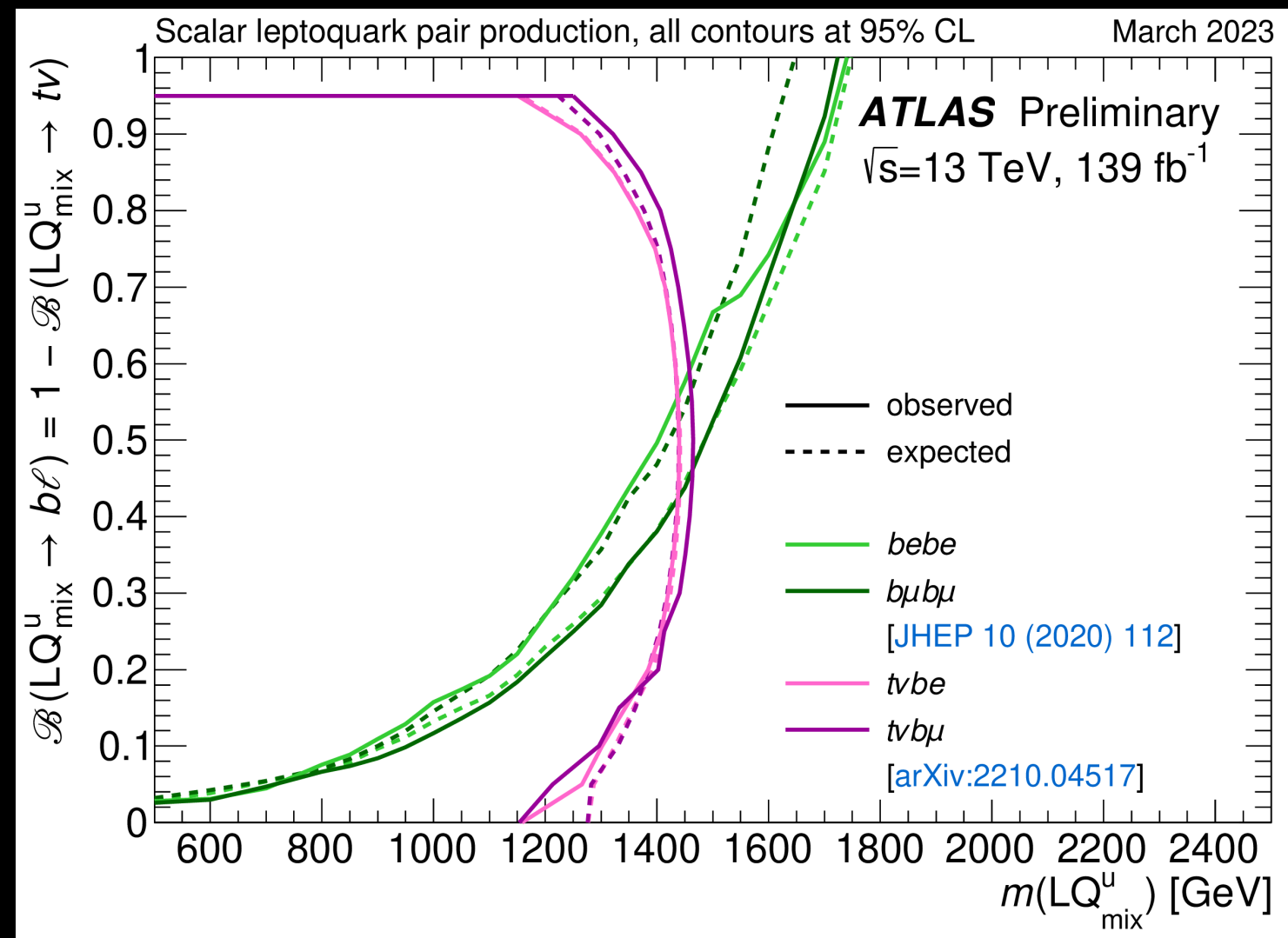
First ATLAS result for the search of singly produced LQs in the  $b\tau\tau$  final state.

The observed limits obtained are less stringent than the expected limits, which is mainly driven by the higher data yields relative to the predicted yields in the highest  $S_T$  bin in the  $\tau_{had}\tau_{had}$  channel.

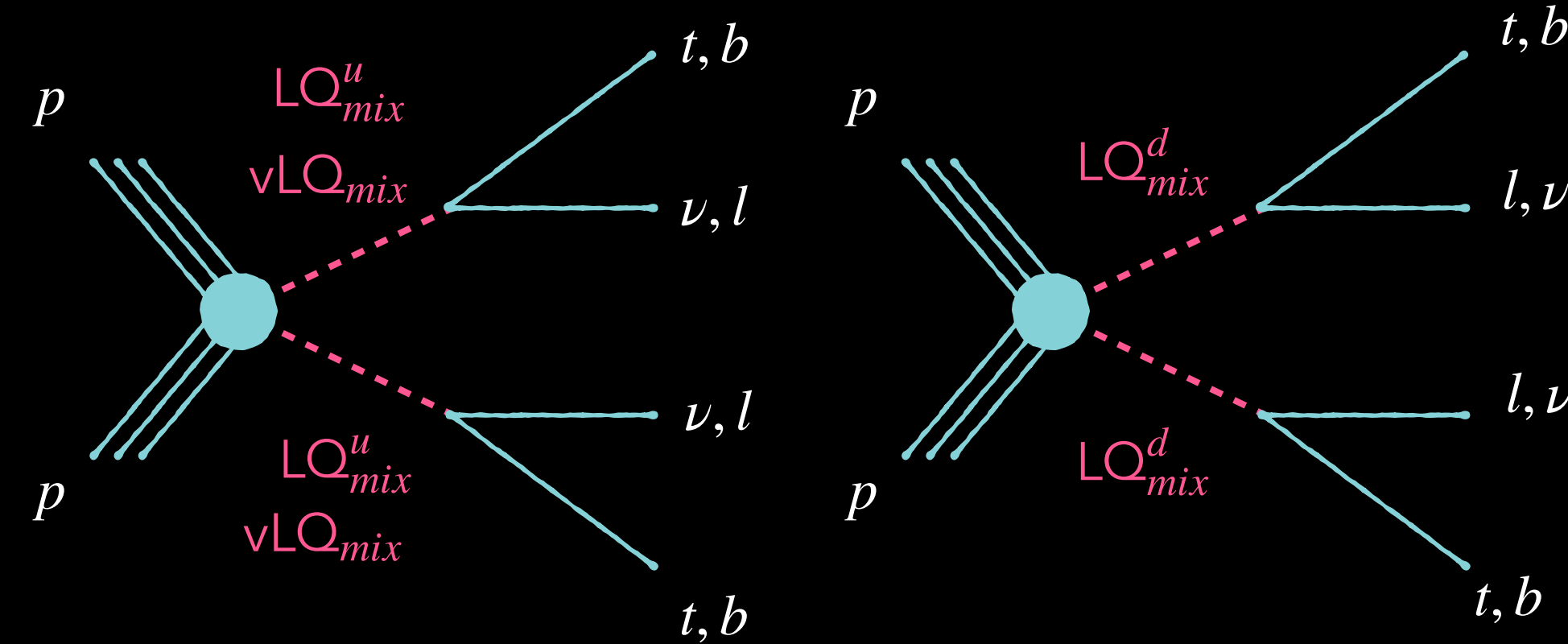
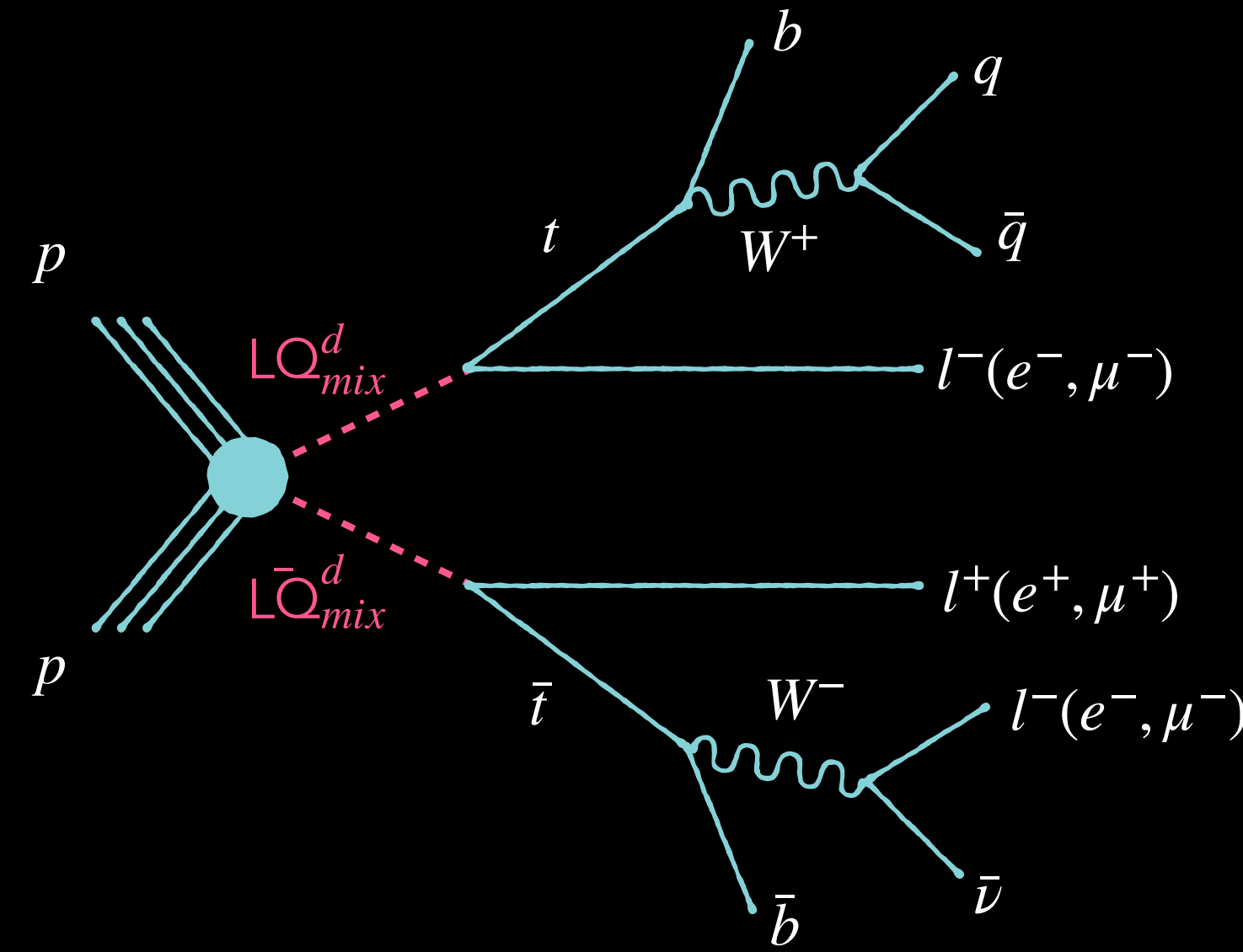


# Final slide - Other results - Leaving the world of third-gen-only coupling

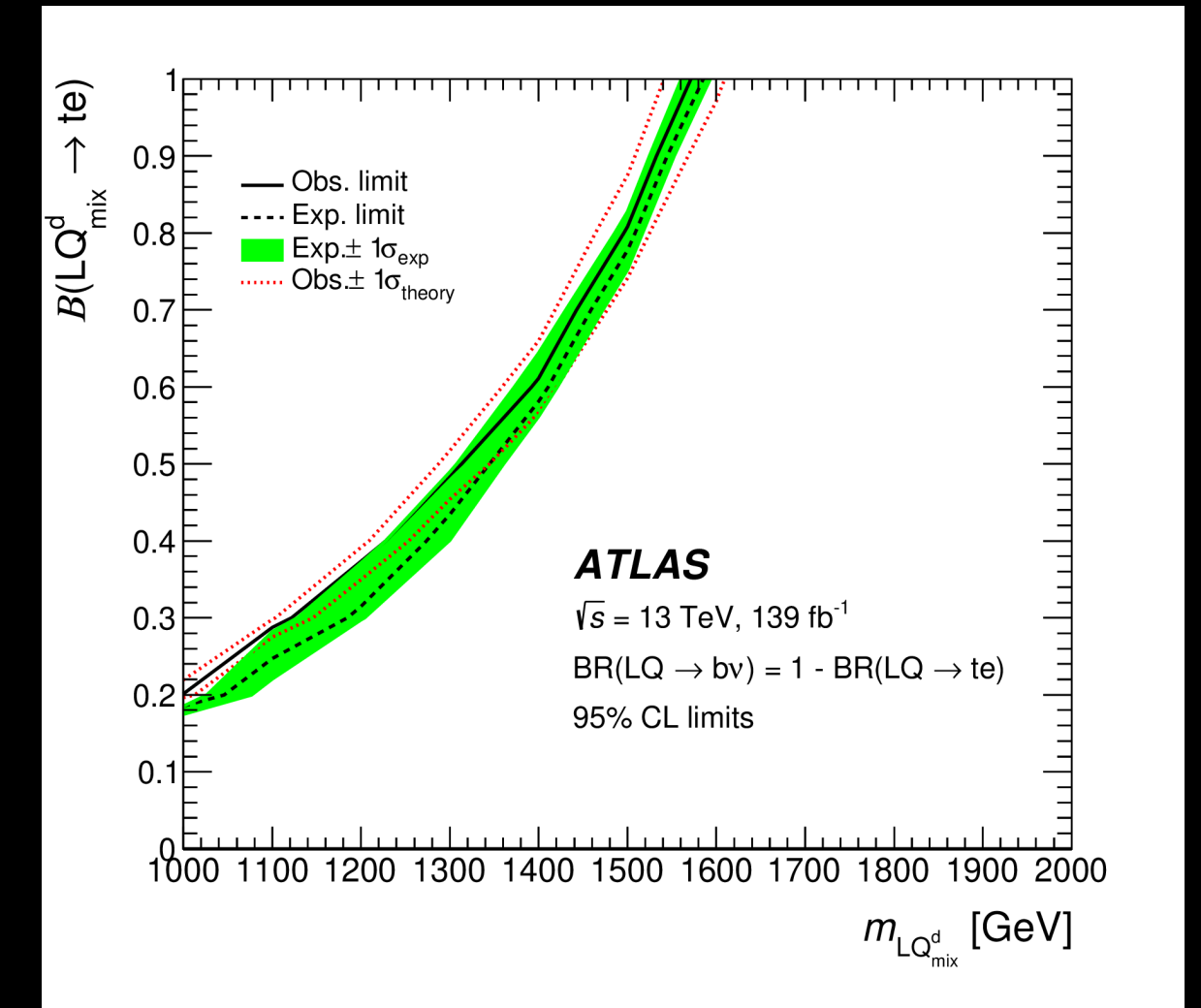
## $LQ_{mix}$ summary plots



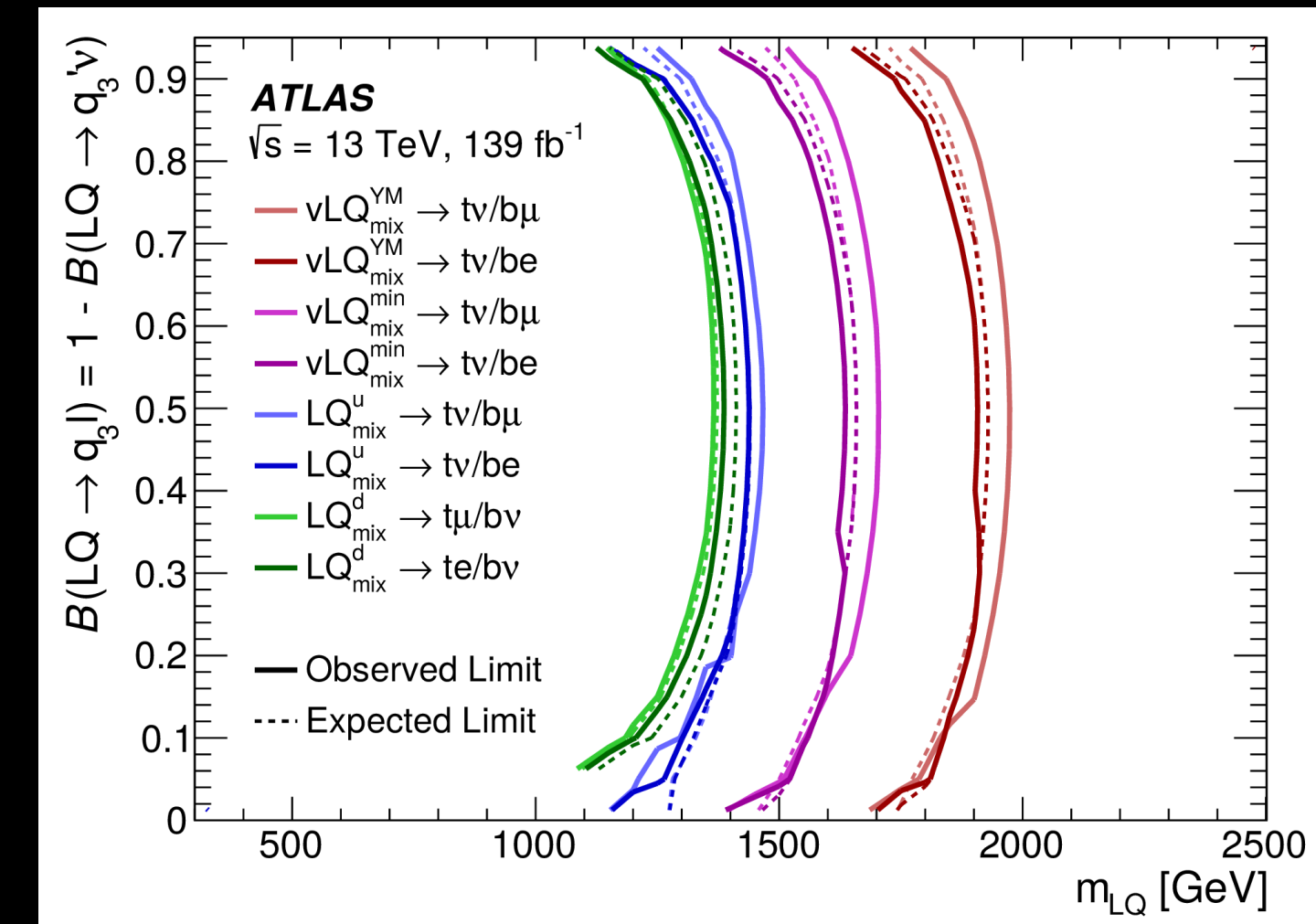
[ATL-PHYS-PUB-2023-006]



$vLQ := \text{vector } LQ$



June 2023 [arXiv:2306.17642](https://arxiv.org/abs/2306.17642)  
+event display on the next slide



October 2022 [arXiv:2210.04517](https://arxiv.org/abs/2210.04517)

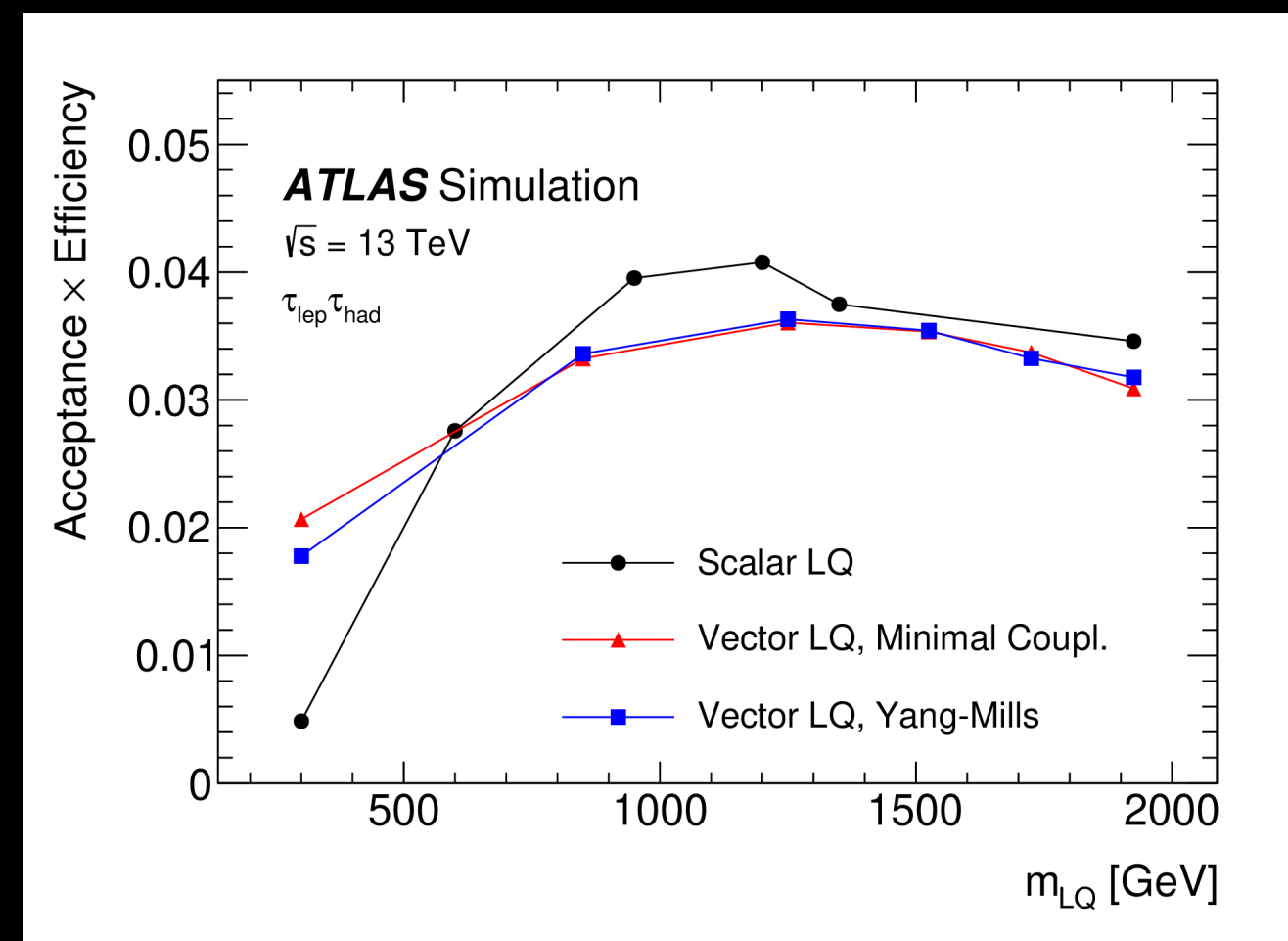
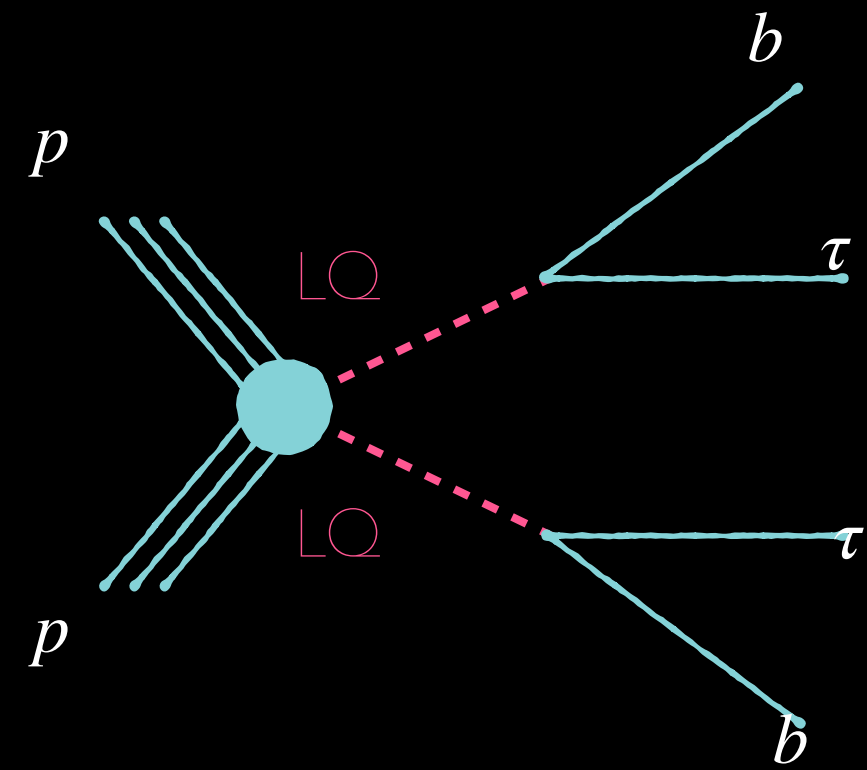


# Conclusion

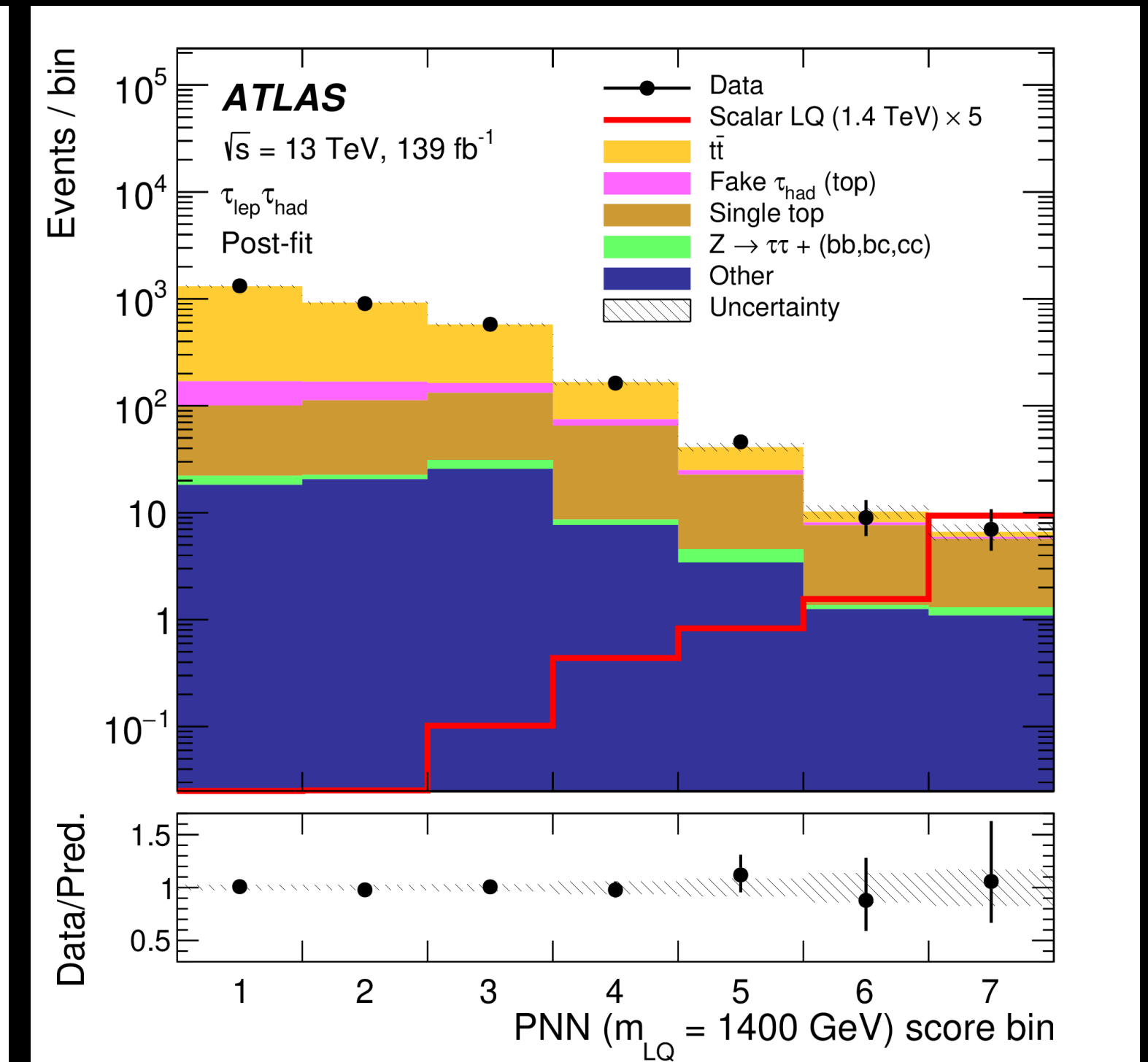
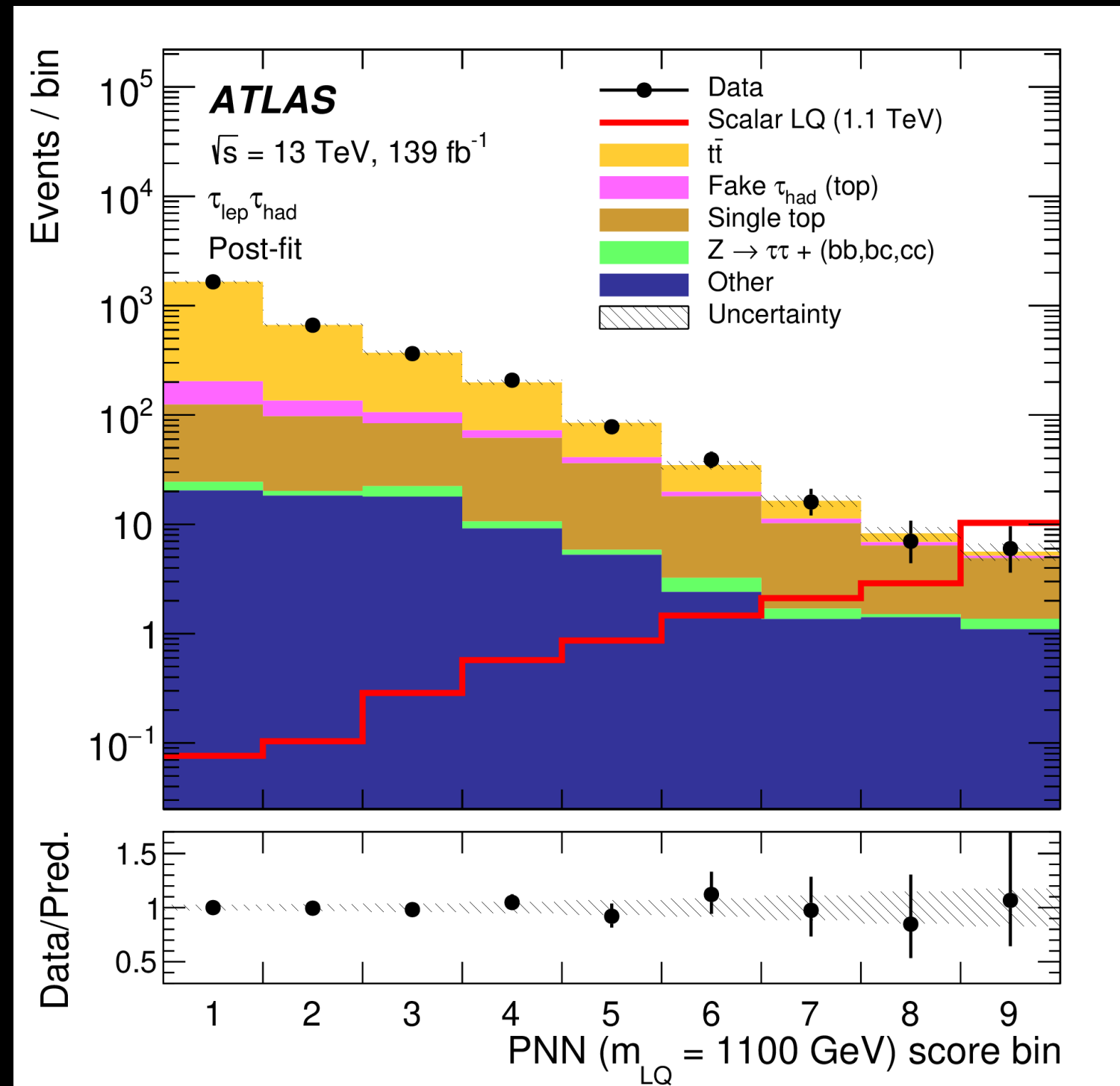
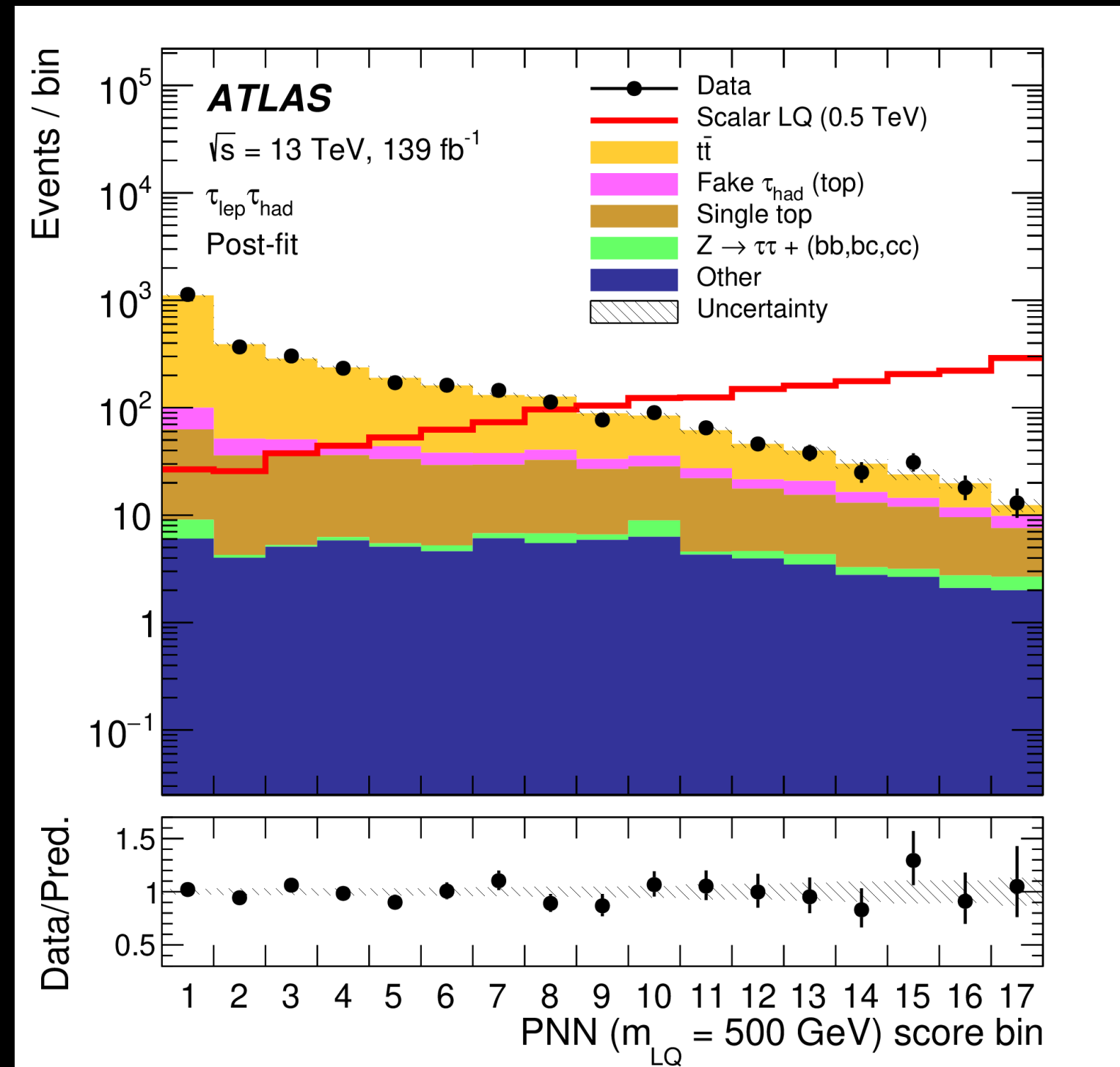
- ★ We use a **broad search program** to look for LQs in ATLAS, which involves **exploring the large LHC Run-2 dataset**.
- ★ There is a wide **variety of models and final states** available.
- ★ The dataset for LHC Run-3 is expanding 

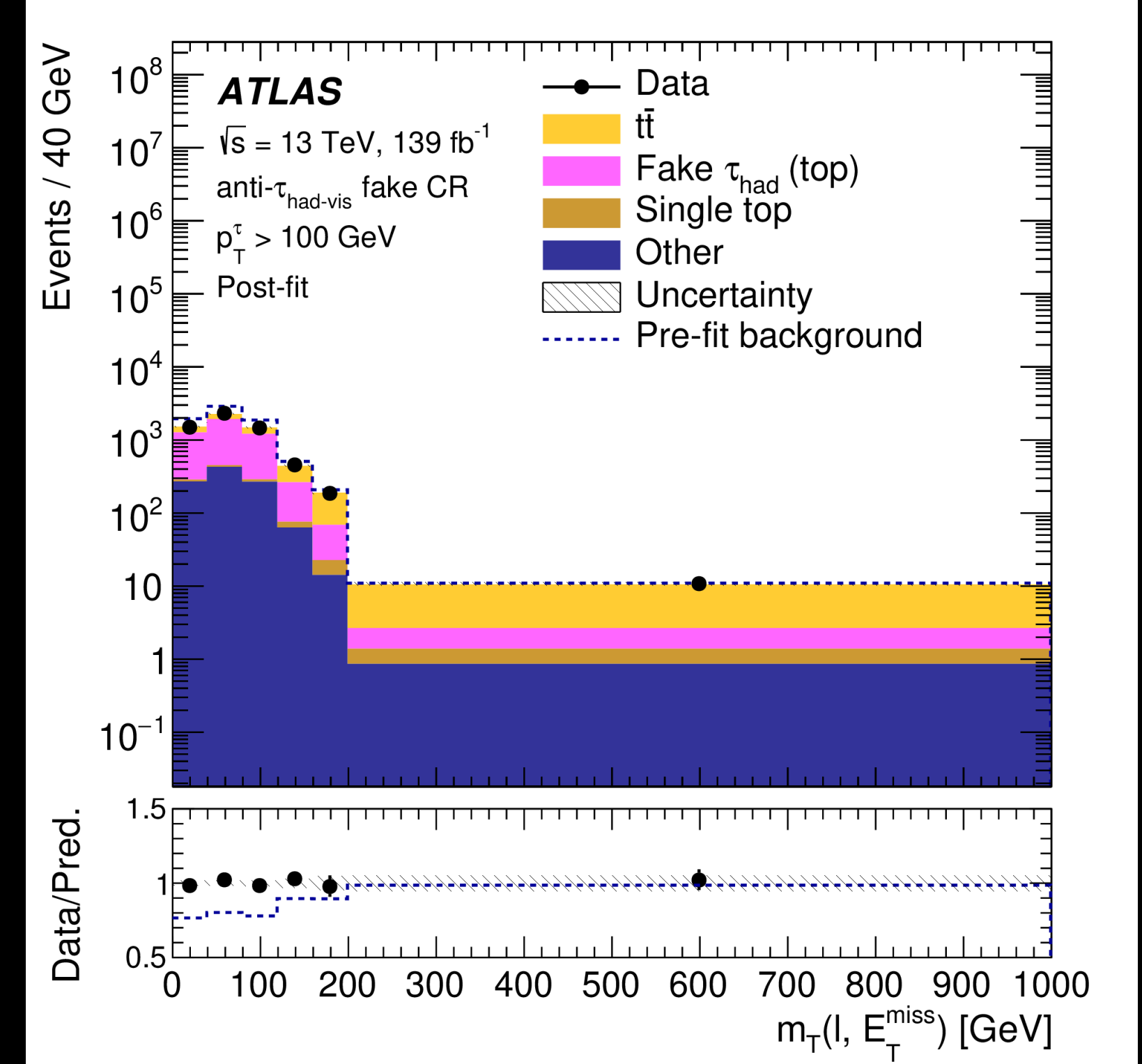
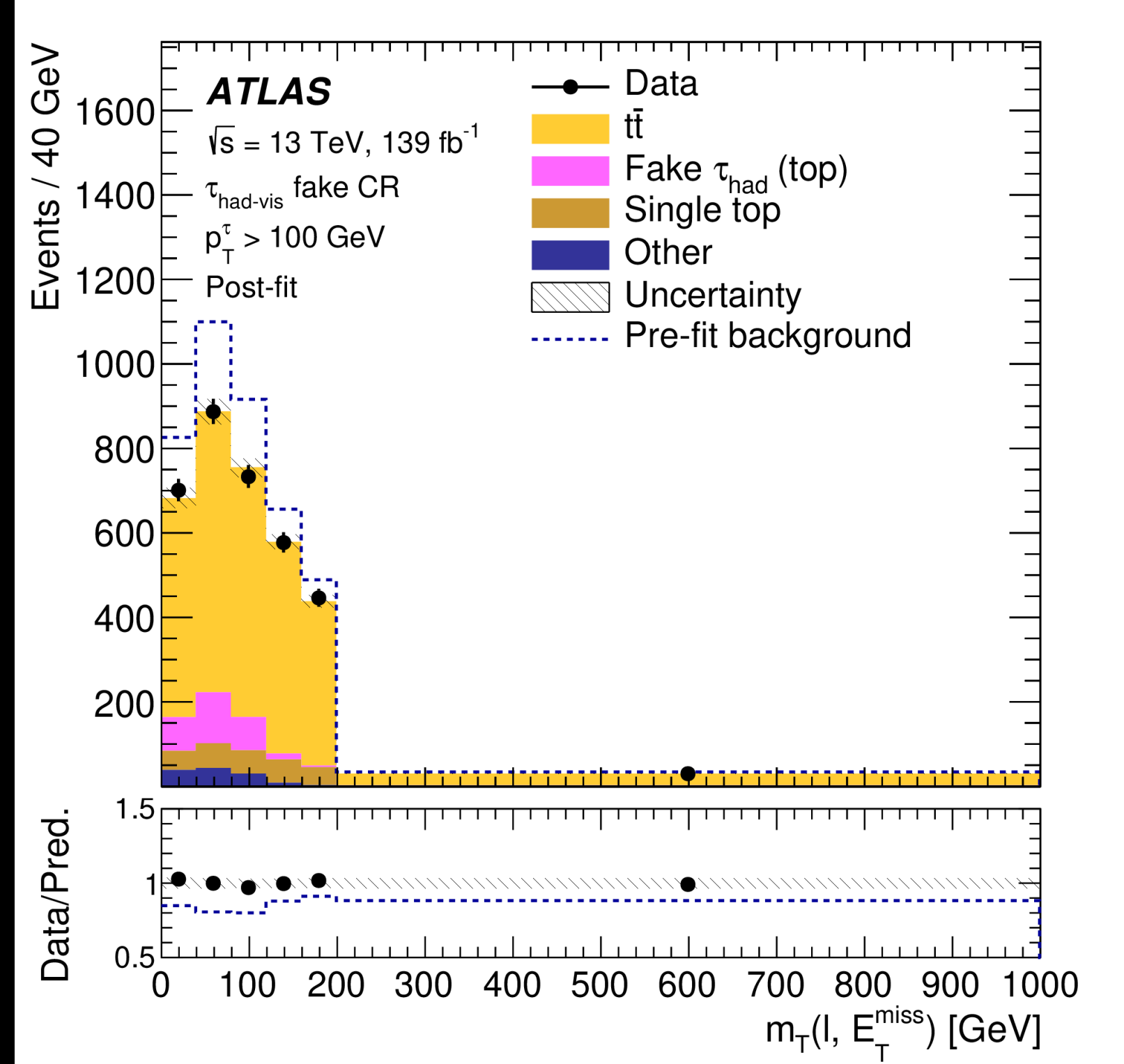
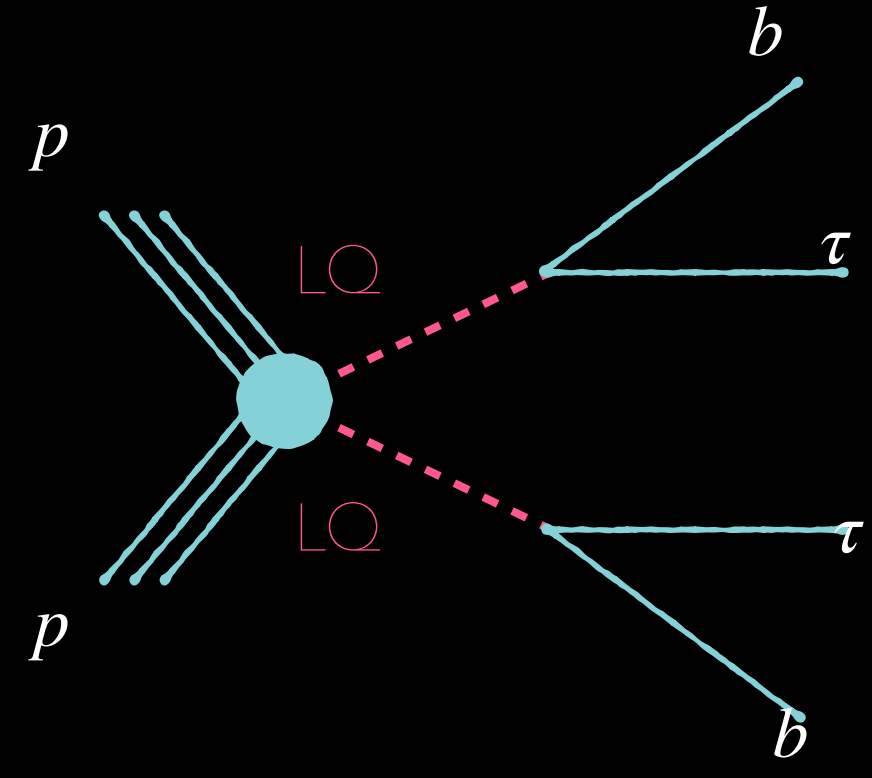


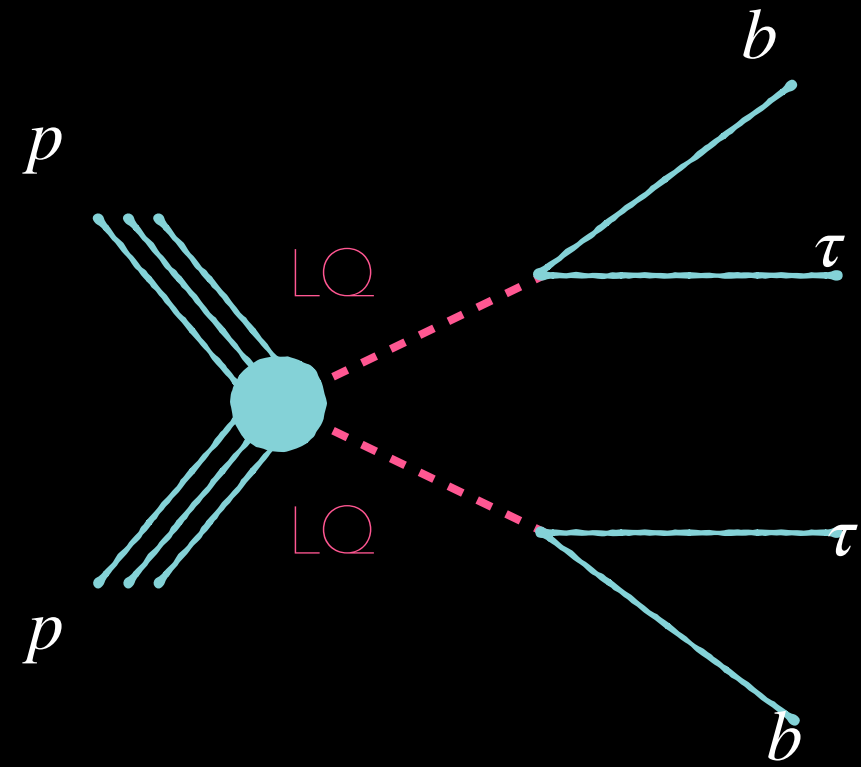




	$\tau_{\text{lep}}\tau_{\text{had}}$ channel	$\tau_{\text{had}}\tau_{\text{had}}$ channel
$t\bar{t}$	2420 $\pm$ 90	93 $\pm$ 9
single-top	355 $\pm$ 27	20 $\pm$ 4
Fake $\tau_{\text{had}}$ (top)	170 $\pm$ 90	43 $\pm$ 18
$Z \rightarrow \tau\tau + (bb, bc, cc)$	13.9 $\pm$ 2.4	10.3 $\pm$ 1.4
Multi-jet	–	22 $\pm$ 11
Other	78 $\pm$ 7	19 $\pm$ 5
<b>Total Background</b>	<b>3040 <math>\pm</math> 60</b>	<b>207 <math>\pm</math> 13</b>
<b>Data</b>	<b>3031</b>	<b>211</b>

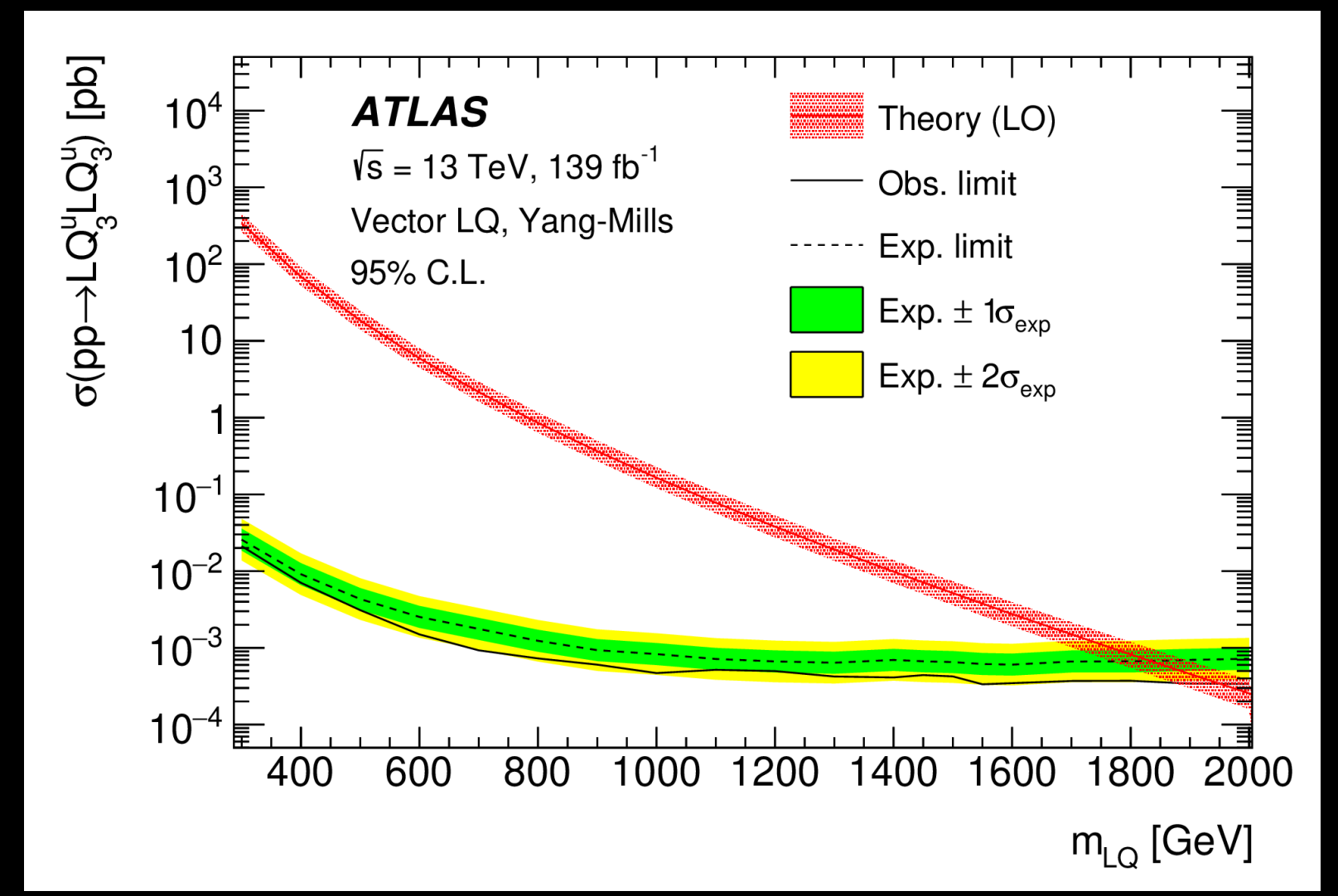
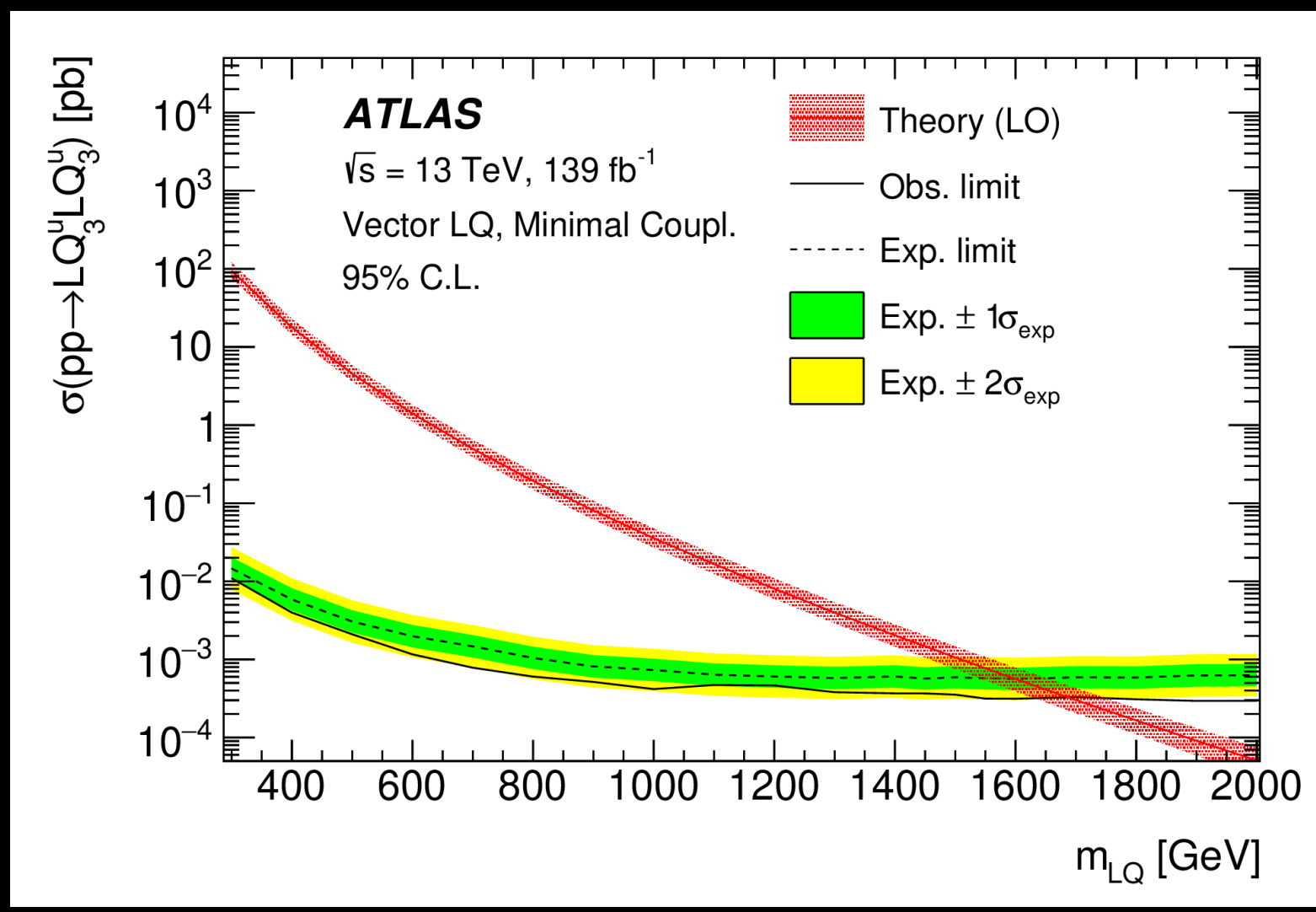
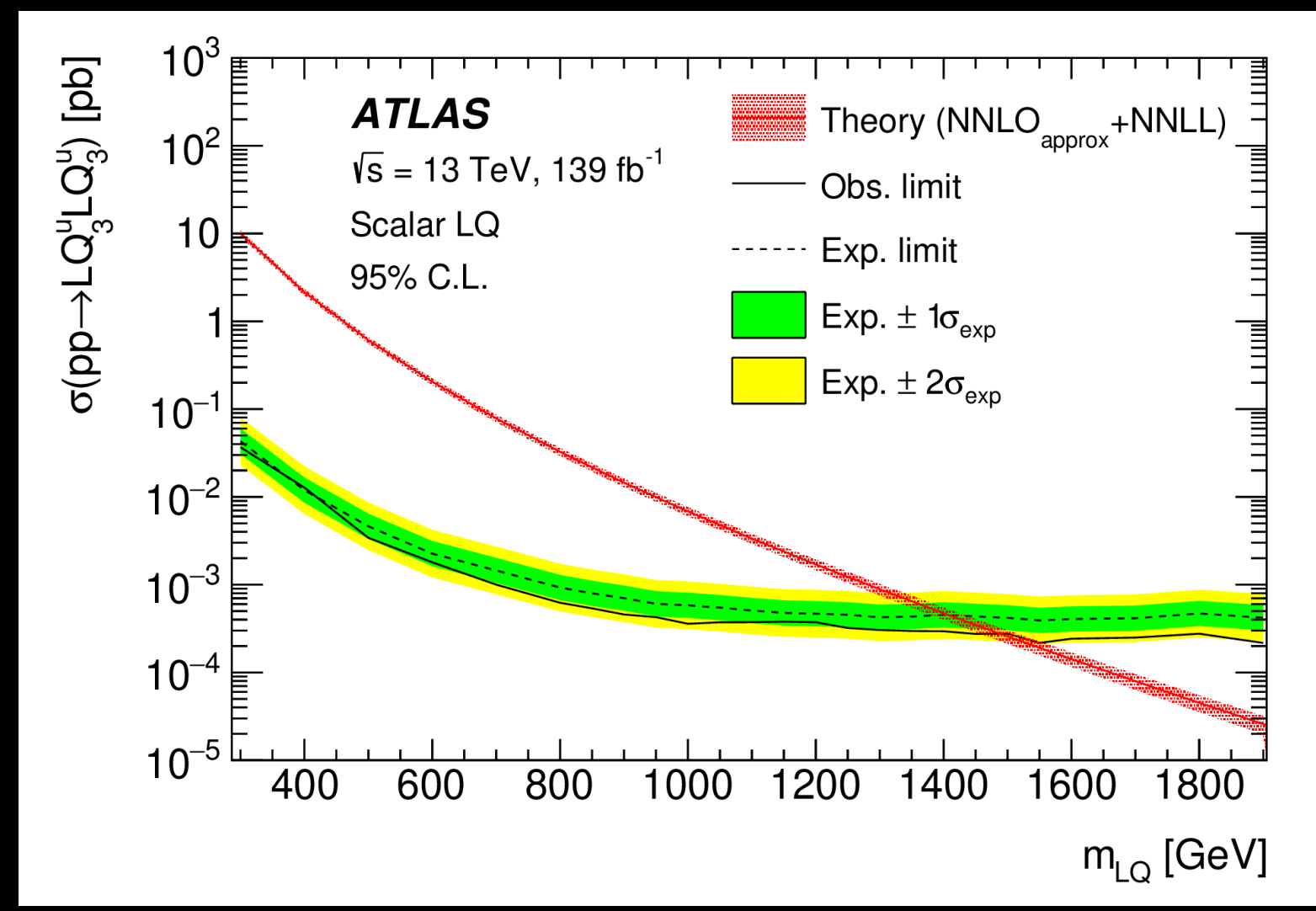
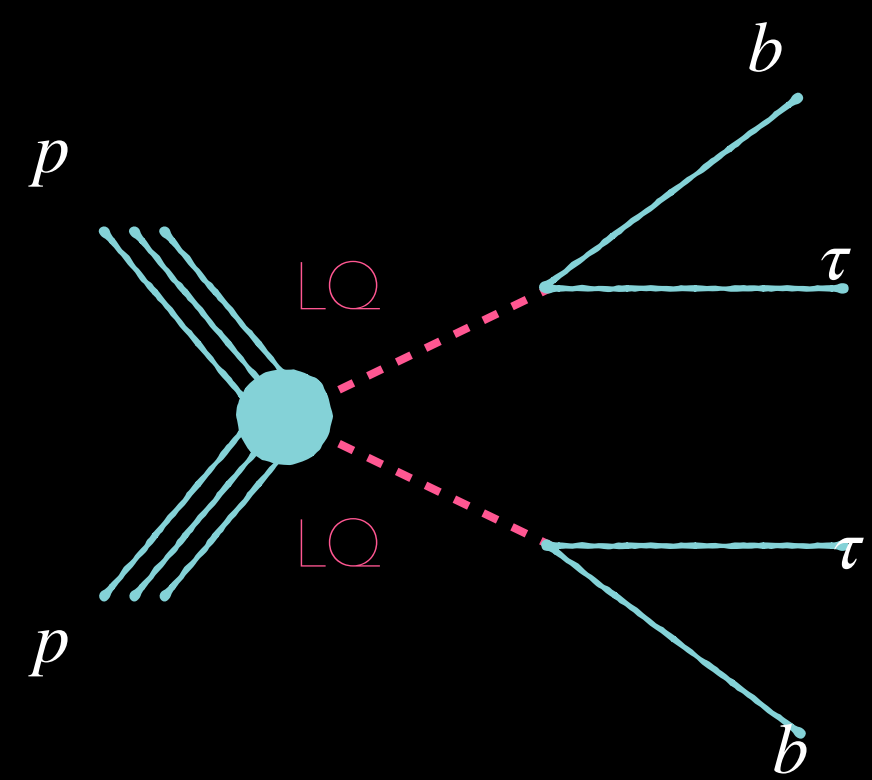


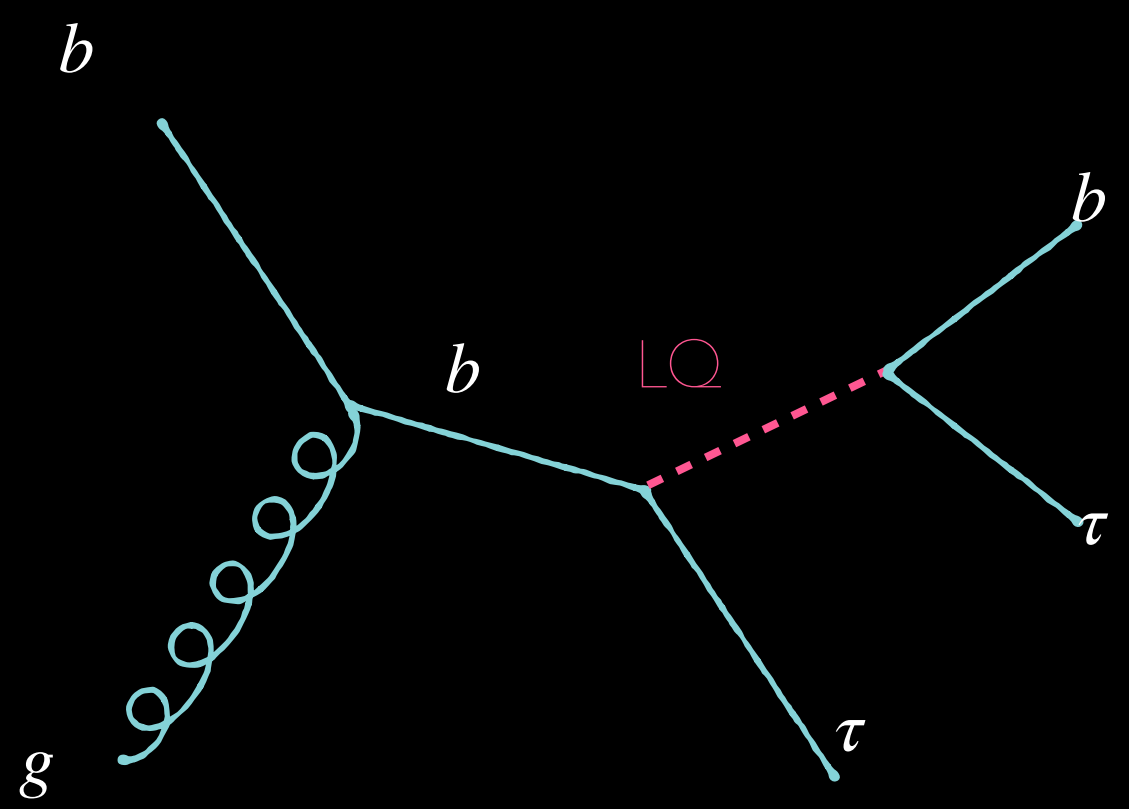




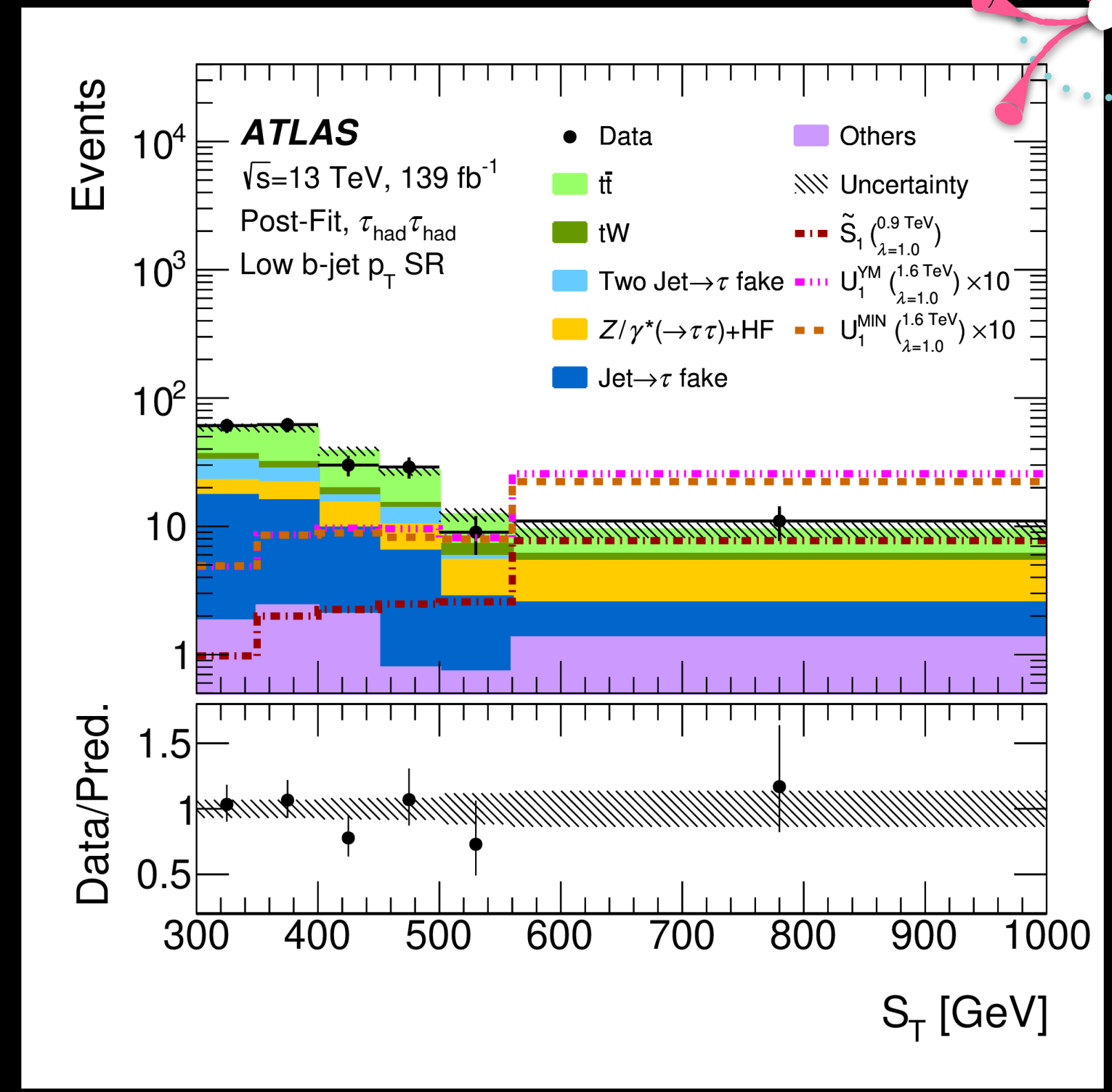
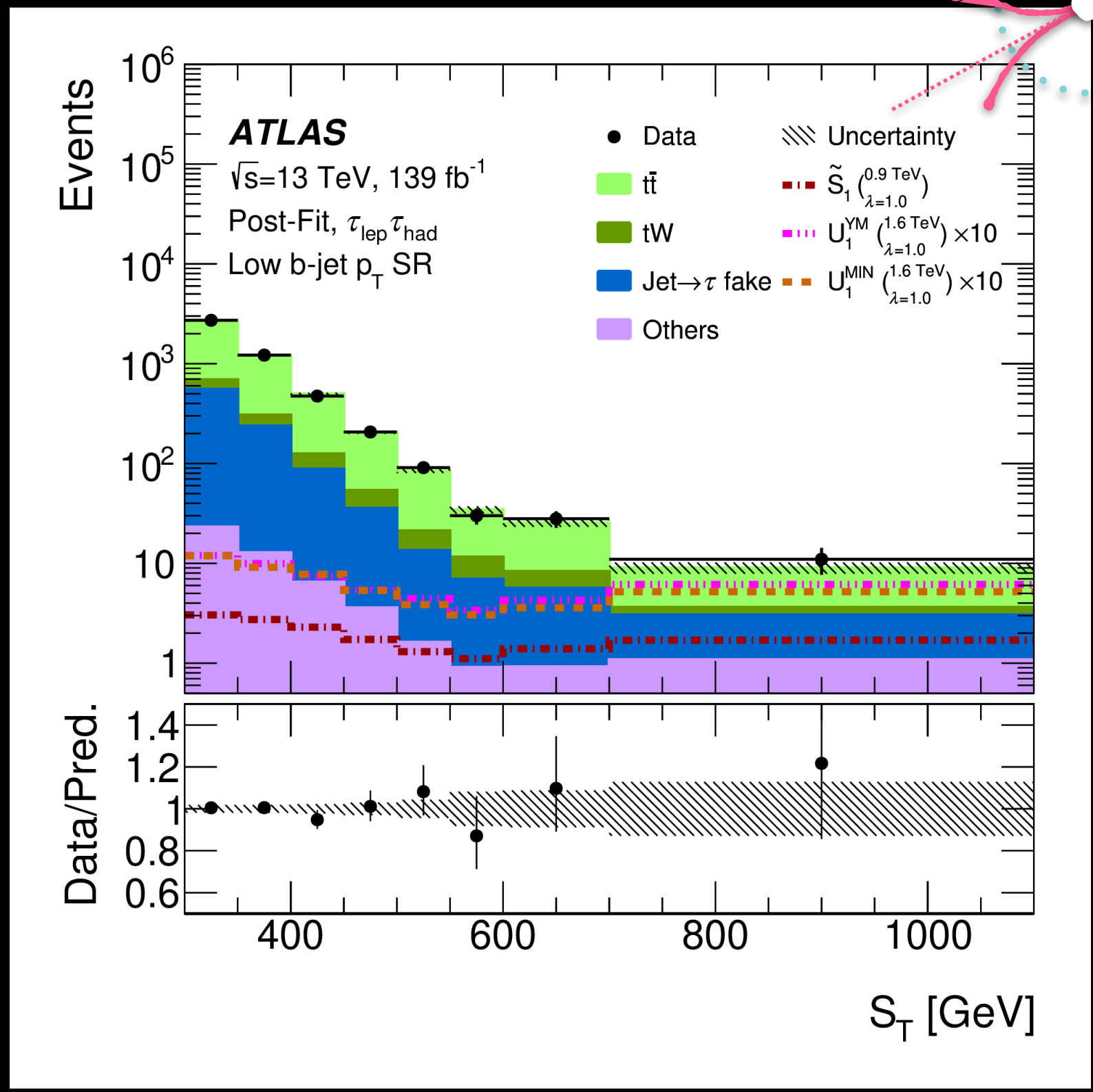
Process	ME generator	ME QCD order	ME PDF	PS and hadronisation	UE tune	Cross-section order
<b>Top-quark</b>						
$t\bar{t}^{(\$)}$	POWHEG-BOX v2	NLO	NNPDF3.0NLO	PYTHIA 8.230	A14	NNLO+NNLL
$t$ -channel	POWHEG-BOX v2	NLO	NNPDF3.0NLO	PYTHIA 8.230	A14	NLO
$s$ -channel	POWHEG-BOX v2	NLO	NNPDF3.0NLO	PYTHIA 8.230	A14	NLO
$Wt^{(\$)}$	POWHEG-BOX v2	NLO	NNPDF3.0NLO	PYTHIA 8.230	A14	NLO
<b>Top-quark + W/Z</b>						
$t\bar{t}Z$	SHERPA 2.2.1	NLO	NNPDF3.0NNLO	SHERPA 2.2.1	Default	NLO <sup>(†)</sup>
$t\bar{t}W$	SHERPA 2.2.8	NLO	NNPDF3.0NNLO	SHERPA 2.2.8	Default	NLO <sup>(†)</sup>
<b>Vector boson + jets</b>						
$W/Z$ +jets	SHERPA 2.2.1	NLO ( $\leq 2$ jets) LO (3,4 jets)	NNPDF3.0NNLO	SHERPA 2.2.1	Default	NNLO
<b>Diboson</b>						
$WW, WZ, ZZ$	SHERPA 2.2.1	NLO ( $\leq 1$ jet) LO (2,3 jets)	NNPDF3.0NNLO	SHERPA 2.2.1	Default	NLO <sup>(†)</sup>
<b>Higgs boson</b>						
ggF	POWHEG-BOX v2	NNLO	NNPDF3.0NLO	PYTHIA 8.212	AZNLO	N3LO(QCD)+NLO(EW)
VBF	POWHEG-BOX v2	NLO	NNPDF3.0NLO	PYTHIA 8.212	AZNLO	NNLO(QCD)+NLO(EW)
$qq \rightarrow WH$	POWHEG-BOX v2	NLO	NNPDF3.0NLO	PYTHIA 8.212	AZNLO	NNLO(QCD)+NLO(EW)
$qq \rightarrow ZH$	POWHEG-BOX v2	NLO	NNPDF3.0NLO	PYTHIA 8.212	AZNLO	NNLO(QCD)+NLO(EW) <sup>(‡)</sup>
$gg \rightarrow ZH$	POWHEG-BOX v2	NLO	NNPDF3.0NLO	PYTHIA 8.212	AZNLO	NLO+NLL
$t\bar{t}H$	POWHEG-BOX v2	NLO	NNPDF3.0NLO	PYTHIA 8.230	A14	NLO

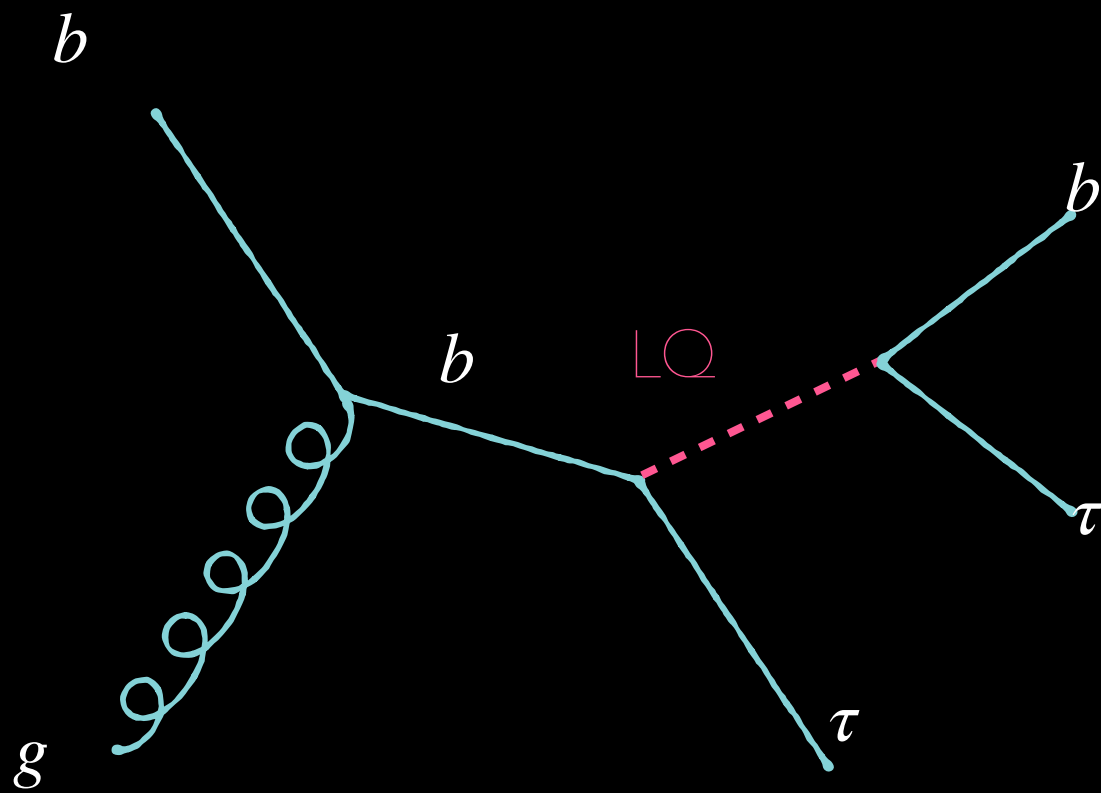






not considered in results





Process	$\tau_{lep} \tau_{had}$	$\tau_{had} \tau_{had}$
$t\bar{t}$	764 ± 82	9.9 ± 2.6
Single top	65 ± 35	3.9 ± 1.0
Jet → $\tau$ fake	215 ± 79	3.9 ± 1.0
Two jet → $\tau$ fake	–	1.34 ± 0.27
Z(→ $\tau\tau$ )+HF jets	5.5 ± 0.4	4.6 ± 1.1
Others	9.7 ± 1.0	1.75 ± 0.30
<b>Total</b>	<b>1059 ± 51</b>	<b>25.4 ± 4.9</b>
<b>Data</b>	<b>1053</b>	<b>29</b>

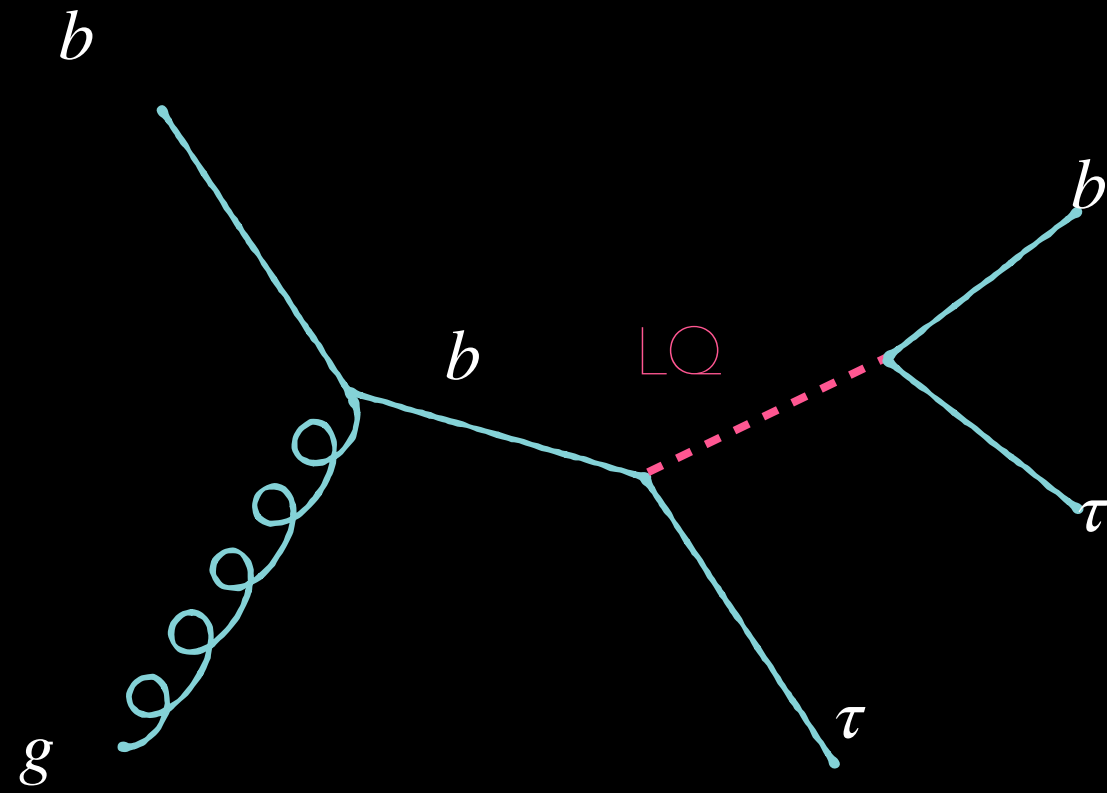
## $\tau_{lep} \tau_{had}$

Signal Regions	Selection	Purpose
Preselection	$\ell$ (trigger, isolated), $\tau_{had-vis}$ (medium $\tau_{had-ID}$ ), $q(\ell) \times q(\tau_{had-vis}) < 0$ , $\Delta\phi(\ell, E_T^{miss}) < 1.5$ , $m_{vis}(\ell, \tau_{had-vis}) > 100$ GeV, $S_T > 300$ GeV, at least one $b$ -jet	
High $b$ -jet $p_T$ SR	Leading $b$ -jet $p_T > 200$ GeV	
Low $b$ -jet $p_T$ SR	Leading $b$ -jet $p_T < 200$ GeV	
Control/Validation Regions	Selection	Purpose
Multijet-CR	$\ell$ (trigger, pass/fail offline isolation), $m_T(\ell, E_T^{miss}) < 30$ GeV, one $b$ -jet, $\tau_{had-ID}$ score $< 0.01$ , $E_T^{miss} < 50$ GeV	Measure lepton fake-factor
Top-CR	Satisfy SR except: $\Delta\phi(\ell, E_T^{miss}) > 2.5$ , no $S_T$ and lead. $b$ -jet $p_T$ req.	Derive top correction
SS-CR	Satisfy SR except: $q(\ell) \times q(\tau_{had-vis}) > 0$ , no $\Delta\phi(\ell, E_T^{miss})$ , and $S_T$ req.	Measure jet → $\tau$ background scale factor
High $b$ -jet $p_T$ VR	Satisfy high $b$ -jet $p_T$ SR except: $1.5 < \Delta\phi(\ell, E_T^{miss}) < 2.5$ , $300$ GeV $< S_T < 600$ GeV	Background modelling validation
Low $b$ -jet $p_T$ VR	Satisfy low $b$ -jet $p_T$ SR except: $1.5 < \Delta\phi(\ell, E_T^{miss}) < 2.5$ , $300$ GeV $< S_T < 600$ GeV	Background modelling validation
b-tag Z-CR	Satisfy SR except: $45$ GeV $< m_{vis}(\ell, \tau_{had-vis}) < 80$ GeV, $p_T(\ell)/p_T(b\text{-jet}) > 0.8$ , $ \Delta\phi(\ell, \tau_{had-vis})  > 2.4$ , no $S_T$ req.	Z+ heavy-flavour jets normalisation factor

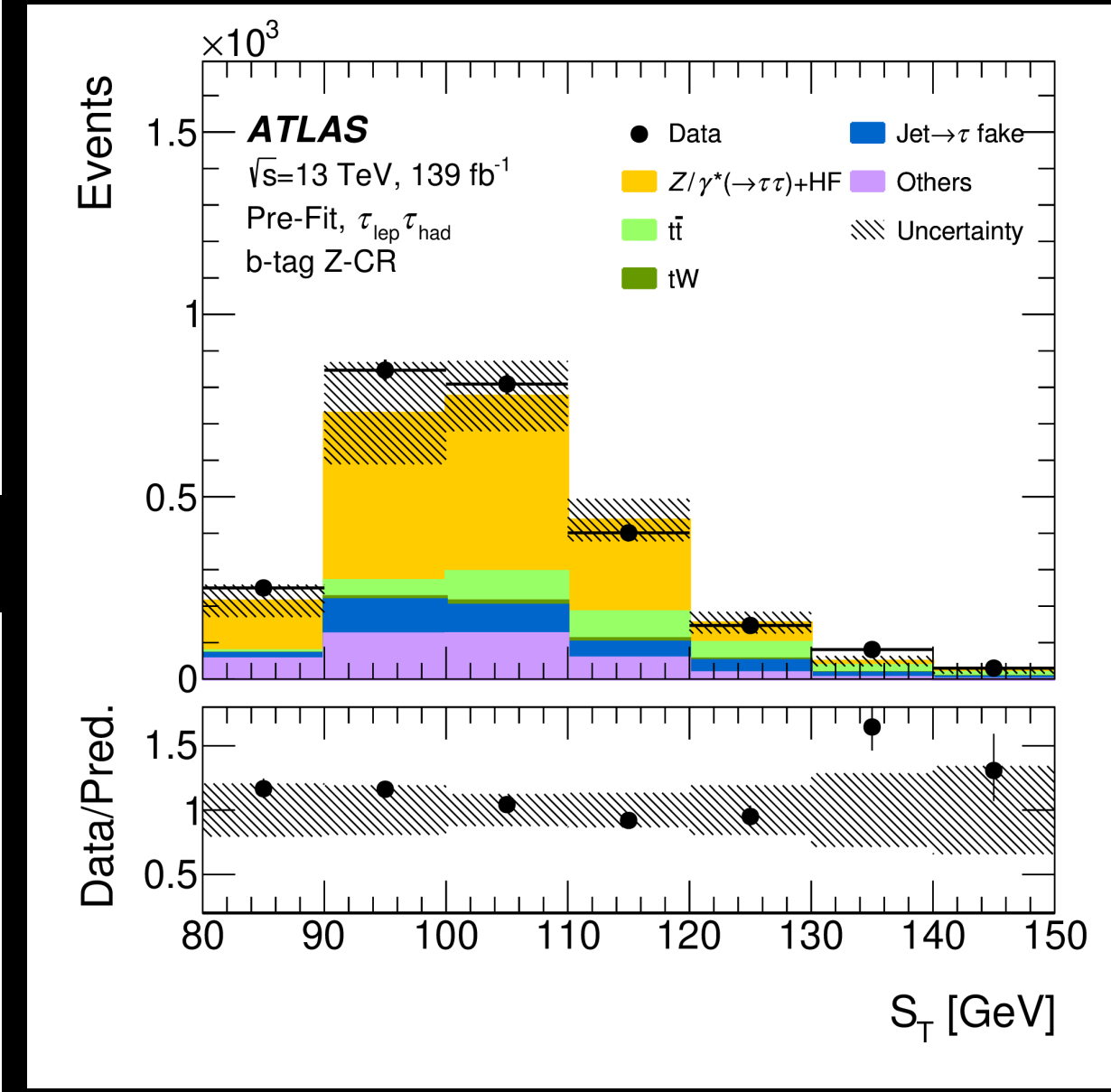
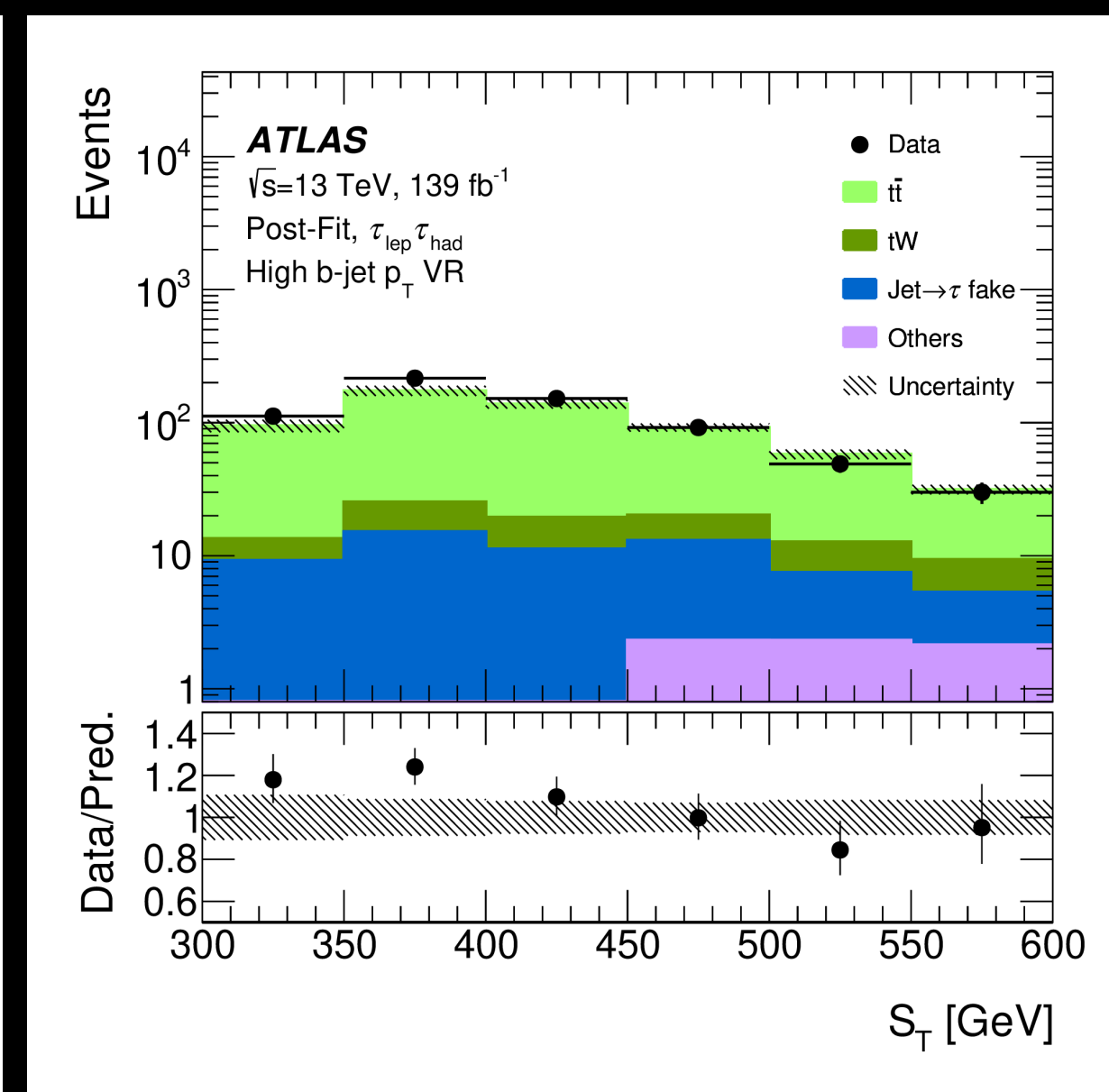
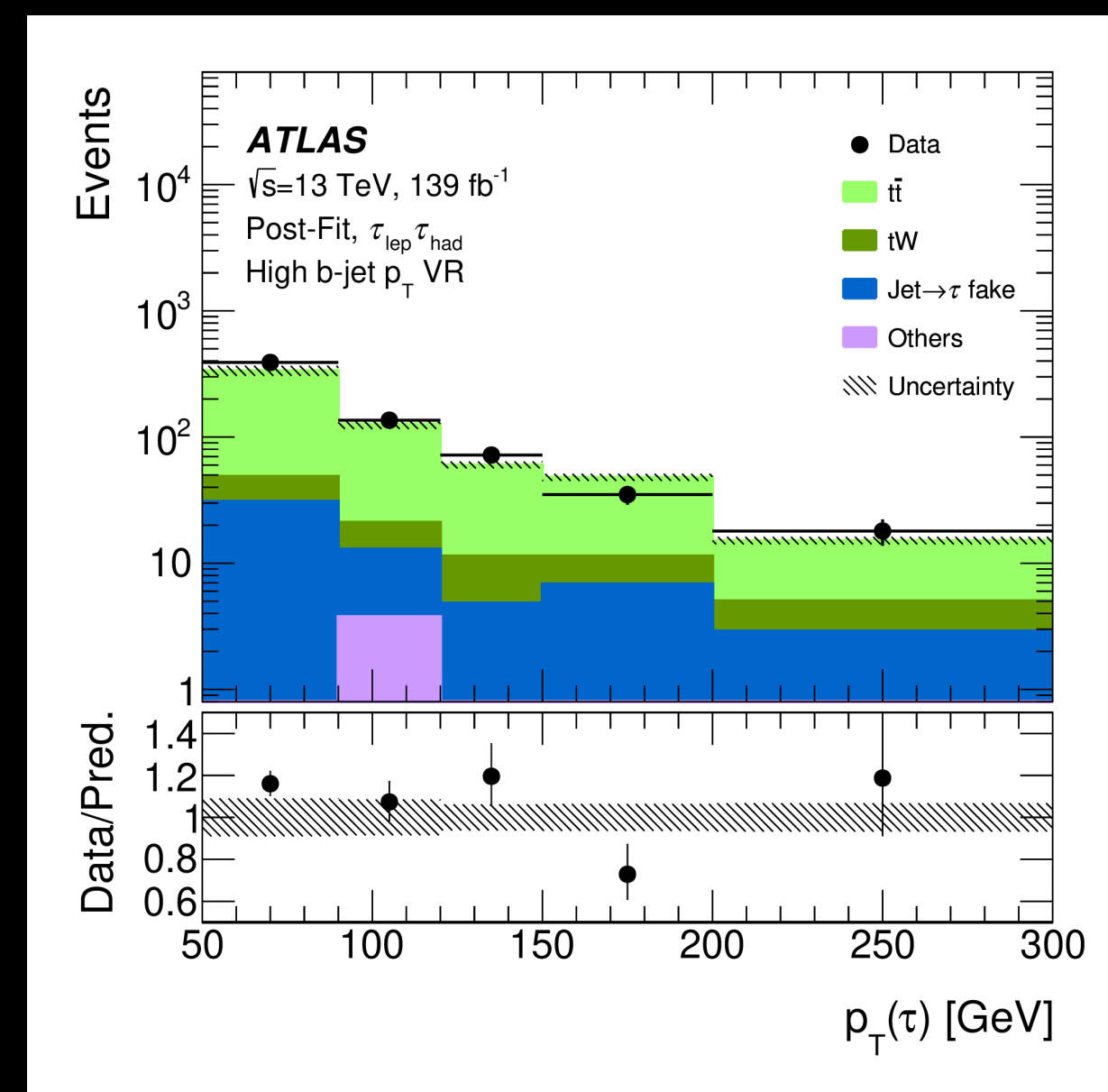
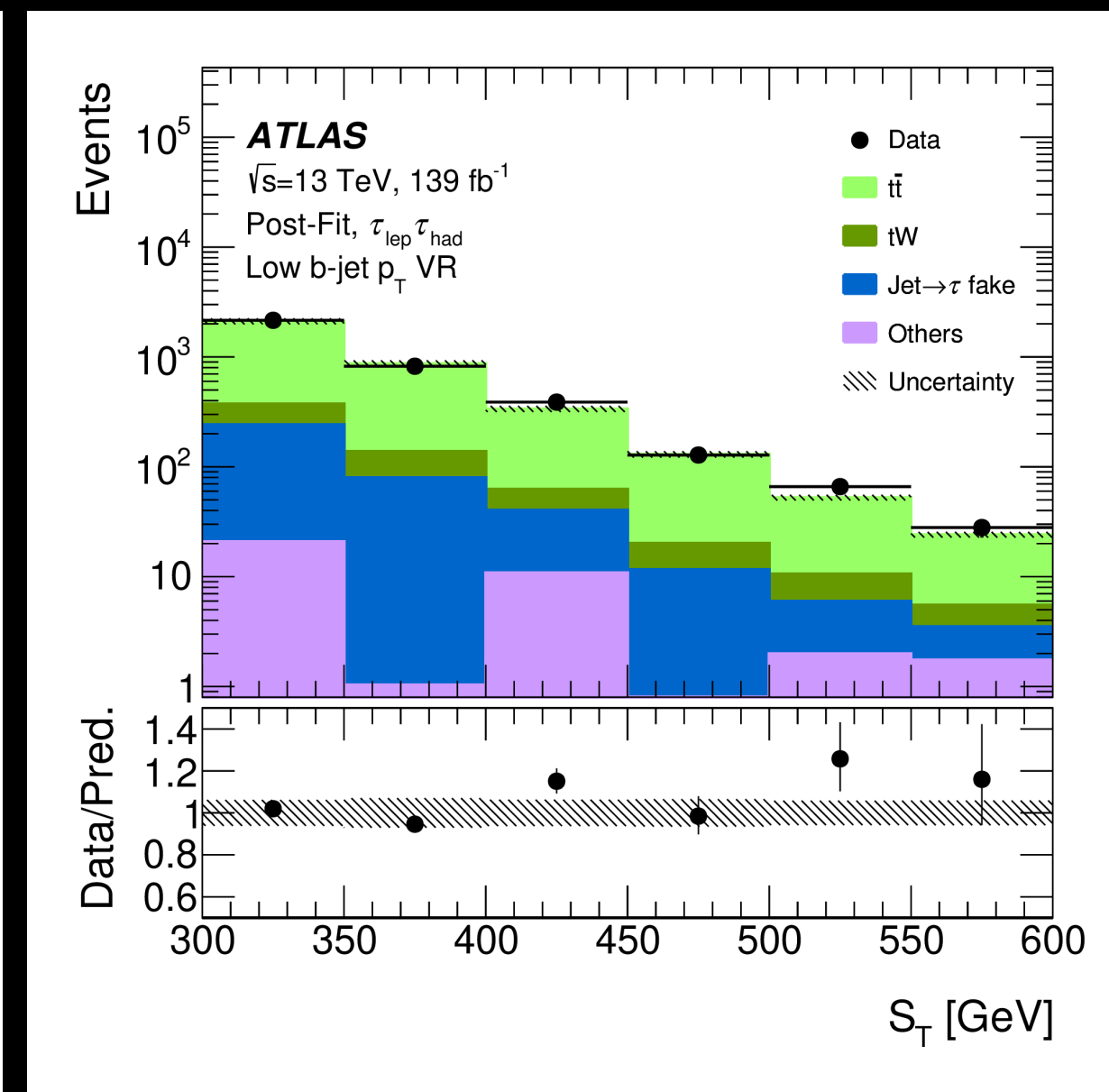
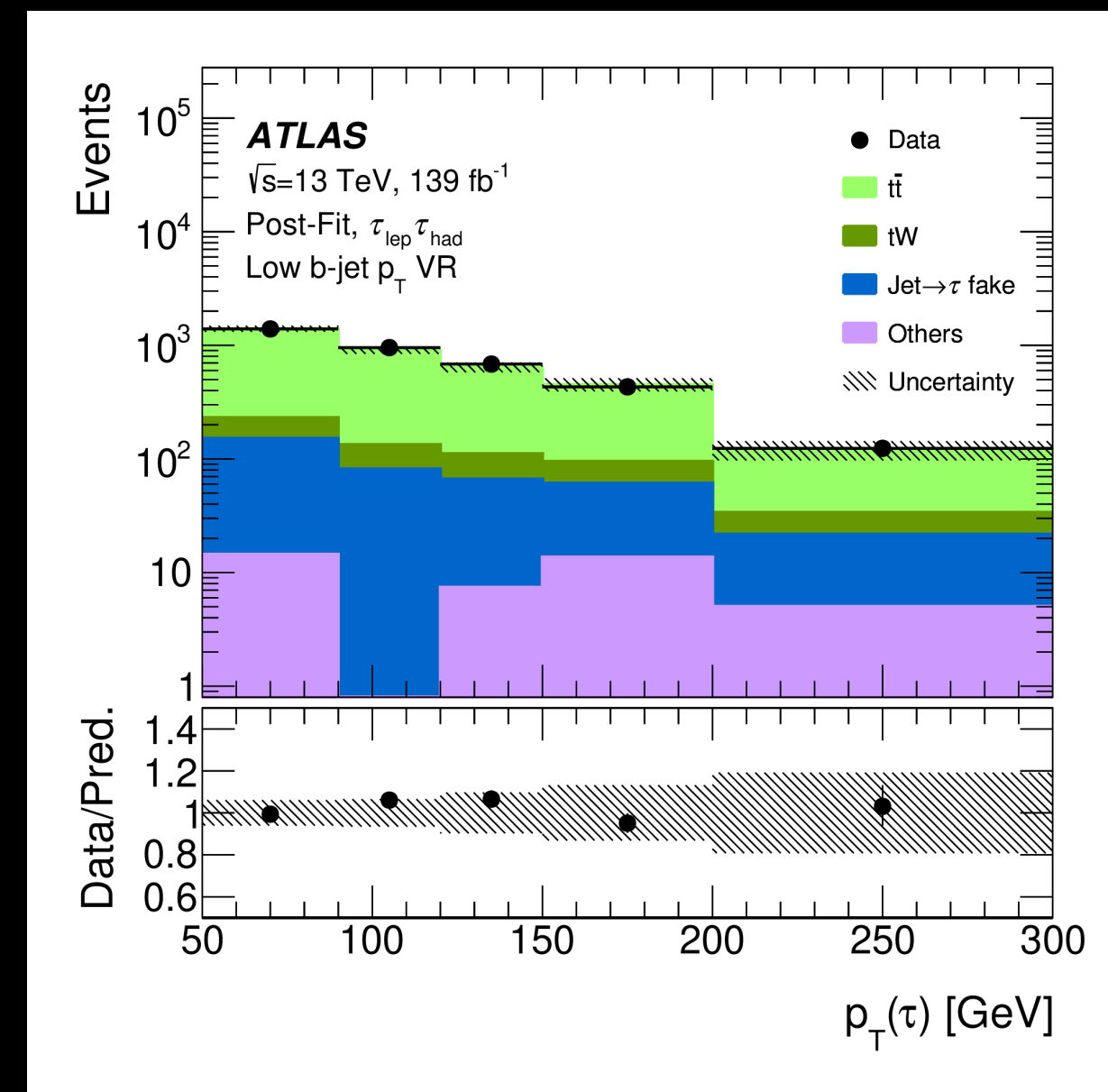
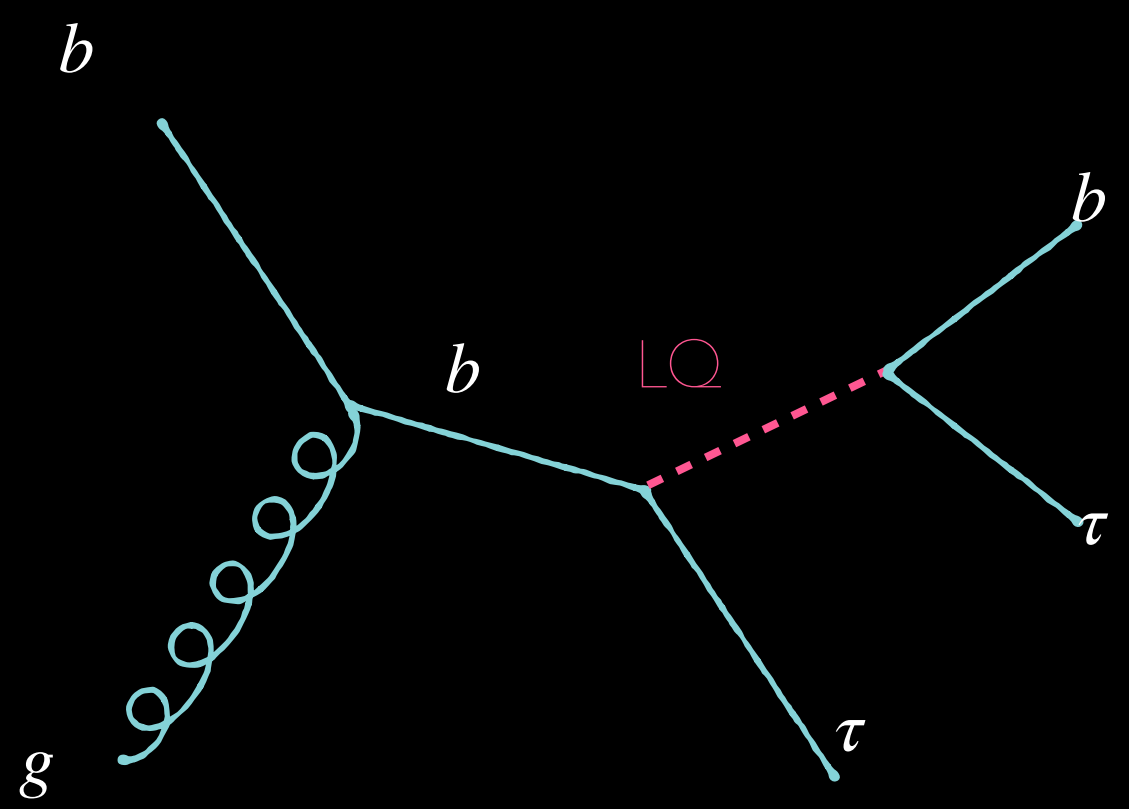
## $\tau_{had} \tau_{had}$

Signal Regions	Selection	Purpose
Preselection	$\tau_{had,1}$ (trigger, medium $\tau_{had-ID}$ ), $\tau_2$ (loose $\tau_{had-ID}$ ), $q(\tau_1) \times q(\tau_2) < 0$ , $m_{vis}(\tau_1, \tau_2) > 100$ GeV, $S_T > 300$ GeV, at least one $b$ -jet	
High $b$ -jet $p_T$ SR	Leading $b$ -jet $p_T > 200$ GeV	
Low $b$ -jet $p_T$ SR	Leading $b$ -jet $p_T < 200$ GeV	
Control/Validation Regions	Selection	Purpose
DJ-CR	$\tau_1$ and $\tau_2$ satisfy very loose $\tau_{had-ID}$ , $q(\tau_1) \times q(\tau_2) < 0$	Measure $\tau_{had-vis}$ fake-factor
CR-1	Satisfy SR except: $\tau_2$ fail loose $\tau_{had-ID}$	Apply $\tau_{had-vis}$ fake-factor
SS-VR	Satisfy SR except: $q(\tau_1) \times q(\tau_2) > 0$	Multijet modelling check
Z+light flavour jets VR	Satisfy SR except: 0 $b$ -jets, $\Delta\phi(\tau_1, \tau_2) > 0.25$ , $m_{vis}(\tau_1, \tau_2) < 100$ GeV, $E_T^{miss} > 60$ GeV	Z+light jets modelling

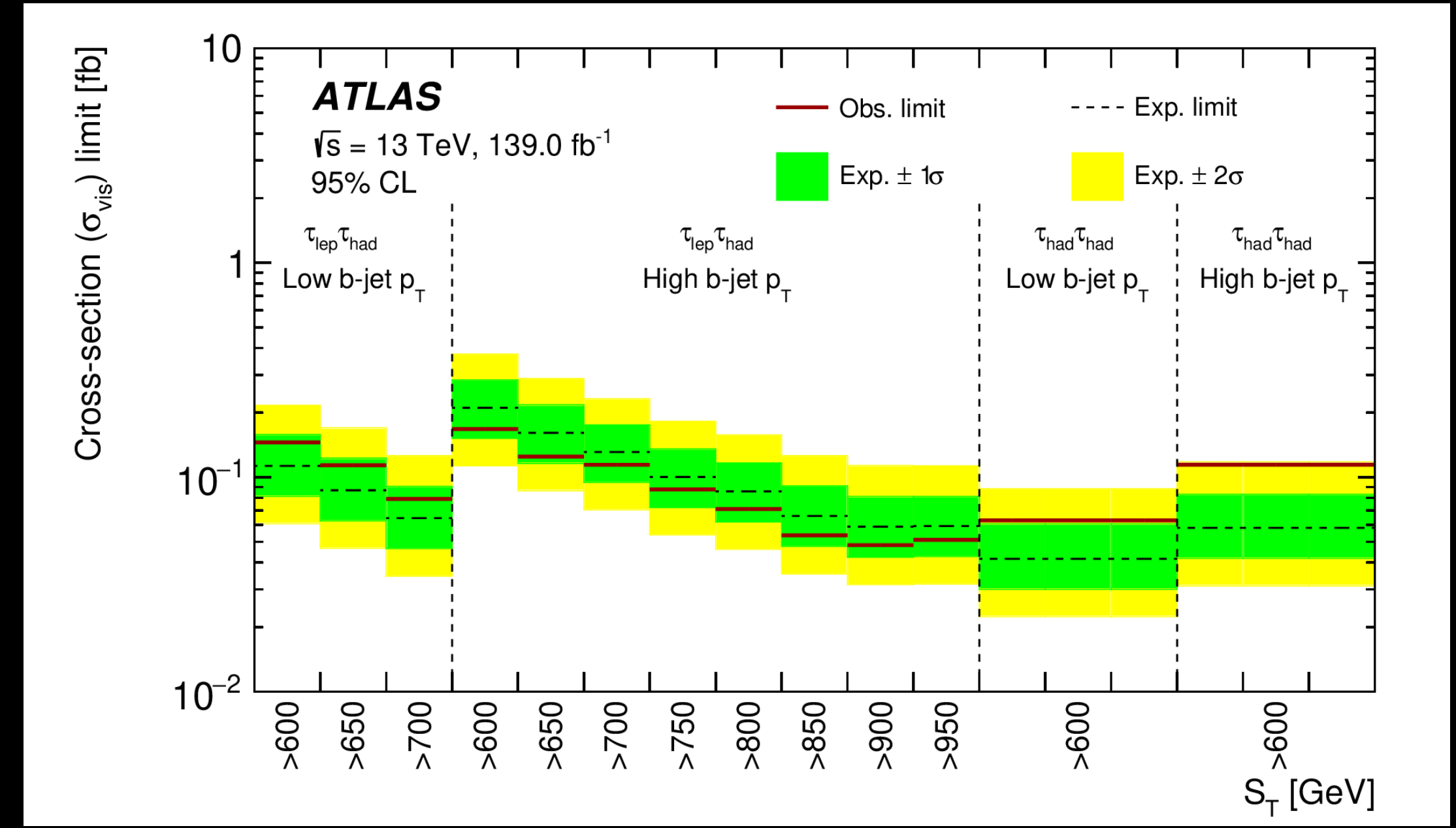
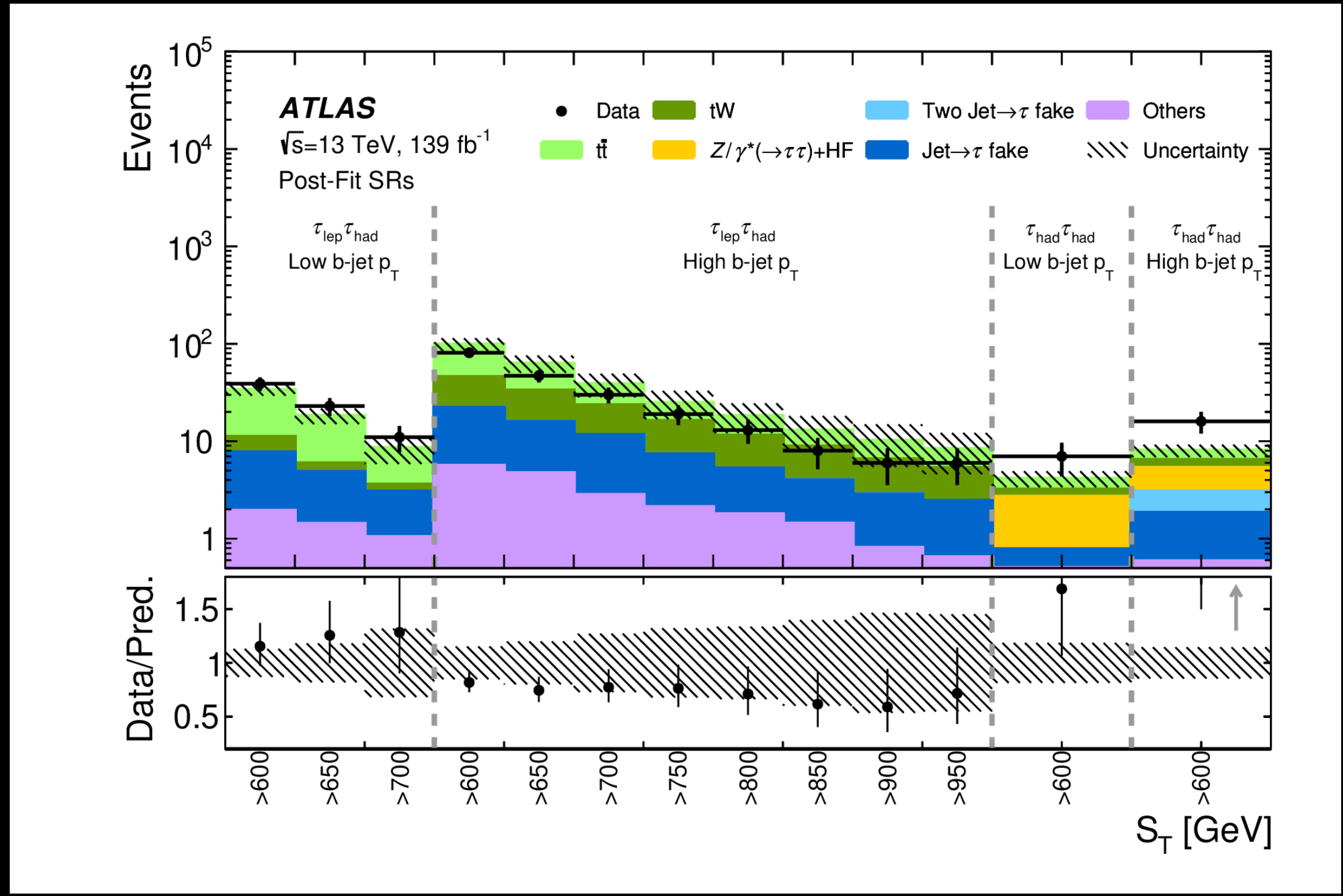
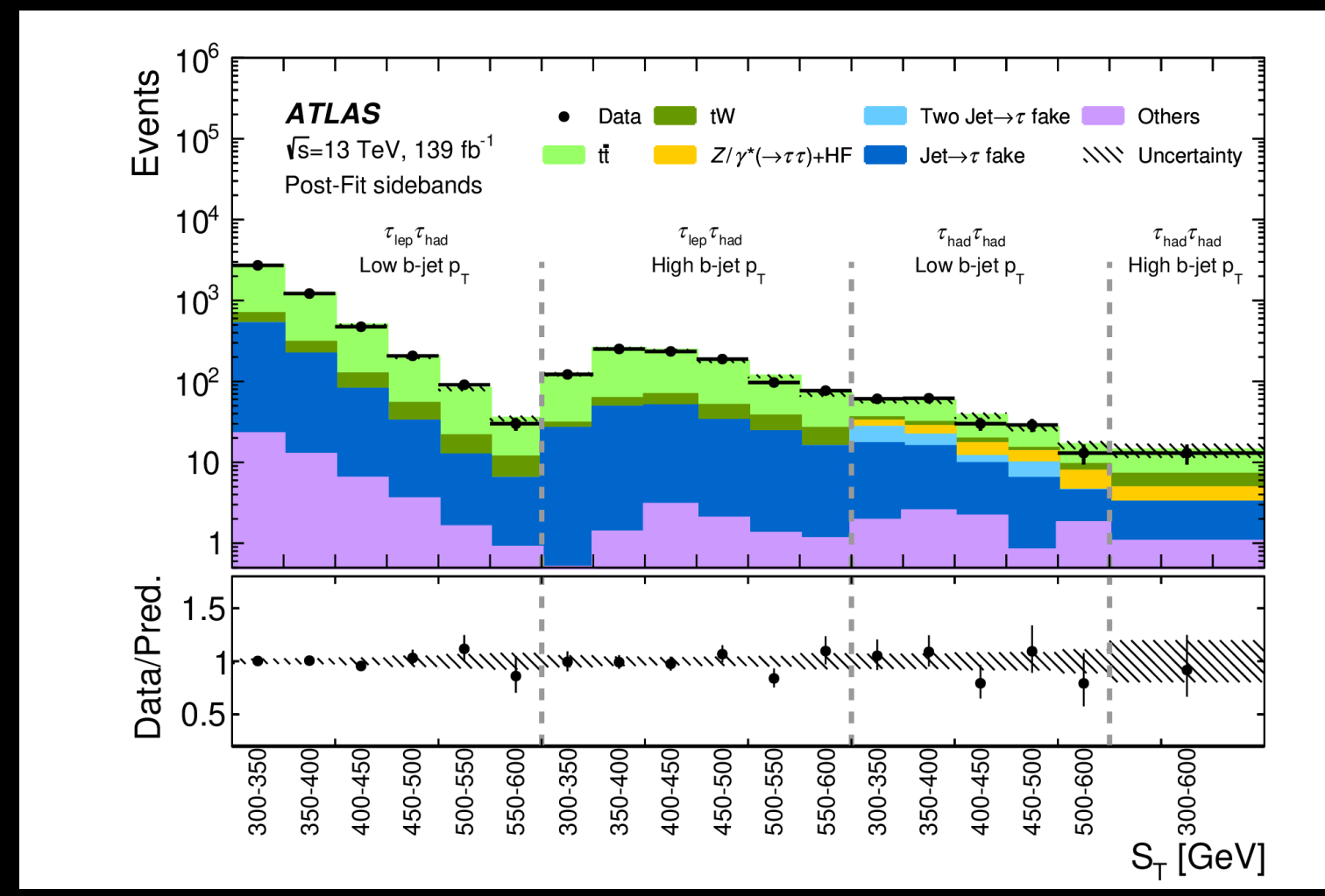
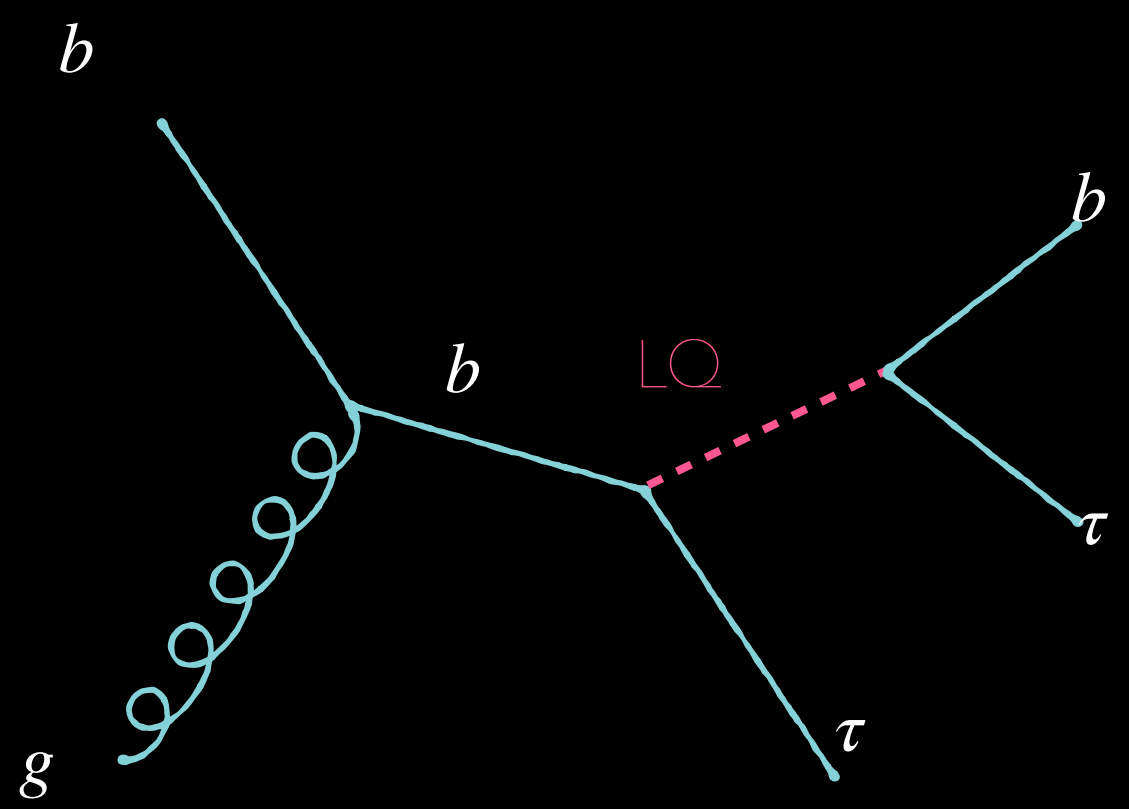


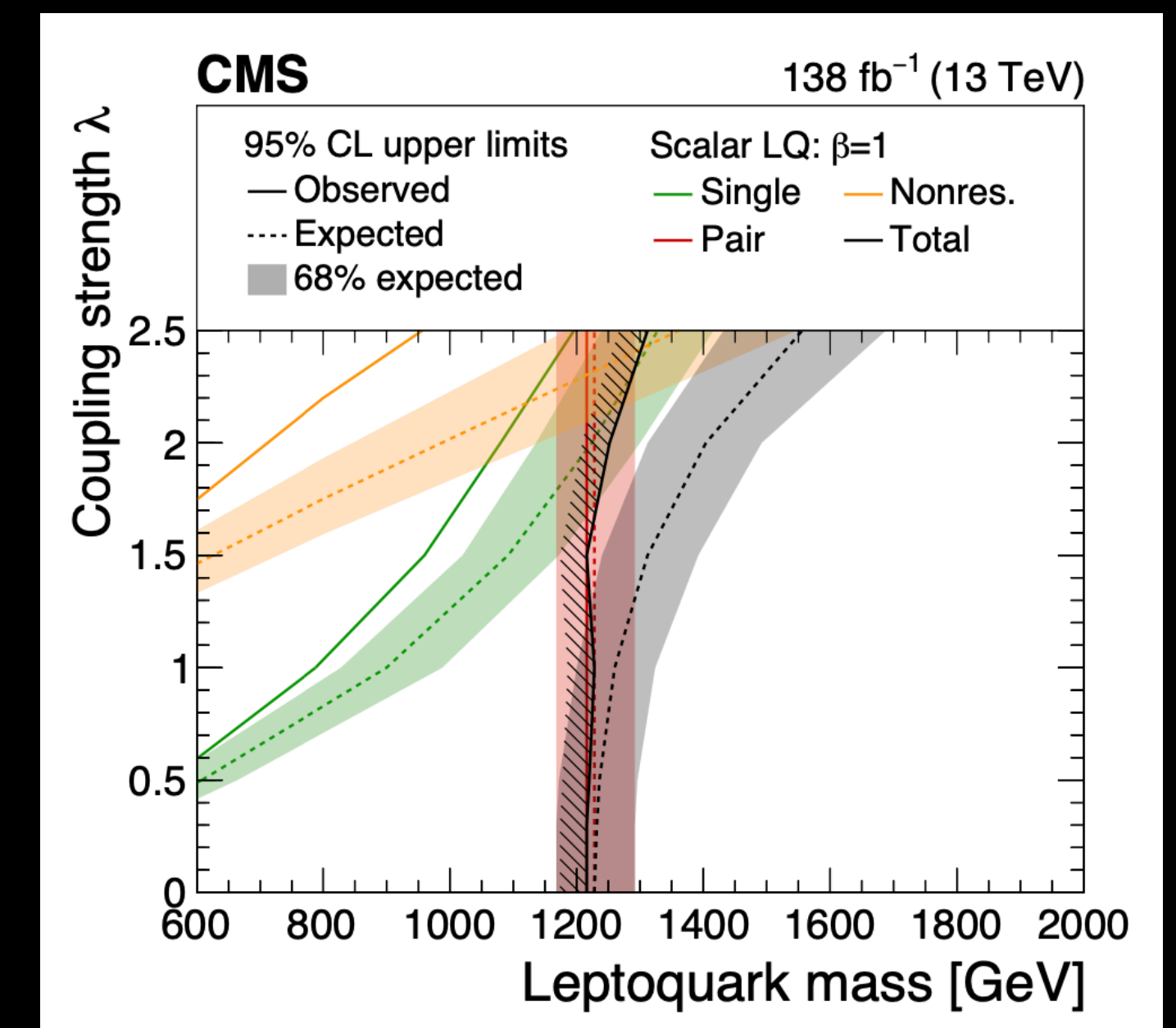
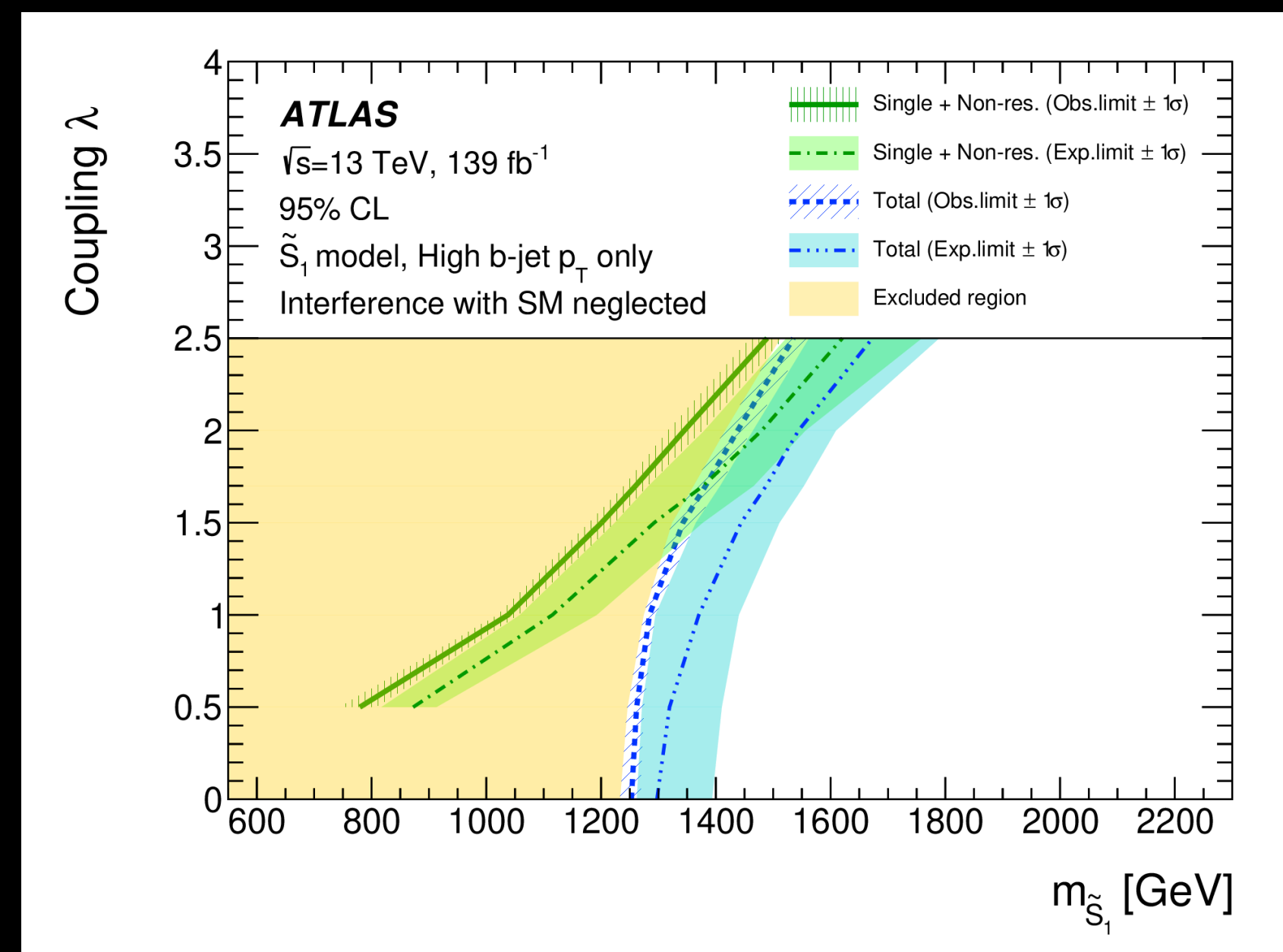
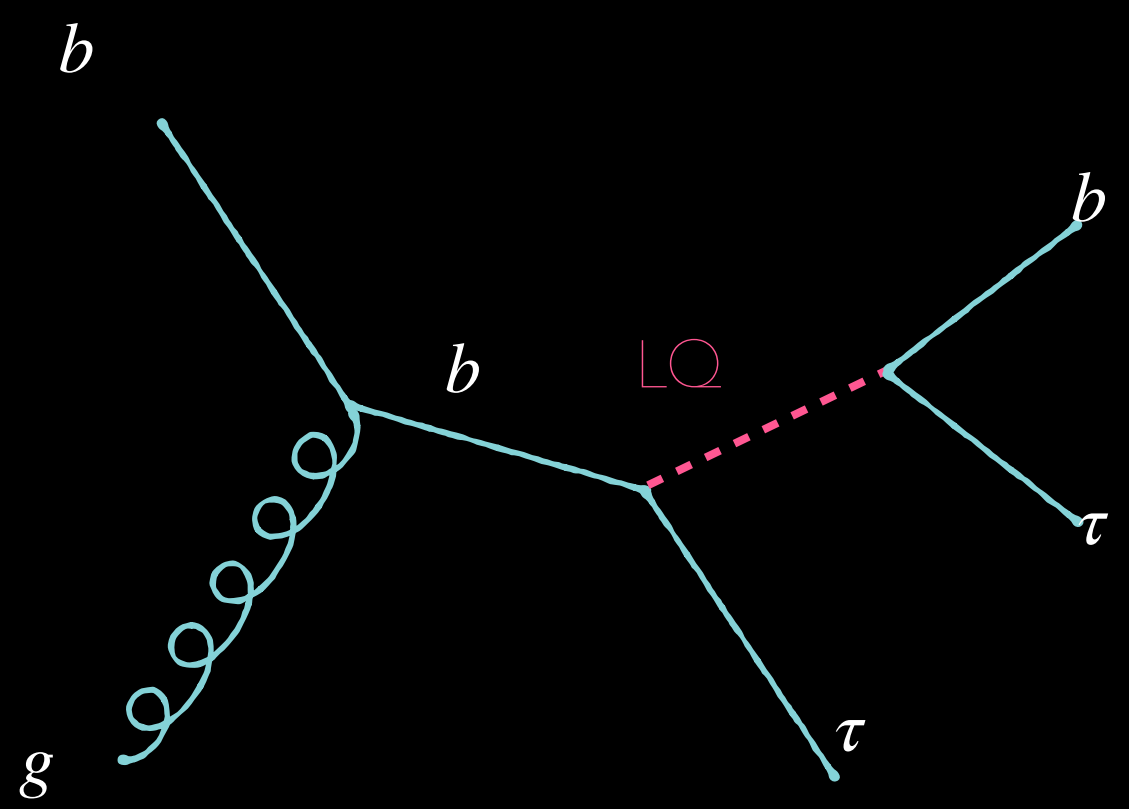


Process	Generator		PDF set		Tune	Normalisation
	ME	PS	ME	PS		
LQ → $b\tau$	MadGraph5_aMC@NLO	PYTHIA 8.244	NNPDF3.0 <sub>NNLO</sub>	NNPDF2.3 <sub>LO</sub>	A14	LO
Scalar LQLQ → $b\tau b\tau$	MadGraph5_aMC@NLO	PYTHIA 8.230	NNPDF3.0 <sub>NNLO</sub>	NNPDF2.3 <sub>LO</sub>	A14	NNLO + NNLL
Vector LQLQ → $b\tau b\tau$	MadGraph5_aMC@NLO	PYTHIA 8.244	NNPDF3.0 <sub>NNLO</sub>	NNPDF2.3 <sub>LO</sub>	A14	LO
$t\bar{t}$	POWHEG BOX v2	PYTHIA 8.230	NNPDF3.0 <sub>NNLO</sub>	NNPDF2.3 <sub>LO</sub>	A14	NNLO + NNLL
Single top	POWHEG BOX v2	PYTHIA 8.230	NNPDF3.0 <sub>NNLO</sub>	NNPDF2.3 <sub>LO</sub>	A14	NLO
$Z/\gamma^*$	POWHEG BOX v1	PYTHIA 8.186	CT10 <sub>NLO</sub>	CTEQ6L1	AZNLO	NLO
W+jets	SHERPA 2.2.1		>NNPDF3.0 <sub>NNLO</sub>		SHERPA	NNLO
Diboson	SHERPA 2.2.1/SHERPA 2.2.2		>NNPDF3.0 <sub>NNLO</sub>		SHERPA	NLO









CMS results (submitted to JHEP)

<https://cms-results.web.cern.ch/cms-results/public-results/publications/EXO-19-016/>

